Model-Based Parameter Estimation for Fault Detection in Process Systems using Multiparametric Programming

A thesis submitted to University College London for the degree of

Doctor of Philosophy

By

Ernie Binti Che Mid

Department of Chemical Engineering

University College London

Torrington Place

London WC1E 7JE

July 2019

DECLARATION

I, Ernie Che Mid, confirm that the work presented in this thesis is my own. Where information has been derived from other sources, I confirm that this has been indicated in the thesis.

Faithfully yours,

Ernie Binti Che Mid

ABSTRACT

Fault detection (FD) has become increasingly important for improving the reliability and safety of process systems. This work presents a model-based FD technique for nonlinear process systems using parameter estimation. For a system described by nonlinear ordinary differential equations (ODEs), estimation of model parameters requires solving an optimisation problem such that the residual between the measurements and model predicted values of state variables is minimised. However, solving an optimisation problem online can be computationally expensive and the solution may not converge in a reasonable time. Thus, a method for parameter estimation for FD using multiparametric programming (MPP) is proposed. In this technique, the nonlinear ODEs model is discretised by using explicit Euler's method to obtain algebraic equations. Then, a square system of parametric nonlinear algebraic equations is obtained by formulating optimality condition. These equations are then solved symbolically to obtain model parameters as an explicit function of the measurements. This allows computation of parameter estimates by simple function evaluation. The detection of fault is carried out by monitoring the changes in the residual between model parameter estimates and 'true' value.

The application of the proposed technique for FD is demonstrated on evaporator, tank, heat exchanger, fermentation and wastewater treatment systems. In a single-stage evaporator, changes in heat transfer coefficient and composition of feed are obtained and estimated for FD. In a quadruple-tank system, tank leakage is investigated by estimating the cross-section of outlet holes. Fouling in heat exchanger is detected where the overall heat transfer coefficient is estimated and the fouling resistance is monitored. In demonstrating the technique in relation to the fermentation and the wastewater treatment systems, kinetic model parameters are estimated for FD. The proposed work successfully estimates the model parameters and detects the faults through simple function evaluations of explicit functions. This demonstrates the advantages of MPP for FD using parameter estimation to detect faults quickly and accurately. In addition, a comparison of the implicit Euler's method and explicit Euler's method for discretisation of nonlinear ODEs model for

parameter estimation using MPP is presented. Complexity of implicit parametric functions, accuracy of parameter estimates and effect of step size are discussed.

IMPACT STATEMENT

Fault detection is an essential element in process monitoring which is gaining importance in the current worldwide discussion. If the faults are not properly handled, they can lead to consequences ranging from failures to meet product quality specifications to plant shutdowns, incurring substantial economic losses, as well as safety hazards to facilities, personnel and environment. A few incidents in aircraft flight provide evidence for the need for FD. Delta Flight 1080, American Airlines DC-10 and EL AL Flight 182, a Boeing 747-2007 freighter, are examples of incidents that could have been avoided. In nuclear power industries, the Three Mile incident and the tragedy at the Chernobyl nuclear power plant led to intensified research in diagnostics and fault-tolerant control. FD is now attracting more and more attention in a wider range of industrial and academic communities. This is due to increased safety and reliability demands beyond what a conventional system can offer. Thus, this work has developed model-based parameter estimation for FD using MPP to develop an efficient and timely response for FD. This work has improved accuracy and speed of parameter estimation in FD by obtaining model parameters as an explicit function of measurements.

The outcome of this work intends to give future directions for academic research and developments in the area of FD using MPP. The proposed parameter estimation approach can be further researched for large-scale process systems to estimate the faulty process parameters. The methodology presented in this work can also be implemented in industrial systems. Results from parameter estimation using MPP can be used in planning for automated FD and tolerant control systems. Automated FD and tolerant control can reduce maintenance costs due to early FD and prevention and better schedule of maintenance services and inspections. The benefits brought by application of FD technique are longer equipment life, better service, reduced service cost and better environmental protection. The research in the area of FD could reduce operating costs over many years.

DISSEMINATION

Journal Publications

CHE MID, E. & DUA, V. 2017. Model-Based Parameter Estimation for Fault Detection Using Multiparametric Programming. *Industrial and Engineering Chemistry Research*, 56, 8000-8015.

CHE MID, E. & DUA, V. 2018. Fault Detection in Wastewater Treatment Systems Using Multiparametric Programming. *Processes,* 6, 231.

CHE MID, E. & DUA, V. 2019. Parameter estimation using multiparametric programming for implicit Euler's method based discretization. *Chemical Engineering Research and Design*, 142, 62-77.

Conference Proceeding

MID, E.C. and DUA, V. 2018. Fault detection of fermentation processes, *Computer Aided Chemical Engineering.* 43, 1171-1176

Oral and Poster Presentations

CHE MID, E. & DUA, V. Model-based fault tolerant control of process systems. ChemEngDayUK 2015, University of Sheffield, 8 – 9 April 2015, Poster Presentation.

CHE MID, E. & DUA, V. Design of a model-based fault tolerant control for nonlinear process systems. ChemEngDayUK 2016, University of Bath, 31 March – 1 April 2016, Poster Presentation.

CHE MID, E. & DUA, V. Model-based fault tolerant control for nonlinear process systems. PSE@ResearchDayUK 2016, Imperial College London, 12 July 2016, Poster Presentation.

CHE MID, E. & DUA, V. Model-based fault detection for nonlinear process systems. 2016 AIChE Annual Meeting, Hotel Nikko San Francisco, 13 – 18 November 2016, Oral Presentation.

CHE MID, E. & DUA, V. Fault detection using multiparametric programming for nonlinear process systems. PSE@ResearchDayUK 2017, Imperial College London, 27 June 2017, Poster Presentation.

CHE MID, E. & DUA, V. Model-Based Fault Detection for Nonlinear Process Systems Using Multiparametric Programming for Parameter Estimation. 2017 AIChE Annual Meeting, Minneapolis Convention Center, 29 – 3 November 2017, Oral Presentation.

ACKNOWLEDGEMENTS

I would like to express my heartfelt gratitude, first of all to my supervisor, Dr Vivek Dua, for his immense contribution towards my PhD programme, through his supervision and guidance during the work. Many of the new ideas were developed through the discussions and I could never have completed the PhD without his help and support. The contributions of the staff at the Department of Chemical Engineering are accordingly recognised. I would like to thank my family for their constant encouragement, support and attention, and for making me more confident in my life. My husband deserves a substantial share of the credit for everything I have done. Also, I thank everyone in the group and my friends for creating a comfortable environment for me to complete my work. Finally, I would like to express my deepest appreciation to my financial sponsor, Ministry of Education Malaysia and University Malaysia Perlis, for the scholarship, which allowed me to undertake the study.

TABLE OF CONTENTS

DECLARATION 2

ABSTRACT 3

IMPACT STATEMENT 5

DISSEMINATION 6

ACKNOWLEDGEMENTS 8

TABLE OF CONTENTS 9

LIST OF FIGURES 14

LIST OF TABLES 18

LIST OF ABBREVIATIONS 20

LIST OF SYMBOLS 21

CHAPTER 1 INTRODUCTION 26

1.1 Introduction 26

1.2 Aim and Objectives 29

1.3 Thesis Organisation 30

CHAPTER 2 LITERATURE REVIEW 32

2.1 Fault Detection 32

2.2 Model-Based Fault Detection Methods 33

2.2.1 Observer/Filter-Based Approaches 35

2.2.2 Parity Relation-Based Approaches 36

2.2.3 Parameter Estimation-Based Approaches 37

2.3 Summary 40

CHAPTER 3 FAULT DETECTION USING MULTIPARAMETRIC PROGRAMMING 41

3.1 Introduction 41

3.2 General Formulation for Fault Detection using Parameter Estimation 41

3.2.1 Discretisation of Ordinary Differential Equation 42

3.2.2 Fault Detection Problem 42

3.3 Parameter Estimation using Multiparametric Programming 43

3.4 Fault Detection Analysis 44

3.5 Illustrated examples of the proposed method 45

3.5.1 Example 1: First-order irreversible chain reactions 46

3.5.2 Example 2: Lotka–Volterra model 50

3.6 Concluding Remarks 54

CHAPTER 4 FAULT DETECTION APPLICATION IN PROCESS SYSTEMS 55

4.1 Introduction 55

4.2 Single-Stage Evaporator 55

4.2.1 Mathematical Model 56

4.2.2 Fault Detection Problem 58

4.2.3 Parameter Estimate using MPP 59

4.2.4 Fault-free Scenario 61

4.2.5 Faulty Scenario 63

4.3 Quadruple-Tank System 66

4.3.1 Mathematical Model 67

4.3.2 Fault Detection Problem 69

4.3.3 Parameter Estimation using MPP 69

4.3.4 Fault-free Scenario 73

4.3.5 Faulty Scenario 75

4.4 Heat Exchanger 77

4.4.1 Mathematical model 79

4.4.2 Fouling Scenario 81

4.4.3 Fault Detection problem 81

4.4.4 Parameter Estimation using MPP 82

4.4.5 Clean Heat Exchanger Scenario 85

4.4.6 Fouling Heat Exchanger Scenario 89

4.5 Glutamic Acid Fermentation Process 91

4.5.1 Mathematical Model 92

4.5.2 Fault Detection Problem 94

4.5.3 Parameter Estimate using MPP 95

4.5.4 Fault-free Scenario 96

4.5.5 Faulty Scenario 99

4.6 Wastewater treatment system 102

4.6.1 Mathematical Model 103

4.6.2 Fault Detection Problem 106

4.6.3 Parameter Estimate using MPP 107

4.6.4 Fault-free Scenario...110

4.6.5 Faulty Scenario 115

4.7 Concluding Remarks..118

CHAPTER 5 PARAMETER ESTIMATION FOR SYSTEM DISCRETISATION USING IMPLICIT EULER’S METHOD.............................119

5.1 Introduction...119

5.2 Discretisation of Ordinary Differential Equation.....................................119

5.3 Parameter Estimation using Multiparametric Programming 120

5.4 Illustrated examples of the proposed method 120

5.4.1 Example 1: First-order irreversible chain reaction 121

5.4.2 Example 2: Lotka–Volterra model 126

5.4.3 Example 3: Single-stage evaporator 132

5.5 Concluding Remarks..142

CHAPTER 6 CONCLUDING REMARKS AND FUTURE DIRECTIONS......143

6.1 Concluding Remarks..143

6.2 Contribution to Knowledge...144

6.3 Future Directions...145

REFERENCES 147

APPENDIX A: ARTIFICIAL NEURAL NETWORK-BASED FORMULATION 158

APPENDIX B: RUNGE-KUTTA FOURTH-ORDER FORMULATION 160

LIST OF FIGURES

Figure 1.1 Parameter estimation using online optimisation approach.......................28

Figure 1.2 Multiparametric programming..29

Figure 1.3 Fault detection using multiparametric programming..............................30

Figure 2.1 Two-stage structure of FD processes (Patton et al., 1995).......................34

Figure 3.1 State variables profile for z_1 and z_2 49

Figure 3.2 Estimated model parameter, θ_1, for different step sizes, Δt 49

Figure 3.3 Estimated model parameter, θ_2, for different step sizes, Δt 49

Figure 3.4 State variables profile for z_1 and z_2 53

Figure 3.5 Estimated model parameter, θ_1, for different step sizes 53

Figure 3.6 Estimated model parameter, θ_2, for different step sizes 53

Figure 4.1 Evaporator configuration and notation..57

Figure 4.2 State variables profile, W, for fault-free scenario....................................61

Figure 4.3 State variables profile, T, for fault-free scenario....................................62

Figure 4.4 Estimated model parameters, UA, for fault-free scenario 62

Figure 4.5 Estimated model parameters, x_F, for fault-free scenario 62

Figure 4.6 Residual of estimated model parameters, UA, for fault-free scenario.....63

Figure 4.7 Residual of estimated model parameters, x_F, for fault-free scenario......63

Figure 4.8 State variables profile, W, for faulty scenario using ANN formulation ..64

Figure 4.9 State variables profile, T, for faulty scenario 65

Figure 4.10 Estimated model parameters, UA, for faulty scenario 65

Figure 4.11 Estimated model parameters, x_F, for faulty scenario 65

Figure 4.12 Residual of estimated model parameters, UA, for faulty scenario 66

Figure 4.13 Residual of estimated model parameters, x_F, for faulty scenario 66

Figure 4.14 Quadruple-tank process 68

Figure 4.15 State variables profile, H_p, for fault-free scenario 74

Figure 4.16 Estimated model parameters, a_p, for fault-free scenario........................74

Figure 4.17 Residual of estimated model parameters, a_p, for fault-free scenario 75

Figure 4.18 State variables profile, H_p, for faulty scenario 76

Figure 4.19 Estimated model parameters, a_p, for faulty scenario 77

Figure 4.20 Residual of estimated model parameters, a_p, for faulty scenario 77

Figure 4.21 Decomposition of the heat exchanger in two sections 81

Figure 4.22 Inlet measurements to the heat exchanger..87

Figure 4.23 Outputs measurements of the clean exchanger (a) T_{h2}, the hot fluid temperature in section 2 (b) T_{c2}, the cold fluid temperature in section 2 87

Figure 4.24 State variables profile of the clean exchanger (a) T_{h1}, the hot fluid.......88

Figure 4.25 Estimated model parameter value for the clean heat exchanger scenario 88

Figure 4.26 Estimated fouling factor, R_f, for the clean heat exchanger scenario 88

Figure 4.27 Outputs measurements of fouling exchanger (a) T_{h2}, the hot fluid temperature in section 2 (b) T_{c2}, the cold fluid temperature in section 2 90

Figure 4.28 State variables profile of fouling exchanger (a) T_{h1}, the hot fluid temperature in section 1 (b) T_{c1}, the cold fluid temperature in section 1 90

Figure 4.29 Estimated model parameter value for fouling heat exchanger scenario . 90

Figure 4.30 Estimated fouling factor, R_f, for fouling heat exchanger scenario 91

Figure 4.31 Batch fermentation diagram 92

Figure 4.32 State variables profile of concentration in fault-free scenario 97

Figure 4.33 Estimated model parameters for fault-free scenario (a) Maximum growth rate of the biomass, μ_m (b) Yield coefficient of product, Y_P 98

Figure 4.34 Residual evaluation of estimated model parameters for fault-free scenario (a) Maximum growth rate of the biomass, μ_m (b) Yield coefficient of product, Y_P 98

Figure 4.35 State variables profile of concentrations in faulty scenarios 100

Figure 4.36 Estimated model parameters for faulty scenarios (a) Maximum growth rate of the biomass, μ_m (b) Yield coefficient of product, Y_P 101

Figure 4.37 Residual evaluation of estimated model parameters for faulty scenarios (a) Maximum growth rate of the biomass, μ_m (b) Yield coefficient of product, Y_P 101

Figure 4.38 The sequencing batch reactor stages 104

Figure 4.39 State variables profile for fault-free scenario 112

Figure 4.40 Estimated model parameters for fault-free scenario (a) Concentration of substrate in the inflow, $S_{c_{in}}$, (b) Inhibition coefficient, K_i, and (c) Specific growth rate, μ_o 113

Figure 4.41 Residual of estimated model parameters for fault-free scenario (a) Concentration of substrate in the inflow, $S_{c_{in}}$, (b) Inhibition coefficient, K_i, and (c) Specific growth rate, μ_o 114

Figure 4.42 Estimated model parameter, $S_{c_{in}}$, for faulty scenario 1 116

Figure 4.43 Residual of the estimated model parameter, $S_{c_{in}}$, for faulty scenario 1 116

Figure 4.44 Estimated model parameter, K_i, for faulty scenario 2....................116

Figure 4.45 Residual of the estimated model parameter, K_i, for faulty scenario 2 117

Figure 4.46 Estimated model parameter, μ_o, for faulty scenario 3....................117

Figure 4.47 Residual of the estimated model parameter, μ_o, for faulty scenario 3 117

Figure 5.1 Estimated model parameter, θ_1, for different step sizes, Δt 124

Figure 5.2 Estimated model parameter, θ_2, for different step sizes, Δt 125

Figure 5.3 Estimated model parameter, θ_1, for different step sizes, Δt 130

Figure 5.4 Estimated model parameter, θ_2, for different step sizes, Δt 130

Figure 5.5 State variables profile for holdup, W 138

Figure 5.6 State variables profile for temperature, T 138

Figure 5.7 Estimated model parameter, UA, for different step sizes, Δt 139

Figure 5.8 Estimated model parameter, x_F, for different step sizes, Δt 139

LIST OF TABLES

Table 2.1 Parameter estimation in FD application 38

Table 3.1 Parameter estimation using the MPP algorithm 45

Table 4.1. Model parameters for the single-stage evaporator system 57

Table 4.2. Faulty scenario for a single-stage evaporator system 64

Table 4.3. Model parameters for the quadruple-tank system 68

Table 4.4. Faulty scenario for the quadruple-tank system 76

Table 4.5. Parameters of the heat exchanger model 86

Table 4.6. Model parameters for glutamic acid fermentation 93

Table 4.7 Faulty scenarios for glutamic acid fermentation 99

Table 4.8. Model parameters for wastewater treatment process reaction................105

Table 4.9. Faulty scenario for the wastewater treatment system 115

Table 5.1. Parameter estimation using MPP algorithm 120

Table 5.2. Comparison of the estimated model parameters, θ_1 for step size $\Delta t = 0.01$ 125

Table 5.3. Comparison of the estimated model parameters, θ_2 for step size $\Delta t = 0.01$ 126

Table 5.4. Comparison of the estimated model parameters, θ_1 for step size $\Delta t = 0.01$ 131

Table 5.5. Comparison of the estimated model parameters, θ_2 for step size $\Delta t = 0.01$ 131

Table 5.6. Comparison of the estimated model parameters, UA for step size $\Delta t = 0.05$ 140

Table 5.7. Comparison of the estimated model parameters, x_F for step size $\Delta t = 0.05$ 141

LIST OF ABBREVIATIONS

ANN	Artificial Neural Network
EKF	Extended Kalman Filter
FD	Fault Detection
GAMS	General Algebraic Modeling System
HVAC	Heating, Ventilation and Air Conditioning
iPDA	Iterated Principal Differential Analysis
KKT	Karush-Kuhn-Tucker
LS	Least Squares
LS-SVM	Least Squares Support Vector Machines
MPC	Model Predictive Control
MPP	Multiparametric Programming
NLP	Nonlinear Programing
NN	Neural Networks
ODE	Ordinary Differential Equations
PCA	Principal Component Analysis
PDA	Principal Differential Analysis
RK	Runge-Kutta
SVM	Support Vector Machine
WWT	Wastewater Treatment

LIST OF SYMBOLS

Roman Symbols

Symbol	Description	Unit
a_p	Cross-section of the outlet holes for tank p	cm^2
A	Area of heat transfer	m^2
A_c	Heat transfer area in cold fluid	m^2
A_h	Heat transfer area in hot fluid	m^2
A_p	Cross-section of tank p	cm^2
b	Endogenous respiration coefficient	h^{-1}
c_c	Specific heat in cold fluid	J/(kg K)
c_h	Specific heat in hot fluid	J/(kg K)
C_p	Heat capacity of the solution	kJ/(kg ˚C)
E_c	Constant	kg/min
f_a	Actuator fault	
f_c	Process fault	
f_s	Sensor fault	
f	Fault	
F	Feed flow rate	kg/min
g	Acceleration of gravity	cm / s^2
h_c	Convection heat transfer coefficients for the cold fluid	$W/(m^2\ K)$
h_h	Convection heat transfer coefficients for the hot fluid	$W/(m^2\ K)$
h_j	Discretisation of nonlinear algebraic equations for each j	

ΔH_V	Heat of vaporisation of the solvent	kJ/kg
H_p	Height of water levels in the tank p	cm
$\hat{H}_p$	Measurement values of H_p	cm
i	Time point	
j	State variable number of ODEs system	
k_{La}	Oxygen mass transfer coefficient	h^{-1}
k_1	Yield coefficient of the substrate to biomass	
k_2	Yield coefficient of oxygen to biomass	
K_i	Inhibition coefficient	g/l
K_s	Half saturation coefficient	g/l
L	Lagrange function	
m	Maintenance coefficient of the biomass	0.105 h^{-1}
$\dot{m}_c$	Mass flow rate of the cold fluid	kg s^{-1}
$\dot{m}_h$	Mass flow rate of the hot fluid	kg s−1
M_c	Mass of the cold fluid	kg
M_h	Mass of the hot fluid	kg
$n_1; n_2$	Rate constant parameter 1,2	
p	Number of tank	
P	Concentration of product	g/l
$\hat{P}$	Measurement values of P	g/l
q_{in}	Inlet flow rate	g/l
Q_L	Rate of heat loss to the surroundings	kJ/min
r	Residual	

$\mathbf{r}$	Vector of r	
R_f	Fouling resistance	m^2 K/W
S	Concentration of substrate	g/l
S_c	Concentrations of organic matter	g/l
$S_{c_{in}}$	Concentration of substrate in the inflow	g/l
S_o	Concentration of dissolved oxygen	g/l
$S_{o_{in}}$	Concentration of dissolved oxygen in the inflow	g/l
S_{o_s}	Dissolved oxygen mass at saturation	g/l
$\hat{S}$	Measurement values of S	g/l
$\hat{S}_c$	Measurement values of S_c	g/l
$\hat{S}_o$	Measurement values of S_o	g/l
t	Time	
Δt	Step size	
T	Temperature	˚C
T_B	Temperature for normal boiling point of the solvent	˚C
T_{ct}	Heat exchanger's temperature in cold fluid	˚C
T_{cin}	Inlet temperature in the cold fluid	˚C
T_F	Temperature of the feed system	˚C
T_{ht}	Heat exchanger's temperature in hot fluid	˚C
T_{hin}	Inlet temperature in the hot fluid	˚C
T_r	Threshold	
$\mathbf{T_r}$	Vector of T_r	
T_S	Steam temperature in the steam chest	˚C

$\hat{T}$	Measurement values of T	˚C
$\hat{T}_{c2}$	Measurement values of T_{c2}	˚C
$\hat{T}_{h2}$	Measurement values of T_{h2}	˚C
u	Control variable	
$\mathbf{u}$	Vector of u	
U_{heat}	Overall heat transfer coefficient	W/(m^2 K)
v_p	Input voltage to tank p	V
V	Volume	l
V_p	Vapour flow rate from the evaporator	
W	Holdup	kg
$\hat{W}$	Measurement values of W	kg
x_j	State variable	
x_F	Composition of feed	Mass fraction
x_m	Maximum biomass concentration	g/l
$\hat{\mathbf{x}}$	Vector measurements of x	
$\hat{x}_j$	Measurement values of x_j	
X	Concentration of biomass	g/l
$\hat{X}$	Measurement values of X	
y	Output	
Y_G	Yield coefficient of the biomass	0.436
Y_P	Yield coefficient of the product	0.645
z_j	State variables of j	
$\hat{z}_j$	Measurement values of z_j	

Greek Symbols

Symbol	Description	Unit
β	Boiling point	
δ	Constant	(kg/min) / kg holdup
ε_{FD}	Error of FD problem	
ε_{MPP}	Error of FD problem using MPP	
κ_1, κ_2	Constant	cm^3 / Vs
ι	Section number in the heat exchanger	
γ_1, γ_2	Constant	
λ_j	Lagrange multipliers for each j	
μ	Growth rate	h^{-1}
μ_o	Specific growth rate	h^{-1}
μ_m	Maximum growth rate	h^{-1}
θ	Estimated model parameter	
$\hat{\theta}$	'True' model parameters	
$\boldsymbol{\theta}$	Vector of θ	
$\hat{\boldsymbol{\theta}}$	Vector of $\hat{\theta}$	

CHAPTER 1 INTRODUCTION

1.1 Introduction

Safety and reliability play a vital role in process systems. Safety is defined as the ability of a system not to cause danger to a person, equipment or the environment, and reliability is the ability of a system to perform a required function under stated conditions within a given scope during a given period of time (Isermann and Ballé, 1997). A conventional feedback control system has the primary design goal to achieve system stability and performance with all components functioning normally. Most conventional control design techniques do not consider scenarios for potential system component faults. With recent developments in technology moving towards greater complexity and automation, if a malfunction occurs the conventional control may result in unsatisfactory performance or instability. Without proper action, even a minor error may lead to destructive consequences. These issues provide the motivation to develop an efficient and timely response to detect faults and accurately locate the faulty equipment so that corrective action can be taken before the faults turn into a catastrophic failure.

Faults can result in fatal damages and economic losses if they the properly. In general, the fault is something that changes the behaviour of a system such that the system no longer satisfies its purpose. It may be an internal event in the system which stops the power supply, breaks an information link or creates a leak in a pipe. It may be a wrong control action given by the human operator that brings the system out of the required operations point, or it may be an error in the design of the system which remains undetected until the system reaches a certain operation point where this error reduces the performance considerably. Fault in terminology for control systems can be defined as an unpermitted deviation of at least one characteristic of a variable from an acceptable behaviour (Isermann and Ballé, 1997). Meanwhile, failure is a permanent interruption of a system's ability to perform a required function under specified operating conditions, and malfunction is an intermittent irregularity in the fulfilment of a system's desired function (Isermann and Ballé, 1997). In any case, the fault is the primary cause of changes in the system's structure or parameters that eventually leads to degrading system performance or even loss of the system function. In large systems, every component has been designed to accomplish a certain function and the overall system works satisfactorily only if all the components provide the service for which they are designed. Therefore, a fault in a single component may change the performance of the overall system. In order to avoid production deterioration or damage to machines and humans, faults have to be identified as quickly as possible and decisions that stop the propagation of their effects have to be made. Hence, process monitoring and FD are becoming ingredients of modern automation control systems. These considerations provide a strong motivation for this work to research the development of FD in order to improve safety and reliability (Isermann, 1997).

This work focus solely on model-based FD method. This approach utilises a mathematical model of the process in order to detect a fault by utilising the concept of analytical redundancy. Analytical redundancy techniques are more cost-effective compared with hardware redundancy but more challenging due to environmental noise/disturbance and modelling errors. Analytical redundancy is achieved through a comparison between measured signals with its estimation from the mathematical model of the system. Hence, the basic idea in a model-based FD scheme is to compare the available system measurements with a priori information represented by the system's mathematical model through the generation of residual quantities. In the residual evaluation, an evaluated residual is compared with a threshold, and a fault existence decision is made if the residual exceeds the threshold (Frank, 1996, Isermann, 2005). The existing model-based FD techniques are based on an observer-based, a parity relation, a parameter estimation approach, or a combination of the three (Venkatasubramanian et al., 2003c, Hwang et al., 2010, Dai and Gao, 2013, Gao et al., 2015). The observer-based FD is a widely used technique in FD. The basic idea of the observer approach is to estimate the outputs of the system from the measurements by using some type of observer and then construct the residual by using an output estimation error (Mhaskar et al., 2006, Mhaskar et al., 2008, Du and Mhaskar, 2014). The parity relation approach uses the parity check on the consistency of the parity equation to generate residuals (parity vector). The inconsistency in the parity relations indicates the presence of faults (Chow and Willsky, 1984, Gertler, 1988, Gertler, 1997).

On the other hand, the parameter estimation approach is based on the assumption that the faults are reflected in the physical system parameters and only the model structure needs to be known (Isermann, 1993, Huang, 2001, Garatti and Bittanti, 2012). The parameter estimation approach is straightforward if the model parameters have an explicit mapping with physical coefficients. In this method, the parameters of the actual process are repeatedly estimated online, and the results are compared with the reference model. The most common method in parameter estimation is the least square (LS) method, which is more practical for the linear system. However, for the nonlinear system, the parameter estimation method requires the solving of an online optimisation problem to estimate the model parameters by minimising an error function given by the sum of the squares of the difference between the observed data and the model predictions (Englezos and Kalogerakis, 2001), as shown in Figure 1.1. The key limitation, these methods are computationally expensive to implement for the online FD method due to the repetitive solution of optimisation problems at regular time intervals (Dua, 2011, Dua and Dua, 2011). The solution of an online optimisation problem is also time-consuming; and, the solution may not converge in a reasonable amount of time. To overcome this problem, the parameter estimates for FD using MPP are presented.

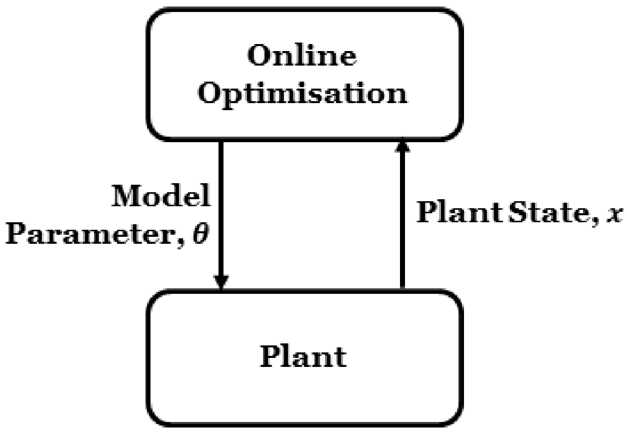

Figure 1.1 Parameter estimation using online optimisation approach

MPP is an optimisation method to obtain the performance criterion and optimisation variables as a function of a parameter which valid over a specific region in the parameter space (Pistikopoulos, 2009, Pistikopoulos et al., 2002). The main advantage of using the MPP method is that the online optimisation problem is solved using simple function evaluations to measure the related optimisation variables, as shown in Figure 1.2. Thus, multiparametric programming solved the computationally expensive and time-consuming issues due to the repetitively solving an optimisation problem.

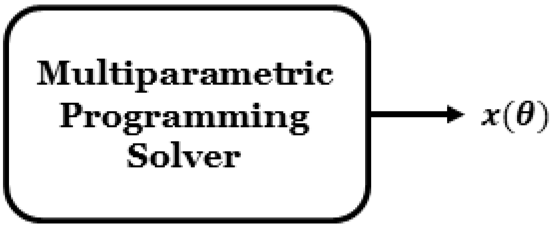

Figure 1.2 Multiparametric programming

1.2 Aim and Objectives

The main aim of the research is to develop a novel approach for FD using offline parameter estimation for process systems that can accurately estimate the online model parameters as fast as possible. Accuracy and speed are vital to avoid false-positive in identify faults and detect quickly enough to enable corrective actions to be taken promptly. Thus, the new algorithm for FD using MPP is proposed. There are two main reasons for using MPP method to detect the fault using the parameter estimation approach. First, MPP provides the optimisation variables as an explicit function of the parameter. Hence, in this work, model parameters are considered as optimisation variables and the measurements as the parameters as shown in Figure 1.3. Second, the computational burden of the online optimisation problem is solved where the model parameter is evaluated as a set of explicit functions of the measurements. This approach provides a significant advancement in the solution of the optimisation problem and online implementation of FD using parameter estimation problems.

The specific objectives of this research are as follows:

(i) to develop a parameter estimation algorithm for the model-based FD method using MPP

(ii) to demonstrate the applicability of the parameter estimation algorithm using MPP for model-based FD applications

(iii) to evaluate the influence of the discretisation of nonlinear ODEs in the MPP algorithm

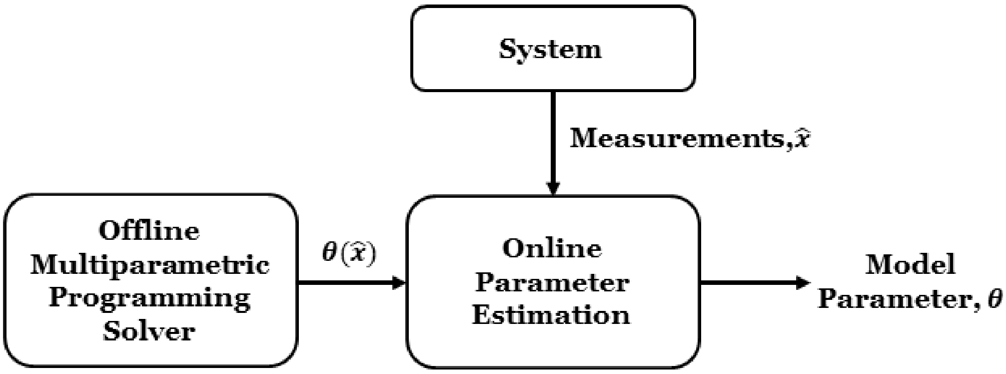

Figure 1.3 Fault detection using multiparametric programming

1.3 Thesis Organisation

The rest of the thesis is outlined as follows:

Chapter 2 gives an overview of the research work on FD, followed by a discussion on model-based FD techniques in the observer, parity relation and parameter estimation method.

Chapter 3 presents a detailed methodology of parameter estimation using MPP. This chapter will also verify the proposed method using two examples and demonstrate the effectiveness of the proposed approach.

Chapter 4 discusses the application of FD using MPP in process systems. Five cases are presented which are the single-stage evaporator, quadruple tank, heat exchanger, fermentation and wastewater treatment systems. In each case, the related parameter faults are discussed and obtained as a parametric function using MPP. A number of faulty and fault-free scenarios are considered to show the effectiveness of the parameter estimation using MPP.

Chapter 5 presents an influence of the discretisation method of ODEs to be work in parameter estimation using MPP. In this chapter, implicit Euler's method is presented and the applicability of this method is demonstrated in three examples. The results of the complexity of implicit parametric functions, the accuracy of parameter estimates and the effect of step size are discussed with comparison to explicit Euler's method.

Chapter 6 summarises the main findings of this research and proposes areas of future work.

CHAPTER 2 LITERATURE REVIEW

2.1 Fault Detection

FD is an active area of research which began in the early 1970s, with different approaches having been proposed since then. Early research into FD relies on limit checking of a directly measured variable. FD can be achieved by monitoring and checking the measured variable of a process if its absolute values or trends exceed certain thresholds. The process is in a normal situation if the monitored variable stays within a certain tolerance limit; if it exceeds the thresholds, this then indicates a fault in the process (Patton et al., 1995, Isermann, 2006). The significant advantage of the classical limit checking FD method is its simplicity and reliability. However, the situation becomes more complicated if the measured variable of a process changes rapidly. In the case of closed loops, changes in the process are covered by control actions and cannot be detected from the output signals, as long as the manipulated process inputs remain in the normal range. Therefore, feedback systems hinder the early detection of process faults. However, they are only able to react to a relatively significant change of a feature after either a large, sudden fault or a long-lasting gradually increasing fault. Unfortunately, the simple limit-checking method becomes invalid as the system complexity increases and in-depth fault diagnosis is usually not possible.

As such, there is a requirement for advanced methods of FD, methods which satisfy the following criteria: (i) the detection of small faults as early as possible; (ii) the accurate diagnosis of the location of faults, whether in the sensor, actuator or process plant; and (iii) the detection of faults in closed loops. The aim of having early FD is so that there is ample time for counteractions such as other operations, reconfiguration, planned maintenance or repair. Due to this, an advanced method for FD has been a subject of interest in control and process systems. FD methods are categorised as model-based and knowledge-based approaches. The model-based method requires the knowledge of a dynamic process model in the form of a mathematical structure (qualitative model-based) either derived from first principles or system identification method. In contrast to the model-based approach, the knowledge-based method performs the FD using a large amount of historical process data. The knowledge-based FD is also referred to as a data-based method where the mathematical model of the system is not available or cannot be derived. Usually, knowledge-based FD methods require significant quantities of data based on both healthy and faulty systems. Despite that, collecting data in the real industry is costly and impossible under certain conditions. An overview of the FD method is presented in these related papers (Venkatasubramanian et al., 2003a, Venkatasubramanian et al., 2003b, Venkatasubramanian et al., 2003c) and books (Chen and Patton, 1999, Isermann, 2006).

2.2 Model-Based Fault Detection Methods

Model-based FD methods require the knowledge of a dynamic process model in the form of a mathematical structure. A model-based FD algorithm can be implemented in software on the process control computer and no additional hardware is required. The significant advantage of the model-based approaches is that it is more cost-effective compared with the hardware redundancy in order to realise an FD algorithm. According to this advantage, model-based FD offers a powerful way of achieving the roles of detection faults by requires only additional storage capacity and possibly higher computer power are needed for the implementation.

The conceptual structure of model-based FD method (Patton et al., 1995) consists of two stages; residual generation and decision making based on these residuals, are shown in Figure 2.1. In a residual generation, the input and the output, with a controlled system subjected to actuator fault, f_a, process fault, f_c, and sensor fault, f_s, are processed by an appropriate algorithm to generate output estimates, parameter estimates and/or state estimates. Checking these estimates with respect to their expected nominal values, a residual, r, is generated and classified. A residual is a fault indicator or an accentuating signal which reflects the faulty situation of the monitored system.

The second step of an FD procedure is to evaluate the residuals. A decision process may consist of a simple threshold test or more sophisticated statistical decision tests, e.g., generalised likelihood ratio testing or sequential probability ratio testing. The residual should be zero-valued when the system is normal and should diverge from zero when a fault occurs in the system given by:

$$r(t) \neq 0 \ \ iff \ \ f(t) \neq 0 \tag{2.1}$$

where $r(t)$ is residual and $f(t)$ is fault. A fault can be detected by comparing the residual evaluation function, $J\left(r(t)\right)$, with threshold function, $T_r(t)$, according to the test given by:

$$J\left(r(t)\right) \leq T_r(t) \ \text{ for } \ f(t) = 0 \tag{2.2}$$

$$J\left(r(t)\right) > T_r(t) \ \text{ for } \ f(t) \neq 0 \tag{2.3}$$

If the threshold is exceeded by the residual evaluation function, a fault is likely to occur. There are many ways of defining $J\left(r(t)\right)$ and $T_r(t)$. For example, $J\left(r(t)\right)$ can be chosen as the residual norm vector and $T_r(t)$ as a positive constant. A classification of the existing residual generation and residual evaluation techniques is given in Zhang and Jiang (2008).

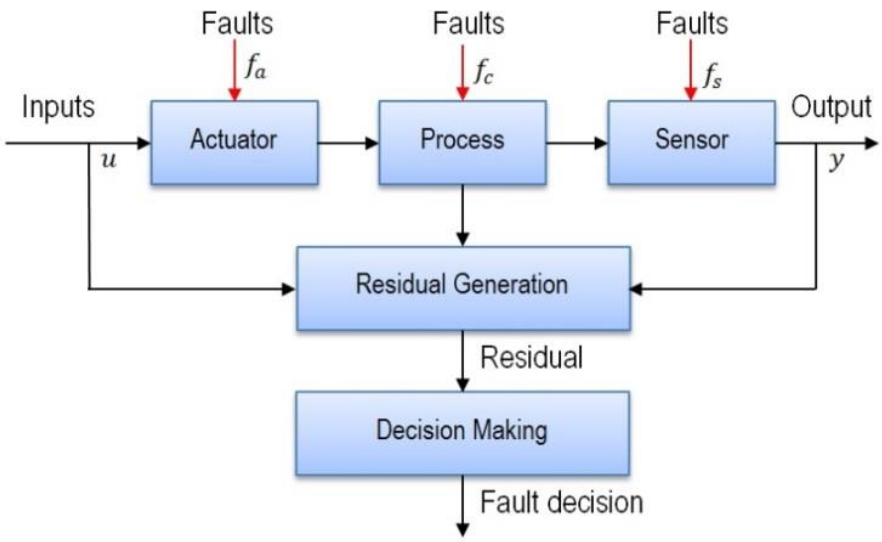

Figure 2.1 Two-stage structure of FD processes (Patton et al., 1995)

In a model-based FD method, as mentioned previously, the mathematical model is utilised to quantify the expected behaviours of the systems. For the nonlinear ODEs system, the mathematical model of the system is given by:

$$\frac{dx_j(t)}{dt} = f_j\left(\mathbf{x}(t), \mathbf{u}(t), \boldsymbol{\theta}, t\right), \quad j \in J \tag{2.4}$$

where $\mathbf{x}(t)$ and $\mathbf{u}(t)$ are *J*-dimensional vectors of state and control variables for the given ODE system and $\boldsymbol{\theta}$ is the vector of model parameters. In these techniques, a fault can be interpreted as a change in state estimation, model parameters or outputs which results in deviations from the normal state (Patton et al., 2000). In order to be useful in practical applications, the residual should be insensitive to noise, disturbances and model uncertainties while maximally sensitive to faults. A good model-based FD ideally has residuals sensitive only to system faults but not to disturbances or uncertainty. The model-based FD techniques can be categorised as observer/filter (Frank and Ding, 1997), parity relation (Chow and Willsky, 1984, Gertler, 1988) and parameter estimation-based approaches (Isermann, 1984).

2.2.1 Observer/Filter-Based Approaches

Observer-based approaches for FD have been well studied and quite a large number of papers exist in the literature. The basic idea for observer-based approaches is to estimate the outputs of the system from the measurements by using either a Luenberger observer in a deterministic setting or by using a Kalman filter in the stochastic setting (Patton and Chen, 1997). This observer provides an estimation of measurements called a residual. The residual is then examined for the likelihood of faults by using a fixed or adaptive threshold. Certain decision rules can then be applied to determine if a fault has occurred. A decision process may be based on a simple threshold test or more sophisticated statistical decision tests. A detailed study of this method can be found in Frank (1996) and Chen and Patton (1999). However, modelling errors and disturbances are inevitable when dealing with nonlinear, uncertain and complex engineering systems. Therefore, robustness issue becomes a crucial aspect in the FD system, which the design should be highly sensitive to faults and insensitive to uncertainty and disturbances (Chen et al., 1996, Patton and Chen, 1997, Chen and Patton, 1999, Patton and Chen, 2000). One way to overcome this problem is to use the unknown input observer (UIO) (Patton and Chen, 1997), which works by decoupling the disturbances and faults into two different input channels. The UIOs are designed such that they are insensitive to certain faults while being sensitive to other faults in the system (Zhang et al., 2010, Du and Mhaskar, 2014). The key limitation in the approaches above is that the proposed FD systems are limited to sensor and actuator faults. Several researchers have developed observers for FD for different classes of nonlinear systems. A review of the principal observer-based approaches for nonlinear systems can be found in Alcorta García and Frank (1997). The approach of the UIO (Fonod et al., 2014) and sliding mode observers (Xing-Gang and Edwards, 2005) were extended to a class of nonlinear systems. An application of actuator and sensor fault in nonlinear process systems can also be found (Zarei and Shokri, 2014, Du and Mhaskar, 2013).

2.2.2 Parity Relation-Based Approaches

Another well-known model-based FD method is the parity relation approach, which was developed in the early 1980s (Chow and Willsky, 1984, Gertler, 1988). Chow and Willsky (1984) first proposed parity equations for a state-space model of the system. A detailed study for this method can be found in Gertler (1997) and Patton and Chen (1991). The parity relation approach is based on the test ('parity check') of the consistency of parity equations with properly modified system equations, by using the measured signals of the actual process. The parity relation approach generates the residual based on consistency checking of the system input and output data over a time window. The modification of the system equations aims at the decoupling of the residuals from the system states and faults to enhance their diagnosability. From the inconsistency (residual) of the parity equations, one can detect the faults but this method required; however storage space and computational load (Gertler, 1997).The parity relation method is similar to the observer-based approach. Two theorems are presented in Ding (2008) that show how to calculate the parity vector corresponding to the observer-based residual generator and vice versa.

A residual generator in parity space can be designed and it transforms the parity vector into diagnostic observer parameters for online implementation. The parity relation approach can be applied to either time-domain state-space model or frequency-domain input-output model, which is well explained in the related literature (Chen and Patton, 1999, Ding, 2008). Recently, the parity relation method has been extended to FD for more complex models such as Takagi–Sugeno fuzzy nonlinear systems and fuzzy tree models (Nguang et al., 2007), and applied to various industrial systems such as aircraft control surface actuators (Odendaal and Jones, 2014) and electromechanical brake systems (Hwang and Huh, 2014).

2.2.3 Parameter Estimation-Based Approaches

The research in the area of parameter estimation has received much attention in recent years due to the development of process optimisation and control technologies. The principle involved in parameter estimation FD is that the specific parameters of the model can be associated with faults. Table 2.1 list the application in process systems related to parameter fault FD. For example, the heat transfer coefficient in the heat exchanger model can be related to fouling (Delmotte et al., 2013), cross-section of outlet holes related to the tank leakage (Johansson, 2000) and specific growth rate, and half-saturation coefficient and inhibition coefficient can be related to the growth behaviour of the biomass on wastewater treatment (Wimberger and Verde, 2008). With this assumption, parameters of a system are estimated online repeatedly using well-known parameter estimation methods. If there is a discrepancy between the estimated parameters and the actual parameters, it indicates faults.

The most common method in parameter estimation is the LS method which involves minimisation of the sum of squared differences between the measurements and the model predictions (Marquardt, 1963, Huang, 2001, Escobet and Travé-Massuyès, 2001). The main advantage of this method is computational simplicity and it is part of statistical software. LS method requires the availability of accurate dynamic models of the process because of its weakness to the robustness due to external disturbances that may affect the system behaviour. The accurate estimation is usually time-consuming and computationally very intensive for large processes. In

Table 2.1 Parameter estimation in FD application

Batch reactor	Hsoumi et al. (2009); Benkouider et al. (2009); Acosta Díaz et al. (2016)
Aircraft flight control	Cimpoesu et al. (2013)
Electric motor	Filbert et al. (1991); Karami et al. (2010); Treetrong et al. (2012); Progovac et al. (2014);
Tank system	Lakhmani et al. (2016); Ganesh et al. (2015)
Heat exchanger	Jonsson et al. (2007); Delrot et al. (2012); Sivathanu and Subramanian (2018)
Fermentation	Zhao et al. (1999); Kabbaj et al. (2001); Çinar et al. (2002); Monroy et al. (2012)

the LS method, the estimation process is only suitable for the linear systems; however, for nonlinear system parameter estimation, the performance of this method cannot be assured.

Several parameter estimation techniques have been presented for nonlinear systems and can be categorised as decomposition and sequential/simultaneous approaches. These approaches were aiming to estimate the unknown parameters by minimising an error function within a given set of equations. In the decomposition method, the direct integration of the ODEs model is not required and the parameter estimation is solved in two steps method involves fitted the experimental data and solved the optimisation problem. This method was introduced by Varah (1982), where measurement data was fitted with spline function; then, the parameters were estimated by finding the solution of LS equation of the spline function and the ODE. Principal differential analysis (PDA) was extended to parameter estimation nonlinear ODEs in Ramsay (1996), where fitted measurements using splines function is differentiated with respect to time to obtain estimate time-derivative curves. This information is substituted into the ODEs; thus, converting the parameter estimation problem into a simple algebraic optimisation problem that can be solved using the LS method. This PDA method is different from the commonly used LS method for dynamic models wherein the parameter values are selected to minimise in the form of differential models and not in integrated models in the PDA method.

However, poor spline fits can result in misleading time-derivative information, which can lead to poor parameter estimates. The integrated PDA (iPDA) had been extended with the introduction of generalized smoothing approach to overcome the issues of precision (Poyton et al., 2006, Varziri et al., 2008). An artificial neural network (ANN) has been proposed in Dua (2011) for the decomposition method. In this method, an ANN model fitted the data and utilised the differential derivatives of ANN approximation to estimate the parameters of nonlinear ODE systems. Although the ANN has good properties such as universal approximation, the solution may become the existence of many local minima solutions. A method using LS-support vector machines (LS-SVM) (Mehrkanoon et al., 2014) and two-stage method (Chang et al., 2015, Chang et al., 2016) are other proposed methods for parameter estimation involving fitting the data and solving the optimisation problem.

Another approach for parameter estimation is involving the solution of the ODEs model in estimating parameters. This method can be performed in two ways. The first way is to solve the numerical solution of the ODEs model separately from the optimisation problem, called sequential approach (Hwang and Seinfeld, 1972, Kim et al., 1991, Bilardello et al., 1993). In the simultaneous approach, the optimisation problem of parameter estimation is solved together with the differential equations model, which is converted into algebraic equations (De et al., 2013, Chen et al., 2016b). Both approaches explicitly require integral of the ODE model to estimate the parameters. Dua and Dua (2011) proposed an ANN implementation for simultaneous parameter estimation wherein this method, the optimisation problem and numerical solution of ODEs are performed simultaneously using the ANN algorithm. This method works very well for the accuracy and computational time; however, the ANN method suffers in choosing the number of hidden units in the ANN model. A collocation approach is also studied for parameter estimation in Villadsen (1982), Tjoa and Biegler (1991) and Chen et al. (2016b). In this method, the optimisation is carried in the full space of discretised ODEs using orthogonal collocation on finite elements where differential equations are satisfied at the converged solution of the NLP only. The solution of the model and the optimisation is carried out simultaneously. The collocation methods are also proposed to improve in the convergence rate and the accuracy (Liu et al., 2019).

The key limitation in the approaches of optimisation parameter estimation in above-mentioned is that they are computationally expensive due to the repetitive solution of the ODEs. Sometime, the solution may not converge in a reasonable amount of time and the optimisation can be difficult due to the presence of nonconvexities (Vassiliadis, 1994, Papamichail and Adjiman, 2002, Sakizlis et al., 2003, Papamichail and Adjiman, 2004).

2.3 Summary

In this chapter, a literature review of FD was presented. An overview of FD was given, followed by a discussion on model-based FD techniques. Based on the above review on parameter estimation-based approaches in Section 2.2.3, it is clear that there is still significant scope for improving the model-based FD method for nonlinear process systems using parameter estimation. The development of the parameter estimation method plays a significant in optimisation research; however, very little thought had been given to the application parameter estimation towards the FD system. Hence, we propose the parameter estimation method for model-based FD for nonlinear ODEs using MPP where this provides the optimisation variables as an explicit function of the parameter (Oberdieck et al., 2016, Charitopoulos and Dua, 2016). The detailed formulation for model-based FD using MPP is discussed in the next chapter.

CHAPTER 3 FAULT DETECTION USING MULTIPARAMETRIC PROGRAMMING

3.1 Introduction

FD using parameter estimation techniques relies on the principle that possible faults in the monitored system can be associated with specific parameters and the mathematical model of the system represented by nonlinear ODEs. Parameter estimation method for FD can be successful if: (a) the mathematical model of the process system is accurate; (b) the experimental data is available; (c) and the model parameters are related to physical system parameters of the equipment or process fluids (Isermann, 2005).

3.2 General Formulation for Fault Detection using Parameter Estimation

This work focuses on developing the method for fault detection by estimating and evaluating the parameter faults for processes systems. In this work, the mathematical model of the system is represented by nonlinear ODEs. The objective of the FD problem is to estimate the model parameters, $\boldsymbol{\theta}$, such that the error, ε_{FD}, between the measurements, $\hat{x}_j(t_i)$, and model predicted values of state variables, $x_j(t_i)$, is minimised as follows (Dua and Dua, 2011):

Problem 3.1

$$\varepsilon_{FD} = \min_{\boldsymbol{\theta}, \mathbf{x}(t)} \sum_{j \in J} \sum_{i \in I} \left\{ \hat{x}_j(t_i) - x_j(t_i) \right\}^2 \tag{3.1}$$

Subject to:

$$\frac{dx_j(t)}{dt} = f_j\left(\mathbf{x}(t), \mathbf{u}(t), \boldsymbol{\theta}, t\right), \; j \in J \tag{3.2}$$

$$x_j(t=0) = x_j^0, \; j \in J \tag{3.3}$$

$$t \in [0, t_f] \tag{3.4}$$

where $x(t)$ is the *J*-dimensional vector of state variables in the given ODEs system, $\hat{x}_j(t_i)$ represents the measurements of the state variables at the time points t_i, $\mathbf{u}(t)$ is the vector of control variables and $\boldsymbol{\theta}$ is the vector of model parameters. The initial condition is given in Equation (3.3).

3.2.1 Discretisation of Ordinary Differential Equation

In this work, the nonlinear ODEs model is converted into algebraic equations using Euler's method, as described next. The ODEs initial value problem in equations (3.2) to (3.3) is to be solved on the time interval, $t \in [0, t_f]$. The Euler method provides:

$$x_j(i+1) = x_j(i) + \Delta t f_j\left(\mathbf{x}(i), \mathbf{u}(i), \boldsymbol{\theta}\right), i \in I,\ j \in J \tag{3.5}$$

where the step size is given by Δt. Equation (3.5) represents the prediction of x_j at time step $i+1$ where $x_j(i)$ is a state variables values at time step i and $f_j\left(\mathbf{x}(i), \mathbf{u}(i), \boldsymbol{\theta}\right)$ is a vector of functions evaluated at step i.

3.2.2 Fault Detection Problem

In this work, Equation (3.5) is substituting in Problem 3.1 and the FD problem is given by the following Nonlinear Programing (NLP) problem:

Problem 3.2

$$\varepsilon_{MPP} = \min_{\boldsymbol{\theta}, \mathbf{x}(i)} \sum_{j \in J} \sum_{i \in I} \left\{ \hat{x}_j(i+1) - x_j(i+1) \right\}^2 \tag{3.6}$$

Subject to:

$$h_j = x_j(i+1) - x_j(i) - \Delta t f_j\left(\mathbf{x}(i), \mathbf{u}(i), \boldsymbol{\theta}\right) = 0, i \in I, j \in J \tag{3.7}$$

$$x_j(0) = x_j^0 \, , \, j \in J \tag{3.8}$$

where h_j represents the set of nonlinear algebraic equations obtained by discretising the ODEs given by Equation (3.5). In this work, we consider $I = \{0,1\}$ represents the ODE is discretised for one-time interval by using Euler's method.

3.3 Parameter Estimation using Multiparametric Programming

In the following paragraphs, we present an MPP approach for solving online optimisation of parameter estimation in Problem 3.2. The MPP provides the optimisation variables as an explicit function of the parameter which avoids the repetitive solution (Dua and Pistikopoulos, 1999, Pistikopoulos et al., 2007b, Pistikopoulos et al., 2007a). In this work, the model parameters, $\boldsymbol{\theta}$, are considered as optimisation variables and the measurements, $\hat{x}_j(i+1)$, as the parameters in the context of MPP.

To obtain the model parameter as explicit function of measurements, the first-order Karush-Kuhn-Tucker (KKT) conditions for Problem 3.2 are first obtained as follows.

The Lagrangian function, L is given by:

$$L = G + \sum_{j \in J} \lambda_j h_j \tag{3.9}$$

Where

$$G = \sum_{j \in J} \sum_{i \in I} \left\{ \hat{x}_j(i+1) - x_j(i+1) \right\}^2 \tag{3.10}$$

$$h_j = x_j(i+1) - x_j(i) - \Delta t f_j \left(\mathbf{x}(i), \mathbf{u}(i), \boldsymbol{\theta} \right) = 0 \, , i \in I \, , \, j \in J \tag{3.11}$$

and λ_j represents the Lagrange multipliers. The KKT conditions are given by the equality constraints as follows:

$$\nabla_{\boldsymbol{\theta}} L = \nabla_{\boldsymbol{\theta}} G + \nabla_{\boldsymbol{\theta}} \sum \lambda_j h_j = 0 \,,\; j \in J \tag{3.12}$$

$$h_j = 0 \tag{3.13}$$

The gradient of the Lagrangian function with respect to $\boldsymbol{\theta}$ and the equality conditions are zero. The KKT conditions are solved analytically using symbolic manipulation software (Dua, 2015) to obtain Lagrange multipliers, λ_j, and model parameters, $\boldsymbol{\theta}$, as an explicit function of measurements, $\hat{\mathbf{x}}$; i.e., $\boldsymbol{\theta}(\hat{\mathbf{x}})$ that satisfy Equations (3.12) and (3.13). The explicit solutions are then screening for validation and ignored solutions with imaginary parts. Note that Equations (3.12) and (3.13) represent a square system of multiparametric nonlinear algebraic equations that can be solved analytically with respect to the optimisation variables. The key principle of the proposed methodology is that it successfully solved the optimisation problem off-line and allows computation of parameter estimates, $\boldsymbol{\theta}$, by simple function evaluation of $\boldsymbol{\theta}(\hat{\mathbf{x}})$. The algorithm for model-based parameter estimation for FD using MPP is summarised in Table 3.1, and FD analysis based upon the model parameter estimates is described in the next section.

3.4 Fault Detection Analysis

FD is carried out by monitoring the residual of model parameters. In order to define the residual generator for the aforementioned analysis, the residual, $\mathbf{r}$, which is a scalar- or a vector-valued signal containing information on the time and location of the occurrence of the fault, is designed. The residual for the FD method is defined as:

$$\mathbf{r} = \left|\boldsymbol{\theta} - \hat{\boldsymbol{\theta}}\right| \tag{3.14}$$

The estimated model parameters, $\boldsymbol{\theta}$, should be close to ‘true’ model parameters, $\hat{\boldsymbol{\theta}}$, when no fault is present. An abnormal condition can be detected by comparing the residual with a decision or threshold functions, $\mathbf{T_r}$. Any substantial discrepancy indicates changes in the process and may be interpreted as a fault. A fault is then declared if the residual, $\mathbf{r}$, surpasses a certain threshold, $\mathbf{T_r}$, as follows:

$$\mathbf{r} < \mathbf{T_r} \Rightarrow \text{ no fault has occurred} \tag{3.15}$$

$$\mathbf{r} \geq \mathbf{T_r} \Rightarrow \text{ a fault has occurred} \tag{3.16}$$

Table 3.1 Parameter estimation using the MPP algorithm

Step 1.	Discretise nonlinear ODEs model in Equation (3.2) to algebraic equations as given in Equation (3.5)
Step 2.	Formulate FD optimisation problem as a NLP problem as given in equations (3.6) to (3.8)
Step 3.	Formulate KKT conditions for equations (3.6) to (3.8) as given in equations (3.9) to (3.13)
Step 4.	Solve the equality constraints in equations (3.12) and (3.13) of the KKT conditions parametrically to obtain Lagrange multipliers and model parameters, $\boldsymbol{\theta}(\hat{\mathbf{x}})$, as a function of measurements, $\hat{\mathbf{x}}$
Step 5.	Screen the solutions obtained in the previous step and ignore solutions with imaginary parts
Step 6.	Calculate the estimated model parameters, $\boldsymbol{\theta}$, using the measurement, $\hat{\mathbf{x}}$, by a simple evaluation of $\boldsymbol{\theta}(\hat{\mathbf{x}})$

3.5 Illustrated examples of the proposed method

This section conducted a preliminary test to verify the effectiveness of the proposed method using two examples for a square system of nonlinear ODEs model where the number of state variables equals to the number of estimated model parameters.

3.5.1 Example 1: First-order irreversible chain reactions

Consider the following first-order irreversible chain reactions (Tjoa and Biegler, 1991, Esposito and Floudas, 2000, Dua, 2011, Dua and Dua, 2011):

$$A \xrightarrow{n_1} B \xrightarrow{n_2} C \tag{3.17}$$

where reactant A to reactant B and then to reactant C is described as the nonlinear ODEs model given by:

$$\frac{dz_1}{dt} = -\theta_1 z_1 \tag{3.18}$$

$$\frac{dz_2}{dt} = \theta_1 z_1 - \theta_2 z_2 \tag{3.19}$$

In this model, there are two state variables of concentration A and B, z_1 and z_2, and two estimated model parameters, θ_1 and θ_2 denote the reaction rate constants of n_1 and n_2. The reaction rate constants are vital in the chemical reaction where it expresses how fast reactants turn into the product. Hence, the objective of the FD problem for Example 1 is to estimate θ_1 and θ_2, such that the error, ε_{FD}, between $\hat{z}_j(t_i)$ and $z_j(t_i)$ is minimised as described in Problem 3.3. The initial values of state variables are given in equations (3.21) and (3.22).

Problem 3.3

$$\varepsilon_{FD} = \min_{\theta_1,\theta_2} \sum_{i \in I} \{(\hat{z}_1(t_i) - z_1(t_i))^2 + (\hat{z}_2(t_i) - z_2(t_i))^2\} \tag{3.20}$$

Subject to :

Equations (3.18) and (3.19)

$$z_1(0) = 1.0 \tag{3.21}$$

$$z_2(0) = 0 \tag{3.22}$$

$$t \in [0,1] \tag{3.23}$$

(a) Discretisation of Ordinary Differential Equations

The nonlinear ODEs model in equations (3.18) and (3.19) is discretised using Euler's method and reformulated as the following algebraic equations:

$$z_1(i+1) = z_1(i) - \Delta t\theta_1 z_1(i) \tag{3.24}$$

$$z_2(i+1) = z_2(i) + \Delta t\theta_1 z_1(i) - \Delta t\theta_2 z_2(i) \tag{3.25}$$

(b) Parameter Estimation Problem

Then, the Equations (3.24) and (3.25) are substituted in Problem 3.3 and parameter estimation problem is reformulated as the following NLP problem:

Problem 3.4

$$\varepsilon_{MPP} = \min_{\theta_1,\theta_2} \sum_{i\in I} \{(\hat{z}_1(i+1) - z_1(i+1))^2 + (\hat{z}_2(i+1) - z_2(i+1))^2\} \tag{3.26}$$

Subject to:

$$h_1 = z_1(i+1) - z_1(i) + \Delta t\theta_1 z_1(i) = 0 \tag{3.27}$$

$$h_2 = z_2(i+1) - z_2(i) - \Delta t\theta_1 z_1(i) + \Delta t\theta_2 z_2(i) = 0 \tag{3.28}$$

Equations (3.21) to (3.23)

Equations (3.27) and (3.28) represent the set of nonlinear algebraic equations and these equations are substituted into Equation (3.26) to obtain:

$$G = (\hat{z}_1(i+1) - z_1(i) + \Delta t\theta_1 z_1(i))^2 + ((\hat{z}_2(i+1) - z_2(i) - \Delta t\theta_1 z_1(i) + \Delta t\theta_2 z_2(i))^2 \tag{3.29}$$

The gradients of G with respect to θ_1 and θ_2 equals to zero are given by

$$\frac{\partial G}{\partial \theta_1} = 2\Delta t z_1(i)(-z_1(i) + \Delta t \theta_1 z_1(i) + \hat{z}_1(i+1)) - 2\Delta t z_1(i)(-\Delta t \theta_1 z_1(i) - z_2(i) + \Delta t \theta_2 z_2(i) + \hat{z}_2(i+1)) = 0 \tag{3.30}$$

$$\frac{\partial G}{\partial \theta_2} = 2\,\Delta t\, z_2(i)\,(-\Delta t\,\theta_1\, z_1(i) - z_2(i) + \Delta t\,\theta_2\, z_2(i) + \hat{z}_2(i+1)) = 0 \tag{3.31}$$

The equality constraints of KKT conditions given in Equations (3.30) and (3.31) denote the square system of multiparametric nonlinear algebraic equations. These equations solved analytically to obtain model parameters, $\boldsymbol{\theta}\left(\hat{z}_j\right)$ in Mathematica. The symbolic solution for reaction rate constants of n_1 and n_2 in Example 1 is given as follows:

$$\theta_1 = -\frac{-z_1(i) + \hat{z}_1(i+1)}{\Delta t\, z_1(i)} \tag{3.32}$$

$$\theta_2 = -\frac{-z_1(i) + \hat{z}_1(i+1) - z_2(i) + \hat{z}_2(i+1)}{\Delta t\, z_2(i)} \tag{3.33}$$

Using the MPP method, the reaction rate constants of n_1 and n_2 can be estimated using the explicit function of measurements in concentrations A and B, $\hat{z}_1(i+1)$ and $\hat{z}_2(i+1)$ at any time point, i.

(c) Results for Example 1

The simulated data for z_1 and z_2, is generated at $t = t_i$ with initial values given in equations (3.21) and (3.22), as is shown in Figure 3.1. The estimated model parameters, θ_1 and θ_2, are calculated using explicit functions as given in equations (3.32) and (3.33), respectively. Three different step sizes, $\Delta t = [0.10, 0.05, 0.01]$, are used to estimate model parameters and the comparison of the estimated model parameters is shown in figures 3.2 and 3.3 for θ_1 and θ_2, respectively. From these figures, for the smallest step size, $\Delta t = 0.01$, the estimated model parameters, θ_1 and θ_2, are close to the actual values of the 'true' model parameters, $\hat{\theta}_1 = 5$ and $\hat{\theta}_2 = 1$.

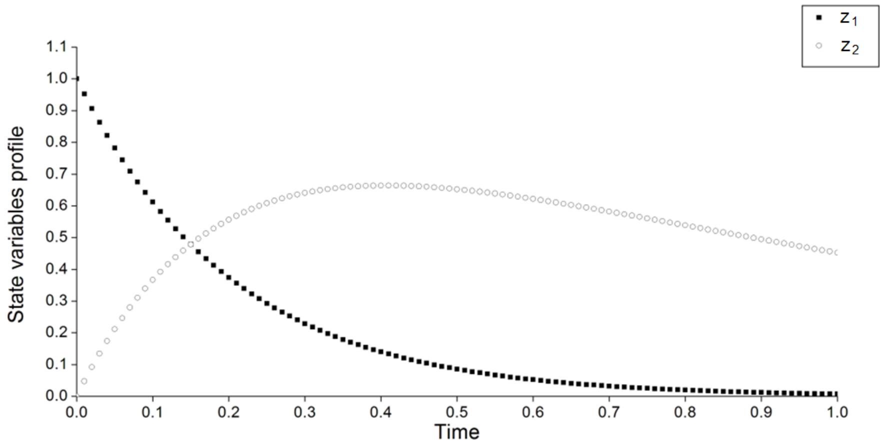

Figure 3.1 State variables profile for z_1 and z_2

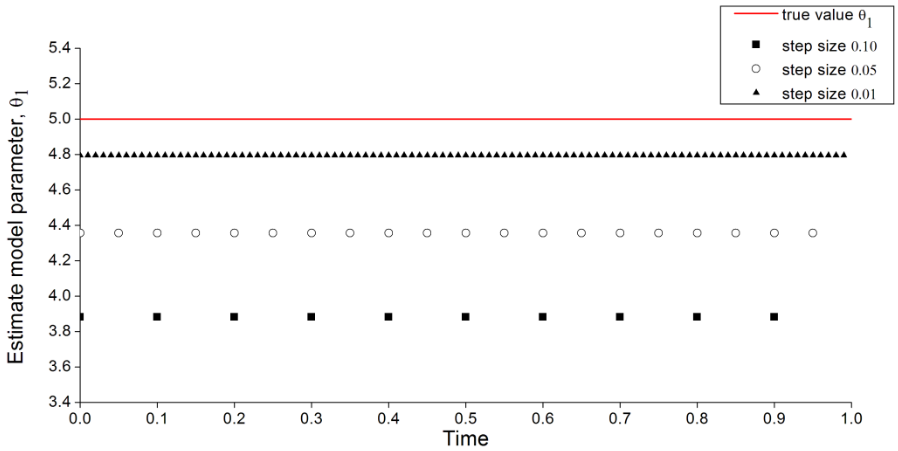

Figure 3.2 Estimated model parameter, θ_1, for different step sizes, Δt

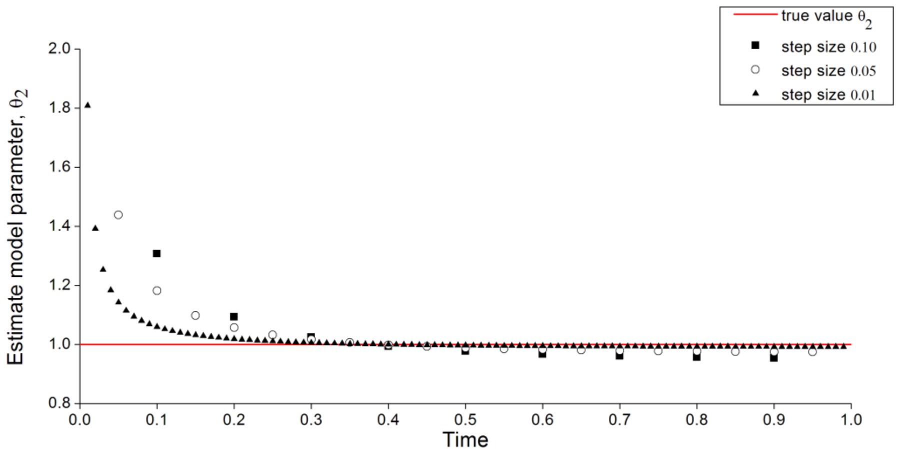

Figure 3.3 Estimated model parameter, θ_2, for different step sizes, Δt

3.5.2 Example 2: Lotka–Volterra model

Example 2 presents the Lotka-Volterra model, which describes an ecological of predator-prey. Consider the following Lotka–Volterra model (Esposito and Floudas, 2000, Dua, 2011, Dua and Dua, 2011), the growth rates of the two populations are described by nonlinear ODEs model:

$$\frac{dz_1}{dt} = \theta_1 z_1 (1 - z_2) \tag{3.34}$$

$$\frac{dz_2}{dt} = \theta_2 z_2 (z_1 - 1) \tag{3.35}$$

where z_1 and z_2 are state variables of prey and predator. The model parameters, θ_1 and θ_2 , represents parameters describing the ecological interaction system. The objective of FD in Example 2 is to estimate the model parameters, θ_1 and θ_2, such that the error, ε_{FD}, between the measurements, $\hat{z}_j(t_i)$, and model predicted values, $z_j(t_i)$, is minimised as described in Problem 3.5. The initial values of state variables are given in equations (3.37) and (3.38).

Problem 3.5

$$\varepsilon_{FD} = \min_{\theta_1,\theta_2} \sum_{i \in I} \{(\hat{z}_1(t_i) - z_1(t_i))^2 + (\hat{z}_2(t_i) - z_2(t_i))^2\} \tag{3.36}$$

Subject to :

Equations (3.34) and (3.35)

$$z_1(0) = 1.2 \tag{3.37}$$

$$z_2(0) = 1.1 \tag{3.38}$$

$$t \in [0,10] \tag{3.39}$$

(a) Discretisation of Ordinary Differential Equations

The nonlinear ODEs model in equations (3.34) and (3.35) is discretised using Euler's method and reformulated as the following algebraic equations:

$$z_1(i+1) = z_1(i) + \Delta t\theta_1 z_1(i) - \Delta t\theta_1 z_1(i)z_2(i) \tag{3.40}$$

$$z_2(i+1) = z_2(i) - \Delta t\theta_2 z_2(i) + \Delta t\theta_2 z_1(i)z_2(i) \tag{3.41}$$

(b) Parameter Estimation Problem

Equations (3.40) and (3.41) are substituted in Problem 3.5 and parameter estimation problem is reformulated as the following NLP problem:

Problem 3.6

$$\varepsilon_{MPP} = \min_{\theta_1,\theta_2} \sum_{i\in I} \{(\hat{z}_1(i+1) - z_1(i+1))^2 + (\hat{z}_2(i+1) - z_2(i+1))^2\} \tag{3.42}$$

Subject to:

$$h_1 = z_1(i+1) - z_1(i) - \Delta t\theta_1 z_1(i) + \Delta t\theta_1 z_1(i)z_2(i) = 0 \tag{3.43}$$

$$h_2 = z_2(i+1) - z_2(i) + \Delta t\theta_2 z_2(i) - \Delta t\theta_2 z_1(i)z_2(i) = 0 \tag{3.44}$$

Equations (3.37) – (3.39)

Equations (3.43) and (3.44) represent the set of nonlinear algebraic equations and these equations are substituted into Equation (3.42) to obtain:

$$\begin{aligned} G = {} & (\hat{z}_1(i+1) - z_1(i) - \Delta t\theta_1 z_1(i) + \Delta t\theta_1 z_1(i)z_2(i))^2 + (\hat{z}_2(i+1) - z_2(i) + \\ & \Delta t\theta_2 z_2(i) - \Delta t\theta_2 z_1(i)z_2(i))^2 \end{aligned} \tag{3.45}$$

The gradients of G with respect to θ_1 and θ_2 equal to zero are given by:

$$\frac{\partial G}{\partial \theta_1} = 2(-\Delta t z_1(i) + \Delta t z_1(i) z_2(i))(-z_1(i) - \Delta t \theta_1 z_1(i) + \hat{z}_1(i+1) + \Delta t\ \theta_1 z_1(i) z_2(i)) \tag{3.46}$$
$$= 0$$

$$\frac{\partial G}{\theta_2} = 2(\Delta t z_2(i) - \Delta t z_1(i) z_2(i))(-z_2(i) + \Delta t \theta_2 z_2(i) - \Delta t \theta_2 z_1(i) z_2(i) + \hat{z}_2(i+1)) \tag{3.47}$$
$$= 0$$

The KKT conditions are given by the equality constraints in equations (3.46) and (3.47) are solved analytically in Mathematica. The solution of model parameters, θ_1 and θ_2, is given by

$$\theta_1 = \frac{z_1(i) - \hat{z}_1(i+1)}{\Delta t\ z_1(i)(-1 + z_2(i))} \tag{3.48}$$

$$\theta_2 = \frac{-z_2(i) + \hat{z}_2(i+1)}{\Delta t(-1 + z_1(i)) z_2(i)} \tag{3.49}$$

The model parameters, θ_1 and θ_2, given in equations (3.48) and (3.49) are obtained as an explicit function of measurements, $\hat{z}_1(i+1)$ and $\hat{z}_2(i+1)$.

(c) Results for Example 2

The simulated data for state variables profile, z_1 and z_2, is generated at $t = t_i$ with initial values given in equations (3.37) and (3.38), as is shown in Figure 3.4. The model parameters, θ_1 and θ_2, are estimated using the explicit functions as given in equations (3.48) and (3.49). Three different step sizes are used to estimate model parameters, $\Delta t = [0.10, 0.05, 0.01]$, and the results are shown in figures 3.5 and 3.6. As the step size decreased, the estimated model parameters for θ_1 and θ_2 are close to the true values of the model parameters, $\hat{\theta}_1 = 3$ and $\hat{\theta}_2 = 1$.

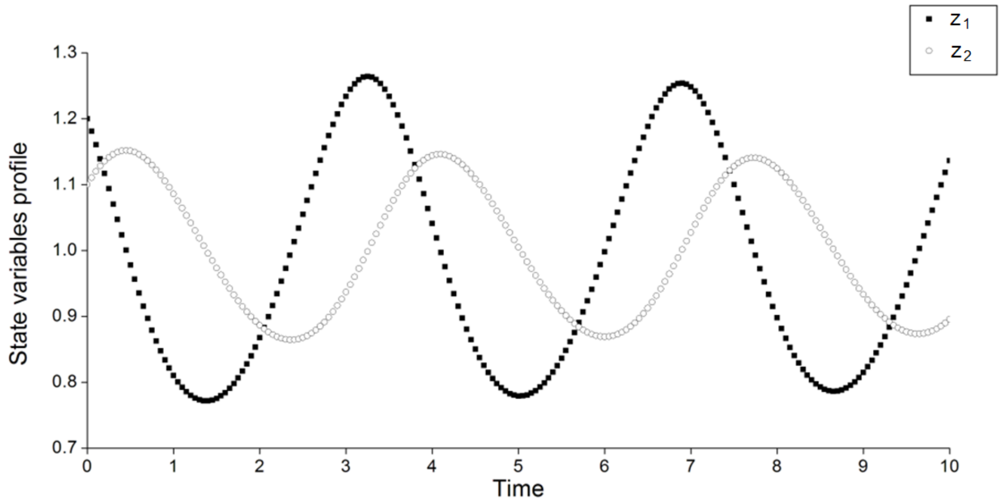

Figure 3.4 State variables profile for z_1 and z_2

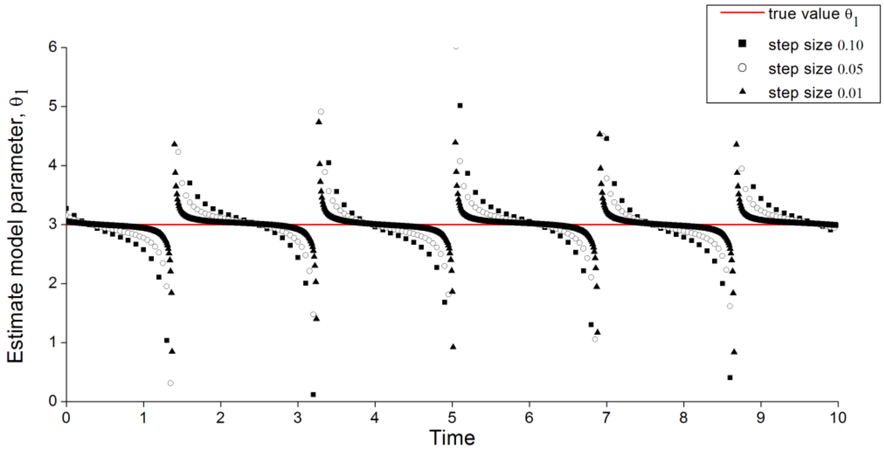

Figure 3.5 Estimated model parameter, θ_1, for different step sizes

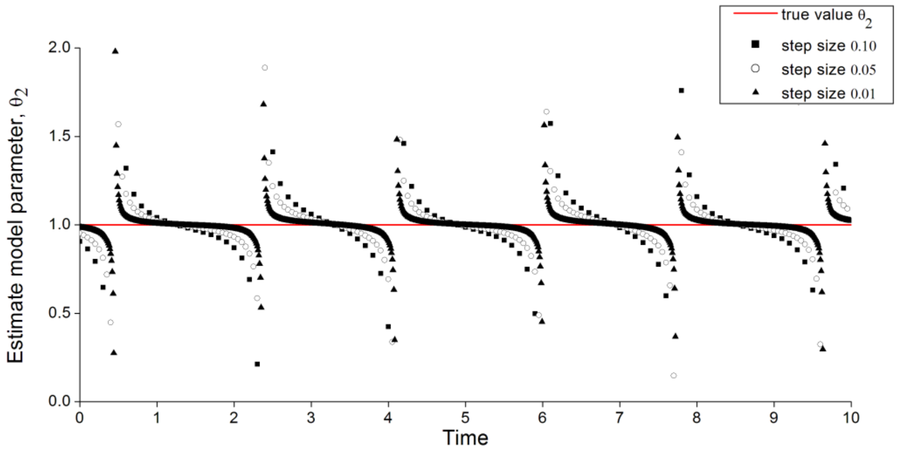

Figure 3.6 Estimated model parameter, θ_2, for different step sizes

3.6 Concluding Remarks

(i) Parameter estimation using the MPP approach is developed and proposed for the FD. In this method, model parameters are obtained as an explicit function of measurements where the estimated model parameters, $\boldsymbol{\theta}$, are considered as optimisation variables and the measurements, $\hat{x}_j$, as the parameters in the context of MPP. The algorithm presented in this work relies on converting the ODEs system into a set of nonlinear algebraic equations and then converting the resulting NLP into another set of nonlinear algebraic equations using the KKT conditions. If these equations can be solved analytically / symbolically, the proposed MPP algorithm for FD method is applicable.

(ii) Preliminary verification of the proposed method is performed by testing the proposed method on two examples of nonlinear ODEs model. The proposed method is successfully obtained model parameters as an explicit function of measurements in the square system of ODEs. The results show that model parameters are accurately obtained compared to 'true value' by performing simple function evaluations. The proposed FD approach using MPP thus provides quick and accurate fault detection by performing simple function evaluations. Another significant advantage is an explicit parametric function able to reduce the computational burden and time-consuming issues in the optimisation problem.

CHAPTER 4 FAULT DETECTION APPLICATION IN PROCESS SYSTEMS

4.1 Introduction

In this chapter, five case studies of process systems are presented to demonstrate the applicability of MPP for the FD in evaporator, tank, heat exchanger, fermentation and wastewater treatment systems. The formulation of parameter estimation using MPP will be discussed and presented to obtain the solution of model parameters. A number of faulty and fault-free scenarios are considered to show the effectiveness of the present approach of parameter estimation using MPP. The detection of fault is carried out by monitoring the residual of model parameters. In this work, the simulations of state variables are obtained using ANN approximation method and validated using the fourth-order Runge–Kutta (RK) method. Both simulations are solved and obtained using the General Algebraic Modeling System (GAMS). Noise is also added to the system as random data to evaluate the effectiveness of the proposed method using MPP. The ANN formulation and fourth-order RK formulation are presented in Appendices A and B.

4.2 Single-Stage Evaporator

Various researches on the FD have been conducted on evaporator systems. An actuator fault of a pilot plant double effect evaporator is discussed in Phatak and Viswanadham (1988) using an unknown input observer. Escobar et al. (2015) discussed a sensor fault in a heat pump's helical evaporator using a high-gain observer and regulated the steam temperature using model predictive control (MPC). The high-gain observer is easy to tune and implement, which provides an adequate estimation of the process output. The evaporator fault in heating, ventilation and air conditioning (HVAC) systems is discussed in Kim and Kim (2005) by observing the variation of cooling capacity. An extended Kalman filter (EKF) is presented in a single-stage evaporator system (Dalle Molle and Himmelblau, 1987) to estimate fault model parameters, i.e., the heat transfer coefficient and the feed composition. The results show that the EKF can estimate the faulty parameters but it required longer computational time. Thus, FD using MPP is proposed in this case study to overcome the limitation in computational time and give more accurate estimated model parameters in Dalle Molle and Himmelblau (1987). Here, the estimated model parameters of UA and x_F will be obtained as an explicit function of measurements, then evaluate the model parameter using symbolic solutions of UA and x_F for fault-free and fault scenarios.

4.2.1 Mathematical Model

In this work, a simplified model of the single-effect evaporator used by Dalle Molle and Himmelblau (1987) is considered. A mathematical model of a single-stage evaporator system is described as:

$$\frac{dW}{dt} = F - \left(\delta W + E_c\right) - V_p \tag{4.1}$$

$$\frac{dT}{dt} = \frac{\beta F x_F + (V_p - F)(T - T_B)}{W} \tag{4.2}$$

where

$$V_p = \left(\frac{UA(T_S - T) - FC_p(T - T_F) - Q_L}{\Delta H_V}\right) \tag{4.3}$$

Here, W and T are the state variables representing the holdup and temperature, respectively, and the estimated model parameters for this process system are UA and x_F. Also, V_p is the vapour flow rate from the evaporator, F is the feed flow rate, T_S is the steam temperature, T_B is the temperature for standard boiling point of the solvent, T_F is the temperature of the feed system, C_p is the heat capacity of the solution, Q_L is the rate of heat loss to the surroundings, and ΔH_V is the heat of vaporisation of the solvent. Figure 4.1 provides a diagram of the evaporator system.

The parameter values used for the simulation of the reactor are shown in Table 4.1 (Dalle Molle and Himmelblau, 1987). In this system, the evaporator operation is assumed to be at 1 atm (101.3 kPa) of pressure.

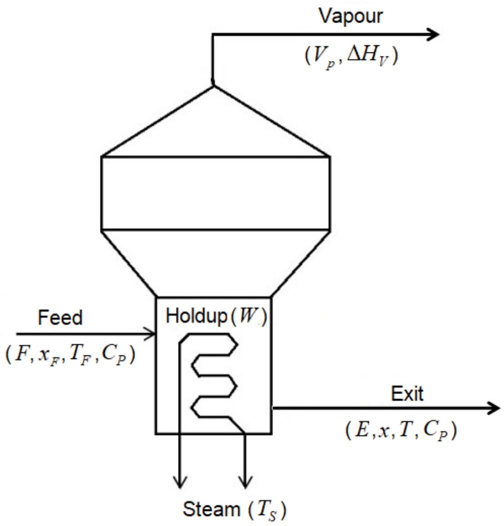

Figure 4.1 Evaporator configuration and notation

Table 4.1. Model parameters for the single-stage evaporator system

Parameter	Value	Description
U	43.6 kJ/(min m ˚C)	overall heat transfer coefficient
A	0.93 m^2	area of heat transfer
x_F	0.032 mass fraction	composition of the feed
T_S	136 ˚C	steam temperature in the steam chest
T_B	100 ˚C	normal boiling point of the solvent
C_p	4.18 kJ/(kg ˚C)	heat capacity of the solution
T_F	88 ˚C	temperature of the feed system
Q_L	400.0 kJ/min	rate of heat loss to the surroundings
ΔH_V	2240 kJ/kg	heat of vapourisation of the solvent
β	8.33 ˚C	boiling point elevation per mass fraction of solute

Parameter	Value	Description
δ	0.06 (kg/min)/kg holdup	constant
E_c	0.0454 kg/min	constant
F	2.27 kg/min	feed flow rate

4.2.2 Fault Detection Problem

In parameter estimation approach for FD, faults are related to specific parameters and parameters can be related to the physical features of the process. In the evaporator system, as the heat transfer surface becomes fouled or scaled, the heat transfer rate is decreased and the efficiency of the process is reduced. The input feed composition could be useful in determining if the previous unit was operating properly (Pouliezos and Stavrakakis, 1994). Thus, the two parameters of interest for faulty operation are UA and x_F will be obtained as an explicit function of measurements. The objective of the FD problem for evaporator system is to estimate the model parameters, UA and x_F, such that the error, ε_{FD}, between the measurement of state variables, $\hat{W}(t_i)$ and $\hat{T}(t_i)$, and ecological interaction value of state variables, $W(t_i)$ and $T(t_i)$, is minimised as the following problem:

Problem 4.2.1

$$\varepsilon_{FD} = \min_{UA, x_f} \sum_{i \in I} \{(\hat{W}(t_i) - W(t_i))^2 + (\hat{T}(t_i) - T(t_i))^2\} \tag{4.4}$$

Subject to :

Equations (4.1) to (4.3)

$$W(0) = 13.8\,\text{kg} \tag{4.5}$$

$$T(0) = 107\,^{\circ}\text{C} \tag{4.6}$$

$$t \in [0, 500] \tag{4.7}$$

where the estimated model parameters, UA and x_F, are estimated through an optimisation problem of FD. The initial values of state variables are given in equations (4.5) and (4.6).

4.2.3 Parameter Estimate using MPP

The formulation and solution of the parameter estimation problem using MPP are summarised as follows:

(i) The nonlinear ODEs model in equations (4.1) to (4.3) is discretised using Euler's method and reformulated as the following algebraic equations:

$$W(i+1) = W(i) + \Delta t(F - \left(\delta W(i) + E_c\right) - V) \tag{4.8}$$

$$T(i+1) = T(i) + \Delta t\left(\frac{\beta F x_F + (V-F)(T(i) - T_B)}{W(i)}\right) \tag{4.9}$$

where

$$V = \left(\frac{UA(T_S - T(i)) - FC_p(T(i) - T_F) - Q_L}{\Delta H_V}\right) \tag{4.10}$$

(ii) Then, the Equations (4.8) to (4.10) are substituted in Problem 4.2.1 and parameter estimation problem is reformulated as the following NLP problem:

Problem 4.2.2

$$\varepsilon_{MPP} = \min_{UA, x_f} \sum_{i \in I} \{(\hat{W}(i+1) - W(i+1))^2 + (\hat{T}(i+1) - T(i+1))^2\} \tag{4.11}$$

Subject to:

$$h_1 = W(i+1) - W(i) - \Delta t(F - \left(\delta W(i) + E_c\right) - V) = 0 \tag{4.12}$$

$$h_2 = T(i+1) - T(i) - \Delta t\left(\frac{\beta F x_F + (V-F)(T(i) - T_B)}{W(i)}\right) = 0 \tag{4.13}$$

Equations (4.5) to (4.7)

(iii) Equations (4.12) and (4.13) represent the set of nonlinear algebraic equations and these equations are substituted into Equation (4.11) to obtain:

$$G = (\hat{W}(i+1) - (W(i) + \Delta t(F - \left(\delta W(i) + E_c\right) - ((UA(T_S - T(i)) - FC_p(T(i) - T_F) - Q_L) / \Delta H_V))))^2 + (\hat{T}(i+1) - (T(i) + \Delta t((\beta F x_F + (((UA(T_S - T(i)) - FC_p(T(i) - T_F) - Q_L) / \Delta H_V) - F)(T(i) - T_B)) / W(i))))^2 \quad (4.14)$$

The gradients of G with respect to UA and x_F are given by:

$$\frac{\partial G}{\partial UA} = -(1/\Delta H_V)2(\Delta t T(i) - T_S)(-(1/\Delta H_V(-\Delta H_V \Delta t E_C - \Delta H_V \Delta t F + \Delta t Q_L + C_P \Delta t F T(i) + C_p \Delta t F T_F + \Delta t T(i) UA - \Delta t T_S UA + \Delta H_V W(i) - \delta \Delta H_V \Delta t W(i)) + \hat{W}(i+1)) - (1/\Delta H_V W(i)) 2\Delta t(T(i) - T_B)(-T(i) - T_S)(\hat{T}(i+1) - \Delta t((T(i)/\Delta t)((T(i) - T_B)(-F + ((UA(T_S - T(i)) - FC_p(T(i) - T_F) - Q_L)/\Delta H_V) + \beta F x_F))/W(i)) = 0 \quad (4.15)$$

$$\frac{\partial G}{\partial x_F} = -(2\beta \Delta t F(\hat{T}(i+1) - \Delta t(T(i)/\Delta t + ((T(i) - T_B)(-F + ((UA(T_S - T(i)) - FC_p(T(i) - T_F) - Q_L)/\Delta H_V) + \beta F x_F)/W(i))))/W(i) = 0 \quad (4.16)$$

(iv) The equality constraints in equations (4.15) and (4.16) are solved analytically in Mathematica to obtain model parameters, $\boldsymbol{\theta}(\hat{\mathbf{x}})$ and the solutions of the model parameters are given by

$$UA = -(1/(\Delta t\,(T(i) - T_S)))(-\Delta H_V \Delta t E_c + \Delta H_V \Delta t F + \Delta t Q_L + C_P \Delta t F T(i) - C_P \Delta t F T_F + \Delta H_V W(i) - \delta \Delta H_V \Delta t W(i) - \Delta H_V \hat{W}(i+1)) \quad (4.17)$$

$$x_F = -(1/(\beta \Delta t F))(-\Delta t E_c T(i) + \Delta t E_c T_B + 2T(i)W(i) - \delta \Delta t T(i) W(i) - T_B W(i) + \delta \Delta t T_B W(i) - \hat{T}(i+1)W(i) - T(i)\hat{W}(i+1) + T_B \hat{W}(i+1)) \quad (4.18)$$

(v) The estimated model parameters, UA and x_F, given in equations (4.17) and (4.18) are successfully obtained as an explicit function of measurements, $\hat{W}$ and $\hat{T}$. Simple function evaluation is carried out to estimate the model parameter and detect faults without the need to solve the online optimisation problem. The residual of model parameters is monitored for FD.

4.2.4 Fault-free Scenario

The simulated measured value and model predicted value of state variables for W and T are shown in Figures 4.2 and 4.3, respectively, using simulated data in Table 4.1. These simulated values are then used to estimated model parameters, UA and x_F, using equations (4.17) and (4.18) with step size, $\Delta t = 1$ min. The model parameters are only estimated after state variables have reached the steady-state value at 50 min. The evaluation of UA and x_F are shown in figures 4.4 and 4.5. It can be seen from these figures that the estimated model parameters are close to true model parameters. The detection of fault is carried out by monitoring the value of the residual of model parameters. The residuals of model parameters are shown in Figures 4.6 and 4.7. No fault was detected since the residual is less than the threshold. The threshold is chosen as 5% from the nominal system parameter values.

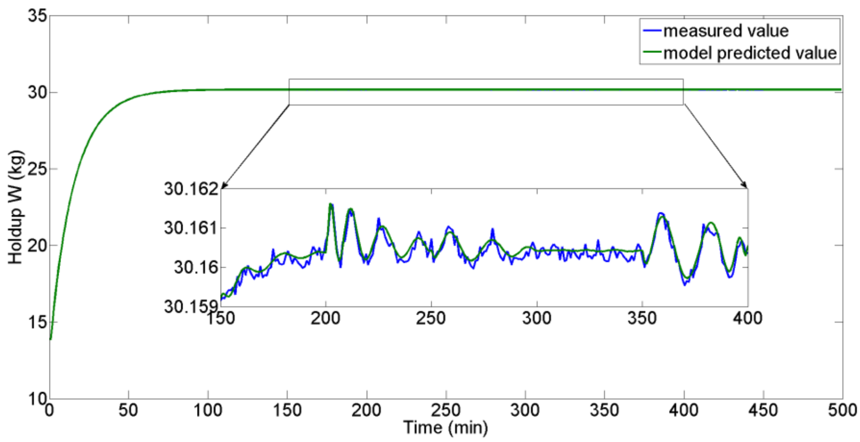

Figure 4.2 State variables profile, W, for fault-free scenario

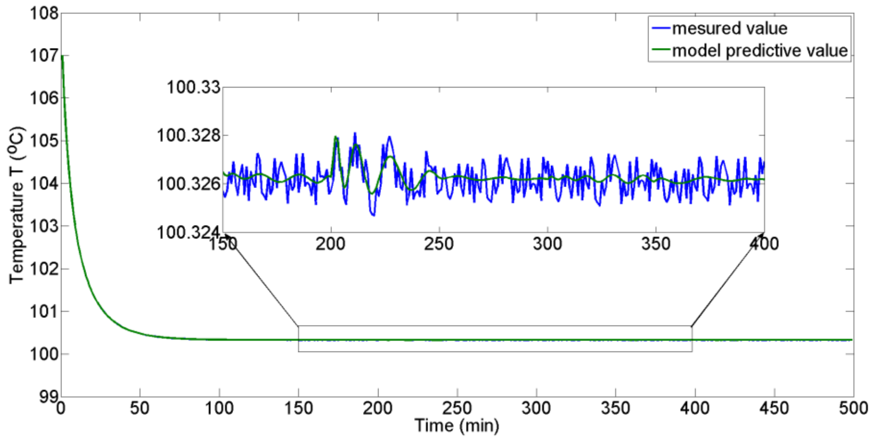

Figure 4.3 State variables profile, T , for fault-free scenario

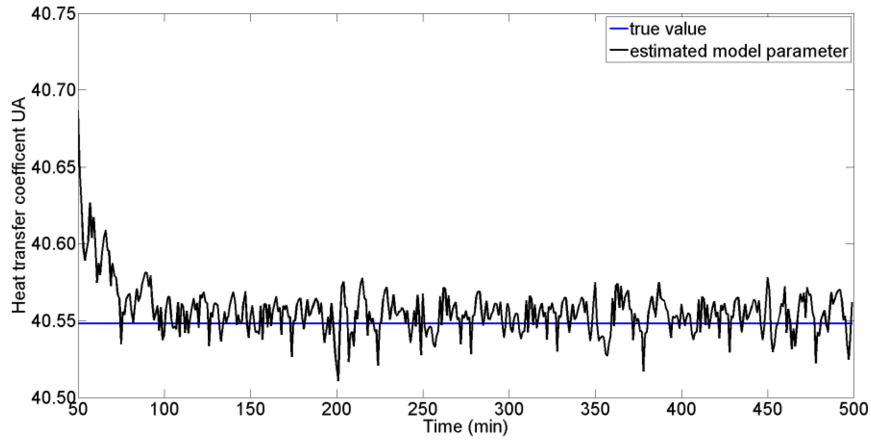

Figure 4.4 Estimated model parameters, UA, for fault-free scenario

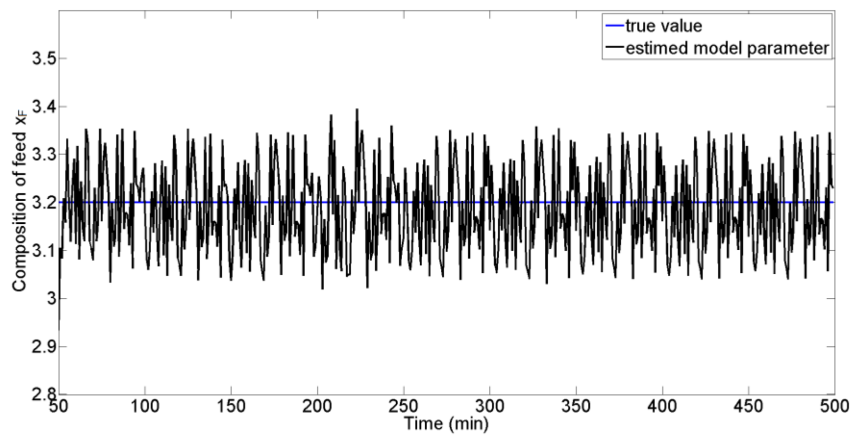

Figure 4.5 Estimated model parameters, x_F , for fault-free scenario

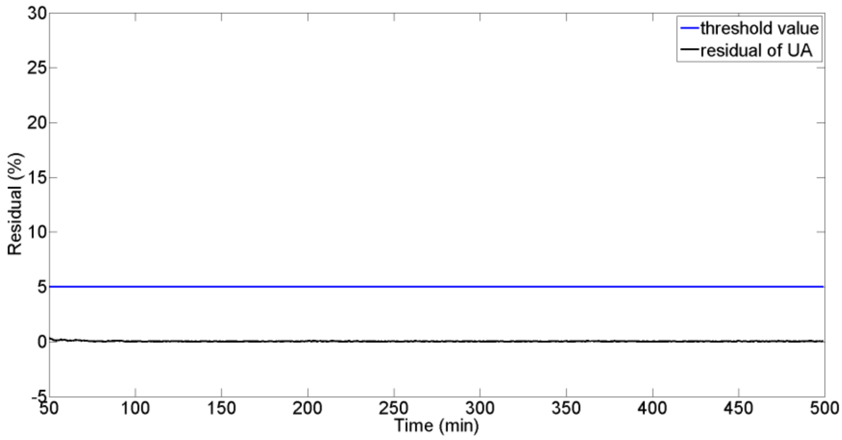

Figure 4.6 Residual of estimated model parameters, UA, for fault-free scenario

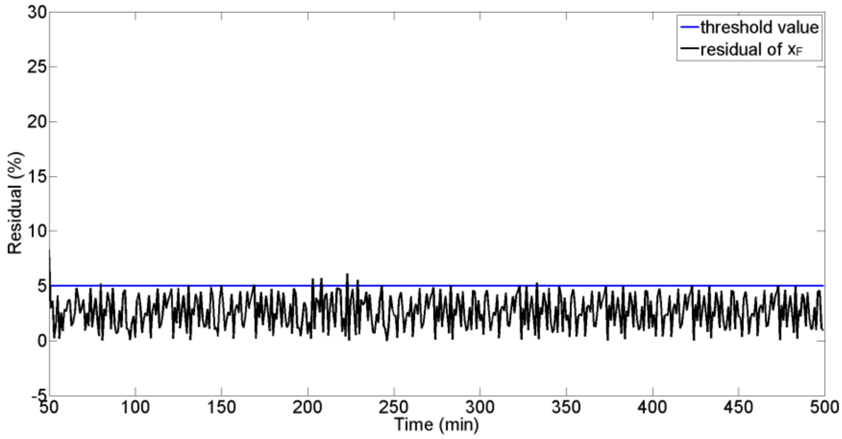

Figure 4.7 Residual of estimated model parameters, x_F, for fault-free scenario

4.2.5 Faulty Scenario

An investigation for a faulty scenario was implemented for this case study. To demonstrate the application of parameter estimation for the evaporator, the estimated model parameters, UA and x_F, are changed as shown in Table 4.2. The faulty state variable for the holdup, W, and temperature, T, are simulated based on faulty conditions as described in Table 4.2 using ANN formulation. Figures 4.8 and 4.9 show the measured value and model predicted value of state variables for a faulty scenario for holdup and temperature. The model parameters are only estimated after state variables have reached the steady-state value at 50 min with step size, $\Delta t = 1$ min. Figures 4.10 and 4.11 show the evaluation of estimated model parameters, UA and x_F, respectively. From these figures, we can see that the estimated parameter,

UA, decreases from 40.548 kJ m/min ˚C at 75 min to 36.50 kJ m/min ˚C (at 375 min). The estimated model parameter for x_F also changes, from 0.032 mass fraction (at 165 min) to 0.025 mass fraction (at 285 min). The detection of fault is carried out by monitoring the value of the residuals of model parameters, and the result is shown in figures 4.12 and 4.13. Figure 4.12 shows that from 75 to 375 min the percentage of residual for UA increases slowly up to 10%, and the fault is declared from 225 to 375 min since the residual for UA is more than or equal to 5% of the threshold value. As shown in Figure 4.13, the fault for x_F is declared at 165 to 285 min as the percentage of residual for x_F is 20 %. The MPP based parameter estimation is thus able to accurately and quickly identify the faults in the evaporator system.

Table 4.2. Faulty scenario for a single-stage evaporator system

Fault parameter	UA	x_F
% change in value	-10.0	-20.0
Type of change	ramp	step
Starting time of change (min)	75	165
Stop time of change (min)	375	285

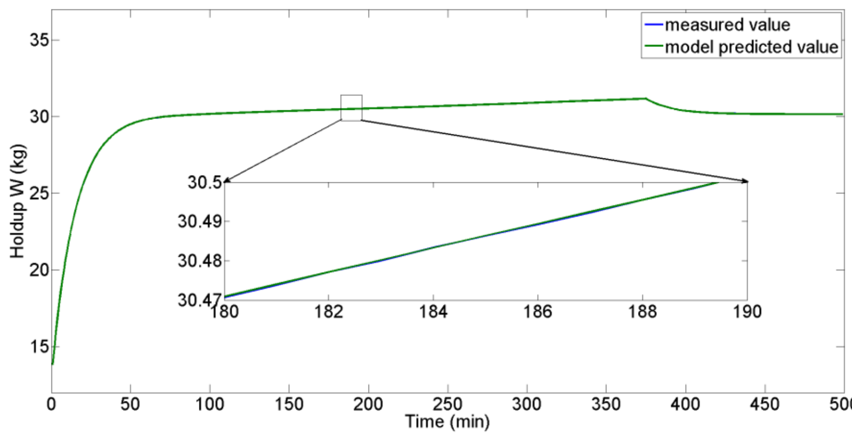

Figure 4.8 State variables profile, W, for faulty scenario using ANN formulation

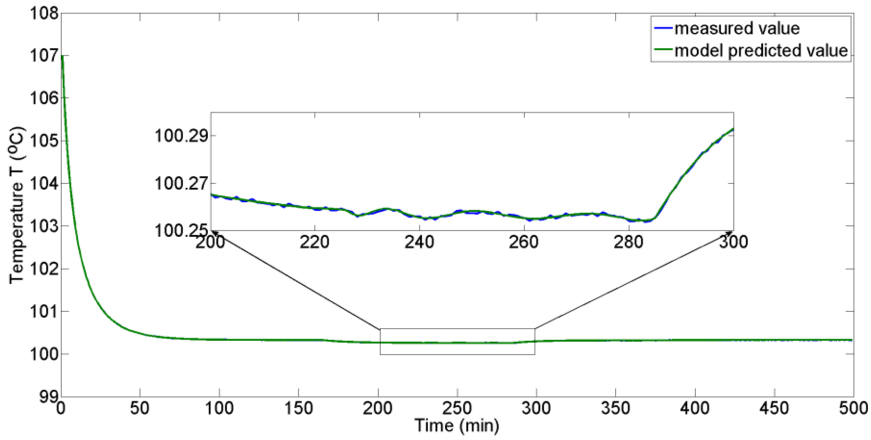

Figure 4.9 State variables profile, T , for faulty scenario

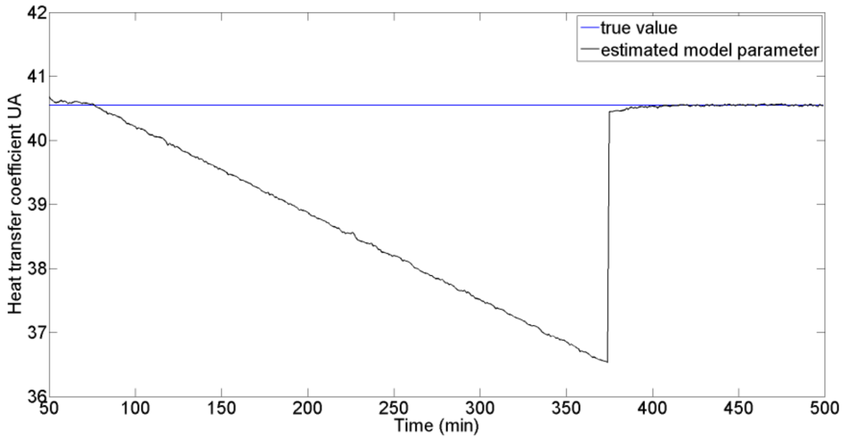

Figure 4.10 Estimated model parameters, UA, for faulty scenario

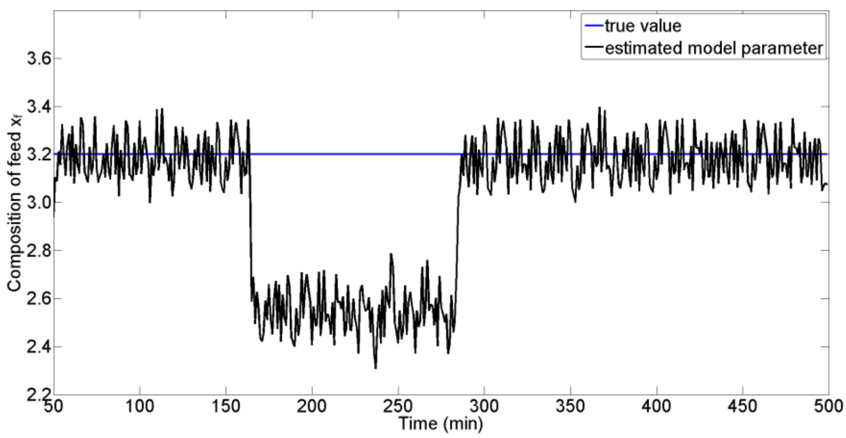

Figure 4.11 Estimated model parameters, x_F , for faulty scenario

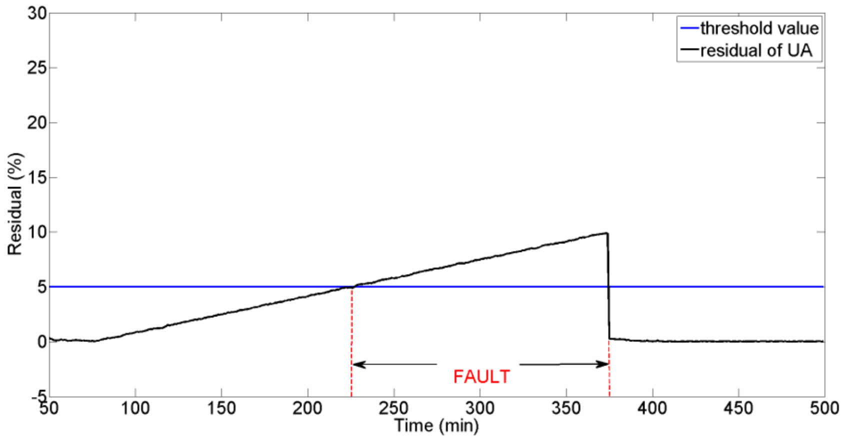

Figure 4.12 Residual of estimated model parameters, UA, for faulty scenario

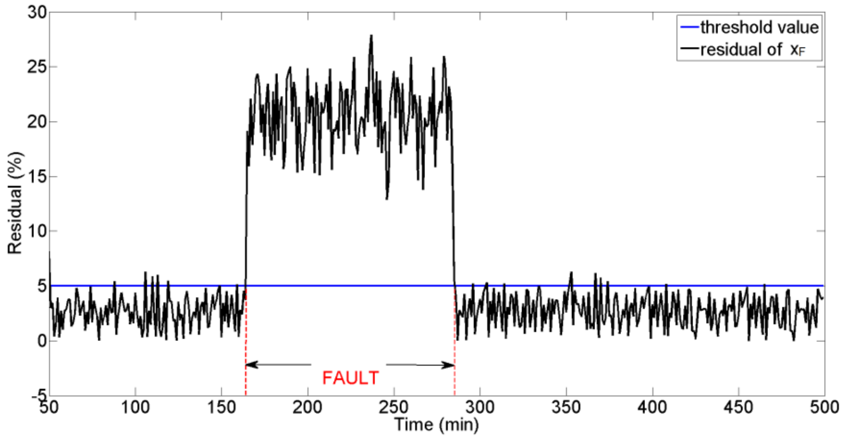

Figure 4.13 Residual of estimated model parameters, x_F , for faulty scenario

4.3 Quadruple-Tank System

The implementation of FD using MPP is further discussed using a quadruple-tank system. Buciakowski et al. (2014) present an actuator fault in the quadruple-tank process using the concept of the fault compensation mechanism. The faults for pumps are estimated and the fault tolerance is implemented with a robust controller. Kamel et al. (2009) discussed the actuator fault using unknown input observer and Lipschitz constraint. In Xuan et al. (2015), the FD of sensor fault using principal component analysis (PCA) is presented. The authors discussed a method for selecting the number of principal components to detect and identified sensor faults in the quadruple-tank system. Leak detection in the tank is presented in Ganesh et al.

(2015) and Lakhmani et al. (2016). A leak occurring at the bottom of a tank is modelled as a change in an appropriate model parameter. A moving-window parameter estimator is presented in Lakhmani et al. (2016) and an extended Kitanidis-Kalman filter in Ganesh et al. (2015) to detect the fault. In this work, a method to detect a leak in the tank using parameter estimation is presented. This leak is assumed to be produced by holes at the bottom of the tanks, such that the outflow is lost. Using the MPP method, the cross-section of the outlet holes is obtained as an explicit function of measurements. The FD is then carried out by monitoring the changes of model parameters.

4.3.1 Mathematical Model

The quadruple-tank system is based on the system presented by Johansson (2000). The system consists of four interacting tanks, two pumps and two valves, as shown in Figure 4.14. The system aims at controlling the liquid levels in the lower tanks. By adjusting the system's bypass valves, the proportion of the liquid pumped into different tanks can be changed to adjust the degree of interaction between the pump throughputs and the water levels. The mathematical model of the quadruple-tank system (Johansson, 2000) is described as:

$$\frac{dH_1}{dt} = -\frac{a_1}{A_1}\sqrt{2gH_1} + \frac{a_3}{A_1}\sqrt{2gH_3} + \frac{\gamma_1\kappa_1}{A_1}v_1 \tag{4.19}$$

$$\frac{dH_2}{dt} = -\frac{a_2}{A_2}\sqrt{2gH_2} + \frac{a_4}{A_2}\sqrt{2gH_4} + \frac{\gamma_2\kappa_2}{A_2}v_2 \tag{4.20}$$

$$\frac{dH_3}{dt} = -\frac{a_3}{A_3}\sqrt{2gH_3} + \frac{(1-\gamma_2)\kappa_2}{A_3}v_2 \tag{4.21}$$

$$\frac{dH_4}{dt} = -\frac{a_4}{A_4}\sqrt{2gH_4} + \frac{(1-\gamma_1)\kappa_1}{A_4}v_1 \tag{4.22}$$

For a tank p, A_p is the cross-section of the tank, a_p is the cross-section of the outlet holes and H_p is the height of water levels in the tank. The input voltage to the pump p is v_p, and the corresponding flow is $\kappa_p v_p$. The parameter values of the quadruple-tank system are given in Table 4.3 (Johansson, 2000).

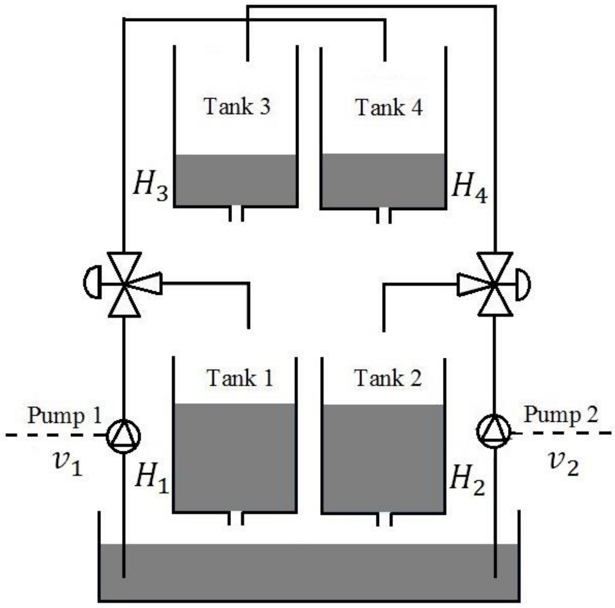

Figure 4.14 Quadruple-tank process

Table 4.3. Model parameters for the quadruple-tank system

Parameters	Values	Units	Description
$A_1; A_2; A_3; A_4$	28; 32; 28; 32	cm^2	cross-section of tank p
$a_1; a_2; a_3; a_4$	0.071; 0.057; 0.071; 0.057	cm^2	cross-section of the outlet hole
$v_1; v_2$	3.00; 3.00	V	input voltage
$\kappa_1; \kappa_2$	3.33; 3.35	cm^3 / Vs	
$\gamma_1; \gamma_2$	0.7; 0.6	-	
g	981.0	cm / s^2	acceleration of gravity

4.3.2 Fault Detection Problem

In this work, a tank leakage fault is considered for testing the proposed FD method. This leak is assumed to be produced by holes at the bottom of the tanks, such that the outflow is lost. Hence, the objective of FD in the quadruple-tank system is to estimate the cross-section of the outlet holes, a_p, such that the error, ε_{FD}, between the measurement of state variables, $\hat{H}_p(t_i)$, and model predicted value of state variables, $H_p(t_i)$, is minimised as described in Problem 4.3.1. The initial values of state variables are given in equations (4.24) to (4.27).

Problem 4.3.1

$$\varepsilon_{FD} = \min_{a_1,a_2,a_3,a_4} \sum_{i\in I} \{(\hat{H}_1(t_i) - H_1(t_i))^2 + (\hat{H}_2(t_i) - H_2(t_i))^2 + (\hat{H}_3(t_i) - H_3(t_i))^2 + (\hat{H}_4(t_i) - H_4(t_i))^2\} \tag{4.23}$$

Subject to :

Equations (4.19) to (4.22)

$$H_1(0) = 12.4\,\text{cm} \tag{4.24}$$

$$H_2(0) = 12.7\,\text{cm} \tag{4.25}$$

$$H_3(0) = 1.4\,\text{cm} \tag{4.26}$$

$$H_4(0) = 1.8\,\text{cm} \tag{4.27}$$

$$t \in [0, 600] \tag{4.28}$$

4.3.3 Parameter Estimation using MPP

The formulation and solution of the parameter estimation problem using MPP are summarised as follows:

i) The nonlinear ODEs model in equations (4.19) to (4.22) is discretised using Euler's method and reformulated as the following algebraic equations:

$$H_1(i+1) = H_1(i) + \Delta t\left(-\frac{a_1}{A_1}\sqrt{2gH_1(i)} + \frac{a_3}{A_1}\sqrt{2gH_3(i)} + \frac{\gamma_1\kappa_1}{A_1}v_1 \right) \tag{4.29}$$

$$H_2(i+1) = H_2(i) + \Delta t\left(-\frac{a_2}{A_2}\sqrt{2gH_2(i)} + \frac{a_4}{A_2}\sqrt{2gH_4(i)} + \frac{\gamma_2\kappa_2}{A_2}v_2 \right) \tag{4.30}$$

$$H_3(i+1) = H_3(i) + \Delta t\left(-\frac{a_3}{A_3}\sqrt{2gH_3(i)} + \frac{(1-\gamma_2)\kappa_2}{A_3}v_2 \right) \tag{4.31}$$

$$H_4(i+1) = H_4(i) + \Delta t\left(-\frac{a_4}{A_4}\sqrt{2gH_4(i)} + \frac{(1-\gamma_1)\kappa_1}{A_4}v_1 \right) \tag{4.32}$$

(ii) Equations (4.29) to (4.32) are substituted in Problem 4.3.1 and the FD problem is formulated as the following NLP problem:

Problem 4.3.2

$$\begin{aligned}\varepsilon_{MPP} = \min_{a_1,a_2,a_3,a_4}\sum_{i\in I}\ &\{(\hat{H}_1(i+1)-H_1(i+1))^2 + (\hat{H}_2(i+1)-H_2(i+1))^2 + \\ &(\hat{H}_3(i+1)-H_3(i+1))^2 + (\hat{H}_4(i+1)-H_4(i+1))^2\}\end{aligned} \tag{4.33}$$

Subject to:

$$h_1 = H_1(i+1) - H_1(i) - \Delta t\left(-\frac{a_1}{A_1}\sqrt{2gH_1(i)} + \frac{a_3}{A_1}\sqrt{2gH_3(i)} + \frac{\gamma_1\kappa_1}{A_1}v_1 \right) = 0 \tag{4.34}$$

$$h_2 = H_2(i+1) - H_2(i) - \Delta t\left(-\frac{a_2}{A_2}\sqrt{2gH_2(i)} + \frac{a_4}{A_2}\sqrt{2gH_4(i)} + \frac{\gamma_2\kappa_2}{A_2}v_2 \right) = 0 \tag{4.35}$$

$$h_3 = H_3(i+1) - H_3(i) - \Delta t\left(-\frac{a_3}{A_3}\sqrt{2gH_3(i)} + \frac{(1-\gamma_2)\kappa_2}{A_3}v_2 \right) = 0 \tag{4.36}$$

$$h_4 = H_4(i+1) - H_4(i) - \Delta t\left(-\frac{a_4}{A_4}\sqrt{2gH_4(i)} + \frac{(1-\gamma_1)\kappa_1}{A_4}v_1 \right) = 0 \tag{4.37}$$

Equations (4.24) to (4.28)

(iii) Equations (4.34) to (4.37) represent the set of nonlinear algebraic equations and these equations are substituted into Equation (4.33) to obtain:

$$
\begin{aligned}
G = {} & (\hat{H}_1(i+1) - (H_1(i) + \Delta t(-(a_1 / A_1)\sqrt{2gH_1(i)} + (a_3 / A_1)\sqrt{2gH_3(i)} + \\
& (\gamma_1\kappa_1 v_1) / A_1)))^2 + (\hat{H}_2(i+1) - (H_2(i) + \Delta t(-(a_2 / A_2)\sqrt{2gH_2(i)} + \\
& (a_4 / A_2)\sqrt{2gH_4(i)} + (\gamma_2\kappa_2 v_2) / A_2)))^2 + (\hat{H}_3(i+1) - (H_3(i) + \\
& \Delta t(-(a_3 / A_3)\sqrt{2gH_3(i)} + ((1-\gamma_2)\kappa_2 v_2) / A_3)))^2 + (\hat{H}_4(i+1) - (H_4(i) + \\
& \Delta t(-(a_4 / A_4)\sqrt{2gH_4(i)} + ((1-\gamma_1)\kappa_1 v_1) / A_4)))^2
\end{aligned}
\tag{4.38}
$$

The gradients of G with respect to the cross-section of the outlet hole, a_p, are given by:

$$
\begin{aligned}
\frac{\partial G}{\partial a_1} = {} & (2.82843\Delta t(gH_1(i))^{0.5}(\hat{H}_1(i+1) - \Delta t((1.H_1(i)) / \Delta t - \\
& (1.41421(gH_1(i))^{0.5} a_1) / A_1 + (1.41421(gH_3(i))^{0.5} a_3) / A_1 + \\
& (1.\kappa_1 v_1 \gamma_1) / A_1))) / A_1 \\
= {} & 0
\end{aligned}
\tag{4.39}
$$

$$
\begin{aligned}
\frac{\partial G}{\partial a_2} = {} & (2.82843\Delta t(gH_2(i))^{0.5}(\hat{H}_2(i+1) - \Delta t((1.H_2(i)) / \Delta t - \\
& (1.41421(gH_2(i))^{0.5} a_2) / A_2 + (1.41421(gH_4(i))^{0.5} a_4) / A_2 + \\
& (1.\kappa_2 v_2 \gamma_2) / A_2))) / A_2 \\
= {} & 0
\end{aligned}
\tag{4.40}
$$

$$
\begin{aligned}
\frac{\partial G}{\partial a_3} = {} & -((2.82843\ \Delta t(g\ H_3(i))^{0.5}(\hat{H}_1(i+1) - \Delta t((1.\ H_1(i)) / \Delta t - \\
& (1.41421(g\ H_1(i))^{0.5} a_1) / A_1 + (1.41421(g\ H_3(k))^{0.5} a_3) / A_1 + \\
& (1.\ \kappa_1 v1 \gamma_1) / A_1))) / A_1) - 2\Delta t(0.\ -(1.41421(gH_3(i))^{0.5}) / A_3)(\hat{H}_3(i+1) - \\
& \Delta t((1.\ H_3(i)) / \Delta t - (1.41421(gH_3(i))^{0.5} a_3) / A_3 + (1.\kappa_2 v_2(1.\ -1.\ \gamma_2)) / \\
& A_3)) \\
= {} & 0
\end{aligned}
\tag{4.41}
$$

$$\frac{\partial G}{\partial a_4} = -2\ \Delta t(0. - (1.41421(g\ H_4(i))^{0.5}) / A_4)(\hat{H}_4(i+1) - \Delta t((1.\ H_4(i)) / \Delta t - (1.41421(g\ H_4(i))^{0.5} a_4) / A_4 + (1.\kappa_1 v_1(1. - 1.\gamma_1)) / A_4)) - (2.82843\Delta t(gH_4(i))^{0.5}(\hat{H}_2(i+1) - \Delta t((1.\ H_2(i)) / \Delta t - (1.41421(gH_2(i))^{0.5} a_2) / A_2 + (1.41421(gH_4(i))^{0.5} a_4) / A_2 + (1.\kappa_2 v_2 \gamma_2) / A_2))) / A_2 = 0 \tag{4.42}$$

(iv) The equality constraints in equations (4.39) to (4.42) are solved analytically in Mathematica to obtain the symbolic solution of a_p and the solutions are given as follows:

$$a_1 = -(1.(-1.((4.\ \Delta t^2 (g\ H_3(i))^{1.}) / A_1^2 - (2.82843\Delta t^2 (g\ H_3(i))^{0.5}(0. - (1.41421(g\ H_3(i))^{0.5}) / A_3)) / A_3)(-((2.82843\Delta t\ H_1(i)(gH_1(i))^{0.5}) / A_1) + (2.82843\Delta t(gH_1(i))^{0.5}\hat{H}_1(i+1)) / A_1 - (2.82843\Delta t^2(gH_1(i))^{0.5}\kappa_1 v_1 \gamma_1) / A_1^2) - 1 / A_1^2\, 4.\Delta t^2 (g\ H_1(i))^{0.5}(g\ H_3(i))^{0.5}\ ((2.82843\Delta t H_1(i)(g\ H_3(i))^{0.5}) / A_1 - (2.82843\Delta t\hat{H}_1(i+1)(gH_3(i))^{0.5}) / A_1 + 2.\Delta t H_3(i)(0. - (1.41421(gH_3(i))^{0.5}) / A_3) - 2.\Delta t(0. - (1.41421(gH_3(i))^{0.5}) / A_3)\hat{H}_3(i+1) + (2.82843\Delta t^2(gH_3(i))^{0.5}\kappa_1 v_1 \gamma_1) / A_1^2 + (2.\Delta t^2(0. - (1.41421(gH_3(i))^{0.5}) / A_3)\kappa_2 v_2(1. - 1.\gamma_2)) / A_3))) / (0. - (16.\Delta t^4 (gH_1(i))^{1.}(gH_3(i))^{1.}) / (A_1^2 A_3^2)) \tag{4.43}$$

$$a_2 = -(0.707107(0. - 1.A_2^3 H_2(i)(gH_2(i))^{1.}(gH_4(i))^{1.} + 1.\ A_2^3(gH_2(i))^{1.}\hat{H}_2(i+1)(g\ H_4(i))^{1.} - 1.\ A_2^2 A4(gH_2(i))^{1.} H_4(i)(gH_4(i))^{1.} + 1.\ A_2^2 A4(gH_2(i))^{1.}(gH_4(i))^{1.}\hat{H}_4(i+1) - 1.\ A_2^2\Delta t(gH_2(i))^{1.}(gH_4(i))^{1.}\kappa_1 v_1 + 1.\ A_2^2\Delta t(gH_2(i))^{1.}(gH_4(i))^{1.}\kappa_1 v_1 \gamma_1 - 1.\ A_2^2\Delta t(gH_2(i))^{1.}(gH_4(i))^{1.}\kappa_2 v_2 \gamma_2)) / (A_2^2\Delta t(gH_2(i))^{1.5.}(gH_4(i))^{1.}) \tag{4.44}$$

$$a_3 = (0.707107(0. - 2.22045\times 10^{-16} A_1^3 H_1(i)(gH_1(i))^{1.}(gH_3(i))^{1.} + 2.22045\times 10^{-16} A_1^3(gH_1(i))^{1.}\hat{H}_1(i+1)(g\ H_3(i))^{1.} + 1.\ A_1^2 A_3(gH_1(i))^{1.} H_3(i)(g\ H_3(i))^{1.} - 1.\ A_1^2 A_3(gH_1(i))^{1.}(gH_3(i))^{1.}\hat{H}_3(i+1) + 1.\ A_1^2\Delta t(gH_1(i))^{1.}(gH_3(i))^{1.}\kappa_2 v_2 - 2.22045\times 10^{-16} A_1^2\Delta t(g\ H_1(i))^{1.}(g\ H_3(i))^{1.}\kappa_1 v_1 \gamma_1 - 1.\ A_1^2\Delta t(g\ H_1(i))^{1.}(g\ H_3(i))^{1.}\kappa_2 v_2 \gamma_2)) / (A_1^2\Delta t(gH_1(i))^{1.}(gH_3(i))^{1.5}) \tag{4.45}$$

$$\begin{aligned} a_4 = &-(1.(1/A_2^2 4.\Delta t^2 (gH_2(i))^{0.5} (gH_4(i))^{0.5} (-((2.82843 \Delta t H_2(i)(gH_2(i))^{0.5})/ \\ &A_2) + (2.82843 \Delta t (gH_2(i))^{0.5} \hat{H}_2(i+1))/A_2 - (2.82843 \Delta t^2 (gH_2(i))^{0.5} \\ &k2v2y2)/A_2^2) + 1/A_2^2 4.\Delta t^2 (gH_2(i))^{1.} ((2.82843 \Delta t H_2(i)(gH_4(i))^{0.5})/ \\ &A_2 - (2.82843 \Delta t \hat{H}_2(i+1)(gH_4(i))^{0.5})/A_2 + 2.\ \Delta t\ H_4(i)(0.\ -(1.41421 \\ &(gH_4(i))^{0.5})/A_4) - 2.\Delta t(0. - (1.41421(gH_4(i))^{0.5})/A_4)\ \hat{H}_4(i+1) + \\ &(2.\ \Delta t^2 (0.\ -(1.41421(gH_4(i))^{0.5})/A_4)\kappa_1 v_1 (1.\ -1.\ \gamma_1))/A_4 + \\ &(2.82843 \Delta t^2 (gH_4(i))^{0.5} \kappa_2 v_2 \gamma_2)/A_2^2)))/(0. + (16.\ \Delta t^4 (gH_2(i))^{1.} \\ &(gH_4(i))^{1.})/(A_2^2 A_4^2)) \end{aligned} \tag{4.46}$$

(v) The parameter faults of a_p are successfully obtained as explicit functions of the measurements, $\hat{H}_p$, as given in equations (4.43) to (4.46). Simple function evaluation is carried out to estimate a_p and the residual is monitored for leakage detection.

4.3.4 Fault-free Scenario

In the fault-free scenario, the simulated measured values and model predicted values for H_p are simulated using parameters in Table 4.3 and shown in Figure 4.15. These simulated values are then used to estimated a_p using equations (4.43) to (4.46) with step size, $\Delta t = 5$ s. The evaluation of the estimation model parameters is shown in Figure 4.16. As shown in Figure 4.16, the estimated model parameters, a_p, are close to true model parameters. The tank leakage is estimated by monitoring the value of the residual of a_p. The result is shown in Figure 4.17 and no leakage was detected in each tank since the residual is less than the threshold value. The threshold value is chosen as 5% from the nominal system.

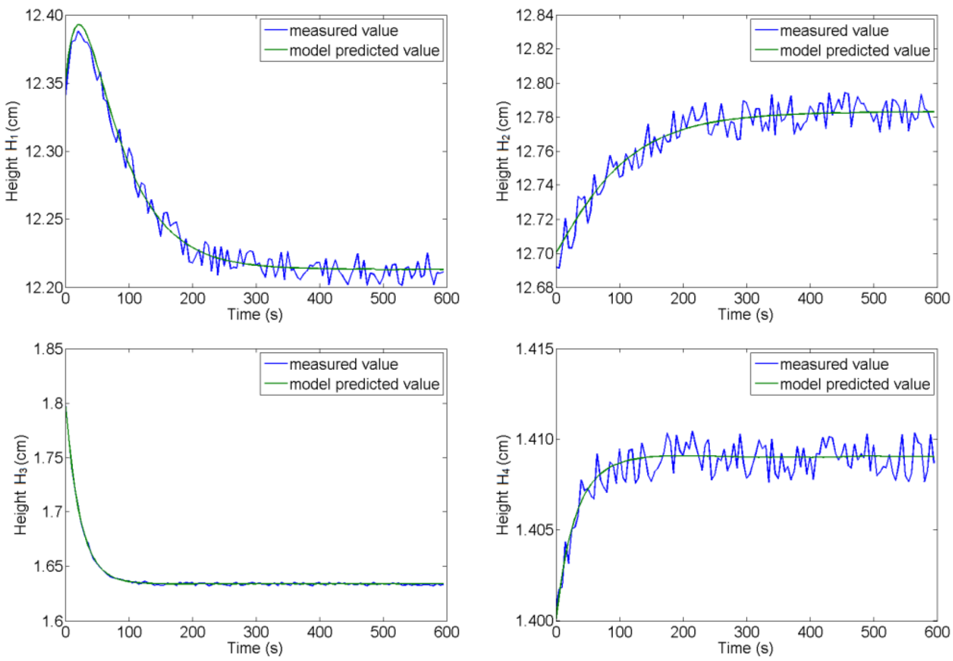

Figure 4.15 State variables profile, H_p, for fault-free scenario

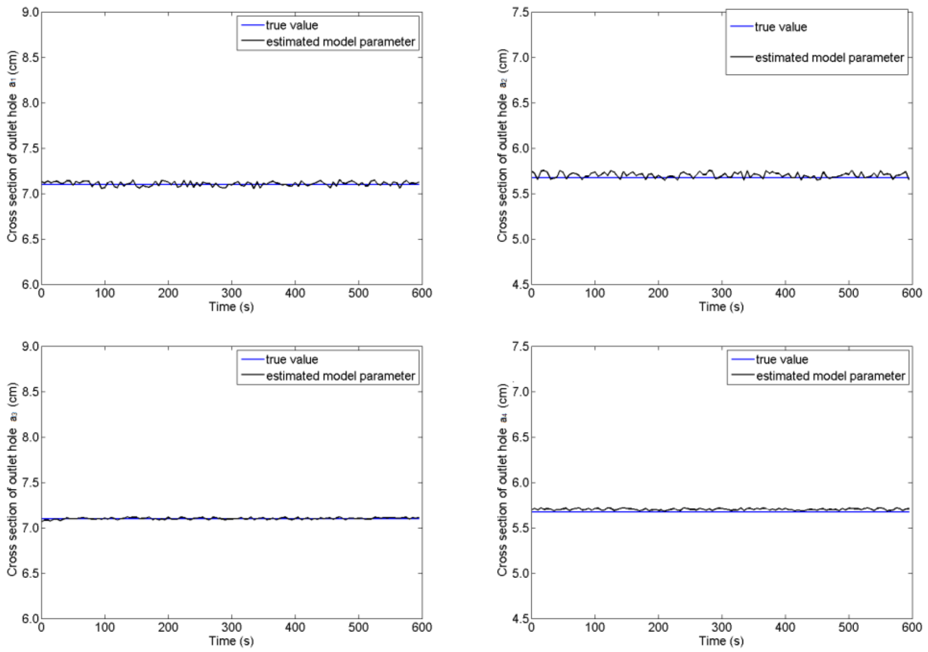

Figure 4.16 Estimated model parameters, a_p, for fault-free scenario

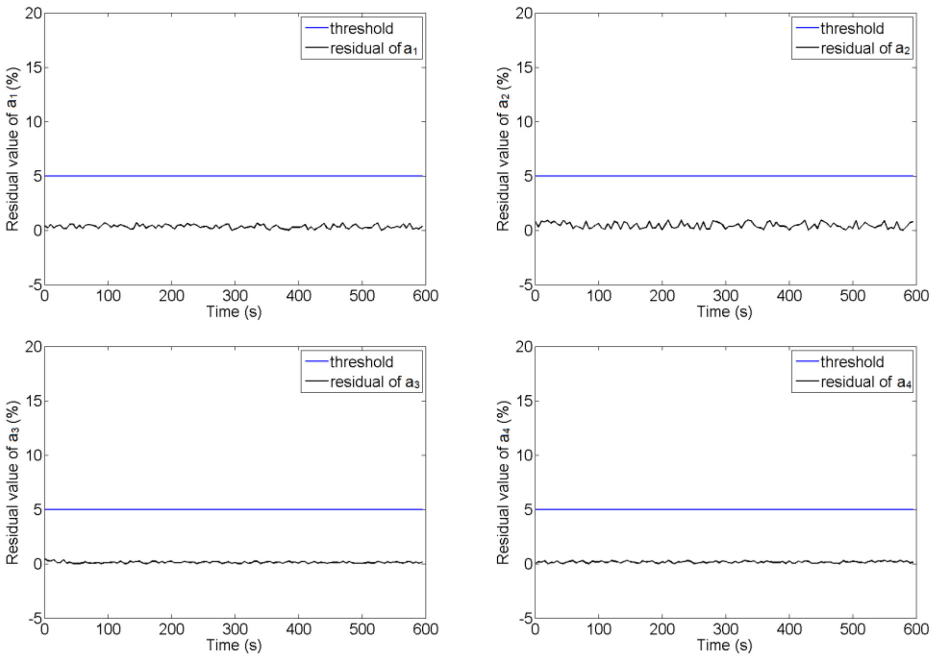

Figure 4.17 Residual of estimated model parameters, a_p, for fault-free scenario

4.3.5 Faulty Scenario

An investigation for the faulty scenario was implemented for this case study. It is assumed that the fault takes place due to leaks in Tank 1 and Tank 2, resulting in changes in the cross-section of outlet holes, a_1 and a_2, in both these tanks. The faults considered are modelled as changes in model parameters, as shown in Table 4.4. Figure 4.18 shows the noisy measured value and model predicted value for H_p would be used to evaluate the model parameters, a_p . Figure 4.19 shows the evaluation of the estimated cross-section of the outlet hole in Tank 1. We can see that the estimated parameter for a_1 has increased from 0.071 to 0.08165 cm^2 at 50 to 150 s and from 0.071 to 0.0781 cm^2 from 350 to 450 s. While estimating the cross-section of the outlet hole in Tank 2, the result shows that from 200 to 300 sec there is an increase in model parameter, a_2, from 0.057 to 0.06556 cm^2 and an increase from 0.057 to 0.0627 cm^2 from 350 to 450 s. There are no changes in cross-sections of the outlet holes in Tank 3 and Tank 4 as the estimated model parameters for a_3 and a_4 show no difference. The residual of model parameters is monitored for FD, and the result is shown in Figure 4.20. This figure shows that the fault is declared for

Tank 1 as the residual for achieving a threshold value at 50 to 150 s and 350 to 450 s, while the fault in Tank 2 is declared at 200 to 300 s and 350 to 450 s. These results indicate that there are leakages in Tank 1 and Tank 2 at specified times, as discussed above. The figure also shows that no leakages are detected in Tank 3 and Tank 4.

Table 4.4. Faulty scenario for the quadruple-tank system

Time	Fault parameter	a_1	a_2
50 – 150 s	% change in value	+ 15.0	0
200 – 300 s	% change in value	0	+ 15.0
350 – 450 s	% change in value	+ 10.0	+ 10.0

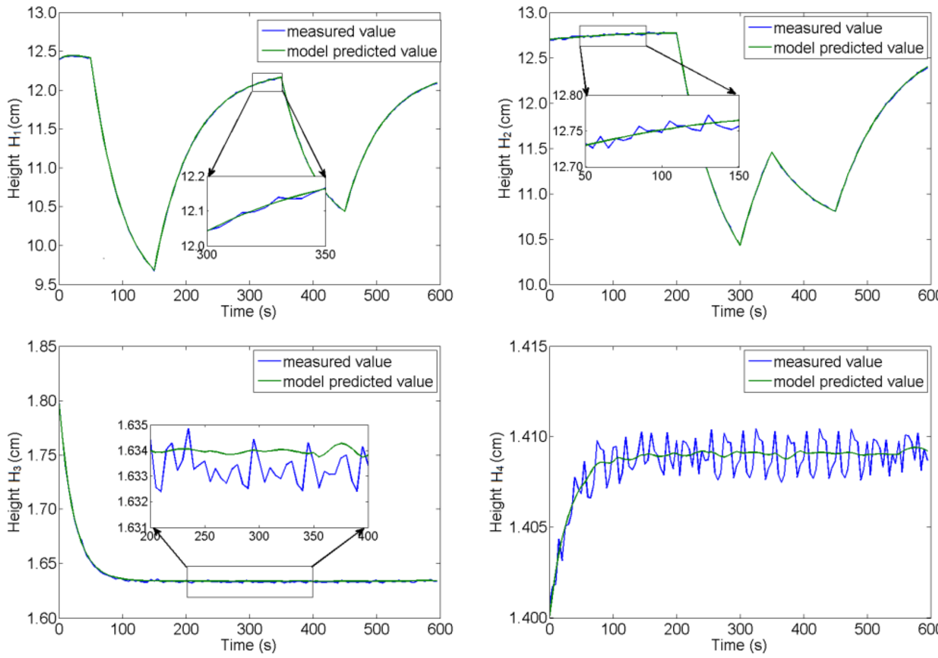

Figure 4.18 State variables profile, H_p, for faulty scenario

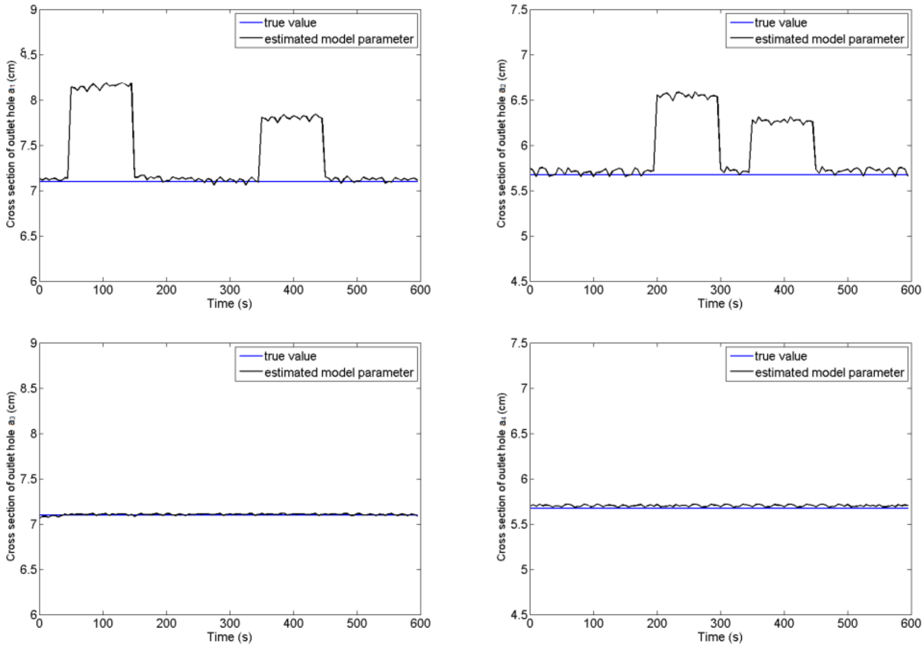

Figure 4.19 Estimated model parameters, a_p, for faulty scenario

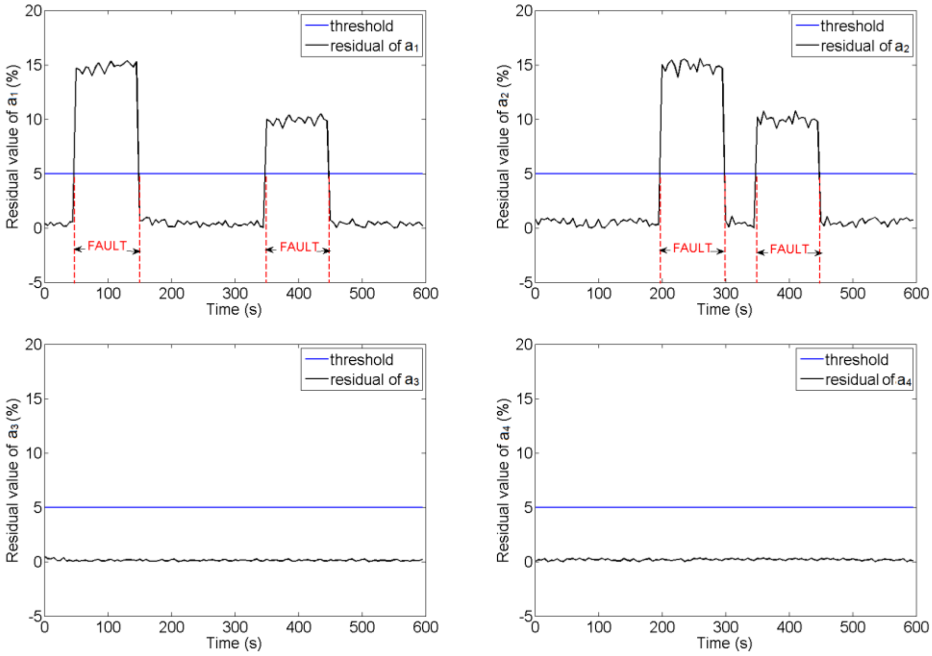

Figure 4.20 Residual of estimated model parameters, a_p, for faulty scenario

4.4 Heat Exchanger

The third case study in the process systems for FD using MPP is heat exchanger. Heat exchanger is widely used in industrial applications including in the oil and gas industry, power stations, chemical plants and more, to transport heat from one fluid to another by conduction through solid walls. Unfortunately, an accumulation of unwanted deposits on the heat exchanger surface – called a fouling film – provides additional resistance to heat transfer and causes deterioration in the effectiveness of heat transfer. When fouling film thickness increases, the heat transfer between fluid decreases, which results in production loss and increased operational costs due to the replacement of equipment and cleaning of the fouling film. Due to the cost and the environmental issues, it is therefore important to minimise or at least to monitor the performance degradation due to fouling in a heat exchanger at its early stages using any fouling detection methods without the need to stop the process. This information helps plan the cleaning or maintenance schedules with minimum impact on production and cost.

Several approaches have been developed to solve the problem of fouling detection in heat exchangers. The classical fouling detection method relies on physical examination of the heat exchanger. However, the examination of the coefficient of heat transfer or simultaneous examinations of pressure drops and mass flow rate requires the system to be in a steady state regime during the fouling detection. Ultrasonic or electric measuring tools can also be used to detect fouling but are only local methods (Withers, 1996).

FD has been presented by online estimation of system parameters (Jonsson and Palsson, 1991, Delmotte et al., 2013) in detecting fouling. This system parameter is represented by a fouling factor which is the measured relative thermal resistance introduced by the fouling film (Gudmundsson et al., 2008) and increases with time with increased thickness of the fouling film. The overall heat transfer coefficient (Astorga-Zaragoza et al., 2007, Astorga-Zaragoza et al., 2008) was estimated by an adaptive observer for heat exchanger maintenance. For a counter-flow heat exchanger, a Takagi-Sugeno observer with parameter estimation was designed by Delrot et al. (2012) to detect fouling. The EKF was utilised to detect fouling in heat transfers (Jonsson and Palsson, 1994, Jonsson et al., 2007, Lalot et al., 2007). Fuzzy observers have been employed to detect fouling of heat transfers to improve the accuracy and robustness of fouling detection (Delrot et al., 2012, Delmotte et al., 2013). PCA and a support vector machine (SVM) were used to extract the feature for detecting fouling in heat exchangers (Lalot and Lecoeuche, 2003). In Chen et al. (2004), a measurement of electric resistance is used to detect fouling build up in the heat exchanger. Batur et al. (2002) combined the LS parameter identification technique and the SVM learning algorithm for FD for heat exchangers. In Liang et al. (2017), the continuous-time Markov chain was used to detect fault propagation in the application of a heat exchanger system. Heat exchangers are modelled with neural networks (NN) in Lalot and Lecoeuche (2003), Lecoeuche et al. (2005), Lalot et al. (2007) and Mohanraj et al. (2015) and were used to detect online fouling but the results were restricted to known operating conditions (Tan et al., 2009). Hence, in this work, the overall heat transfer coefficient is obtained as an explicit function of the measurements. The fouling resistance is introduced to monitor heat exchanger performance. The detection of fouling is carried out by monitoring the changes in the fouling resistance value leading to informed decision making regarding when a heat exchanger needs preventive or corrective maintenance.

4.4.1 Mathematical model

The heat exchanger is used to transport heat from one fluid to another by conduction through solid walls. Consider the case of a counter-flow tubular heat exchanger model where the hot fluid flows in the inner tube while the cold fluid circulates in the annulus and we assume no heat loss to the surroundings. Also, the temperatures for hot and cold streams in each section are uniform and the specific heat capacities are constant. Hence, the heat exchanger model is obtained by dividing the heat exchanger into sections of the same length. Each section is numbered according to the corresponding direction of the fluid flow. The nonlinear ODEs for heat exchanger are given by Delmotte et al. (2013):

$$M_h c_h \frac{dT_{h\imath}}{dt} = \dot{m}_h c_h \left(T_{h\imath-1} - T_{hi}\right) - A_h U_{heat} \Delta T \tag{4.47}$$

$$M_c c_c \frac{dT_{c\imath}}{dt} = \dot{m}_c c_c \left(T_{c\imath-1} - T_{c\imath}\right) - A_c U_{heat} \Delta T \tag{4.48}$$

$$\Delta T = \left(\frac{T_{hin} + T_{h\iota}}{2}\right) - \left(\frac{T_{cin} + T_{c\iota}}{2}\right) \tag{4.49}$$

where ι denotes the section number in the heat exchanger, h denotes the hot fluid, and c denotes the cold fluid, $T_{h0} = T_{hin}$ and $T_{c0} = T_{cin}$. In these equations, A_h and A_c are the heat transfer areas, c_h and c_c are the specific heats, M_h and M_c are the masses of the fluids, $T_{h\iota}$ and $T_{c\iota}$ are the heat exchanger's temperatures in each section, T_{hin} is the inlet temperature in the hot fluid, T_{cin} is the inlet temperature in the cold fluid, $\dot{m}_h$ and $\dot{m}_c$ are mass flow rates of the hot and cold fluids, and U_{heat} is the overall heat transfer coefficient.

In this work, the heat exchanger is divided into two sections (Delrot et al., 2012) and the energy flow indicates by the arrows, as shown in Figure 4.21. Equations (4.47) to (4.49) become as follows:

$$\frac{dT_{h1}}{dt} = \frac{\dot{m}_h}{M_h}\left(T_{hin} - T_{h1}\right) + \frac{A_h U_{heat}}{2M_h c_h}\left(T_{c2} + T_{c1} - T_{h1} - T_{hin}\right) \tag{4.50}$$

$$\frac{dT_{h2}}{dt} = \frac{\dot{m}_h}{M_h}\left(T_{h1} - T_{h2}\right) + \frac{A_h U_{heat}}{2M_h c_h}\left(-T_{h2} + T_{c1} - T_{h1} + T_{hin}\right) \tag{4.51}$$

$$\frac{dT_{c1}}{dt} = \frac{\dot{m}_c}{M_c}\left(T_{cin} - T_{c1}\right) + \frac{A_c U_{heat}}{2M_c c_c}\left(T_{h2} - T_{c1} + T_{h1} - T_{cin}\right) \tag{4.52}$$

$$\frac{dT_{c2}}{dt} = \frac{\dot{m}_c}{M_c}\left(T_{c1} - T_{c2}\right) + \frac{A_c U_{heat}}{2M_c c_c}\left(-T_{c2} - T_{c1} + T_{h1} - T_{hin}\right) \tag{4.53}$$

From equations (4.50) to (4.53), T_{h1} and T_{c1} are the state variables of the heat exchanger model, T_{h2} and T_{c2} are output measurements and T_{hin} and T_{cin} are the input measurements.

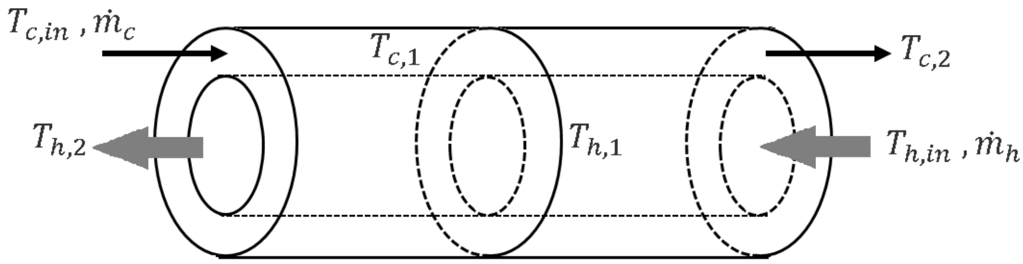

Figure 4.21 Decomposition of the heat exchanger in two sections

4.4.2 Fouling Scenario

In heat transfer, the fouling scenario can be computed by fouling resistance, R_f (Gudmundsson et al., 2008). Here, the overall heat transfer coefficient, U_{heat}, is expanded to introduce R_f. It is defined as follows (Delmotte et al., 2013):

$$\frac{1}{U_{heat}A_h} = \frac{1}{h_h A_h} + \frac{1}{h_c A_c} + \frac{R_f}{A_h} \tag{4.54}$$

where h_h and h_c denote the convection heat transfer coefficients for the hot and cold fluids. Thus, the fouling resistance can be defined as:

$$R_f = \frac{A_c h_c h_h - A_c h_c U_{heat} - A_h h_h U_{heat}}{A_c h_c h_h U_{heat}} \tag{4.55}$$

For a new heat exchanger, the fouling resistance, R_f, is zero and it increases with time with increased fouling.

4.4.3 Fault Detection problem

In this work, the overall heat transfer coefficient is obtained as an explicit function of measurements and estimated for FD. The objective of the FD problem is to minimise the difference between the measurements, $\hat{T}_{h2}(t_i)$ and $\hat{T}_{c2}(t_i)$, and the model predicted value, $T_{h2}(t_i)$ and $T_{c2}(t_i)$, to obtain U_{heat}, as described in Problem 4.4.1. The initial values of output measurements and state variables are given in equations (4.57) to (4.60).

Problem 4.4.1

$$\varepsilon_{FD} = \min_{U} \sum_{i \in I} \{(\hat{T}_{h2}(t_i) - T_{h2}(t_i))^2 + (\hat{T}_{c2}(t_i) - T_{c2}(t_i))^2\} \tag{4.56}$$

Subject to:

Equations (4.50) to (4.53)

$$T_{h1}(0) = 80\,^{\circ}\mathrm{C} \tag{4.57}$$

$$T_{h2}(0) = 50\,^{\circ}\mathrm{C} \tag{4.58}$$

$$T_{c1}(0) = 60\,^{\circ}\mathrm{C} \tag{4.59}$$

$$T_{c2}(0) = 55\,^{\circ}\mathrm{C} \tag{4.60}$$

$$t \in [0,10] \tag{4.61}$$

4.4.4 Parameter Estimation using MPP

The formulation and solution of the parameter estimation problem using MPP are summarised as follows:

(i) The nonlinear ODEs model in equations (4.50) to (4.53) is discretised using Euler's method and reformulated as the following algebraic equations:

$$T_{h1}(i+1) = T_{h1}(i) + \Delta t((\dot{m}_h / M_h)(T_{hin} - T_{h1}(i)) + (A_h U_{heat} / 2M_h c_h)(T_{c2}(i) + T_{c1}(i) - T_{h1}(i) - T_{hin})) \tag{4.62}$$

$$T_{h2}(i+1) = T_{h2}(i) + \Delta t((\dot{m}_h / M_h)(T_{h1}(i) - T_{h2}(i)) + (A_h U_{heat} / 2M_h c_h)(-T_{h2}(i) + T_{c1}(i) - T_{h1}(i) + T_{hin})) \tag{4.63}$$

$$T_{c1}(i+1) = T_{c1}(i) + \Delta t((\dot{m}_c / M_c)(T_{cin} - T_{c1}(i)) + (A_c U_{heat} / 2M_c c_c)(T_{h2}(i) - T_{c1}(i) + T_{h1}(i) - T_{cin})) \quad (4.64)$$

$$T_{c2}(i+1) = T_{c2}(i) + \Delta t((\dot{m}_c / M_c)(T_{c1}(i) - T_{c2}(i)) + (A_c U_{heat} / 2M_c c_c)(-T_{c2}(i) - T_{c1}(i) + T_{h1}(i) - T_{hin})) \quad (4.65)$$

(ii) Equations (4.62) to (4.65) are substituted in Problem 4.4.1 and the discrete-time FD problem is reformulated as the following NLP problem:

Problem 4.4.2

$$\varepsilon_{MPP} = \min_{U} \sum_{i \in I} \{(\hat{T}_{h2}(i+1) - T_{h2}(i+1))^2 + (\hat{T}_{c2}(i+1) - T_{c2}(i+1))^2\} \quad (4.66)$$

Subject to:

$$h_1 = T_{h1}(i+1) - T_{h1}(i) - \Delta t((\dot{m}_h / M_h)(T_{hin} - T_{h1}(i)) + (A_h U_{heat} / 2M_h c_h)(T_{c2}(i) + T_{c1}(i) - T_{h1}(i) - T_{hin})) = 0 \quad (4.67)$$

$$h_2 = T_{h2}(i+1) - T_{h2}(i) - \Delta t((\dot{m}_h / M_h)(T_{h1}(i) - T_{h2}(i)) + (A_h U_{heat} / 2M_h c_h)(-T_{h2}(i) + T_{c1}(i) - T_{h1}(i) + T_{hin})) = 0 \quad (4.68)$$

$$h_3 = T_{c1}(i+1) - T_{c1}(i) - \Delta t((\dot{m}_c / M_c)(T_{cin} - T_{c1}(i)) + (A_c U_{heat} / 2M_c c_c)(T_{h2}(i) - T_{c1}(i) + T_{h1}(i) - T_{cin})) = 0 \quad (4.69)$$

$$h_4 = T_{c2}(i+1) - T_{c2}(i) - \Delta t((\dot{m}_c / M_c)(T_{c1}(i) - T_{c2}(i)) + (A_c U_{heat} / 2M_c c_c)(-T_{c2}(i) - T_{c1}(i) + T_{h1}(i) - T_{hin})) = 0 \quad (4.70)$$

Equations (4.57) to (4.61)

(iii) Equations (4.67) and (4.69) are represented the set of nonlinear algebraic equations and these equations are substituted into Equation (4.66) to obtain:

$$G = (\hat{T}_{h2}(i+1) - (T_{h2}(i) + \Delta t((\dot{m}_h / M_h)(T_{h1}(i) - T_{h2}(i)) + (A_h U_{heat} / 2M_h c_h) \\ (-T_{h2}(i) + T_{c1}(i) - T_{h1}(i) + T_{hin}))))^2 + (\hat{T}_{c2}(i+1) - (T_{c2}(i) + \Delta t((\dot{m}_c / M_c) \\ (T_{c1}(i) - T_{c2}(i)) + (A_c U_{heat} / 2M_c c_c)(-T_{c2}(i) - T_{c1}(i) + T_{h1}(i) - T_{hin}))))^2 \tag{4.71}$$

The gradient of G with respect to overall heat transfer coefficient function, U_{heat} is given by:

$$\frac{\partial G}{\partial U_{heat}} = -(1/(c_h M_h))(A_h \Delta t T_{c1}(i) + A_h \Delta t T_{cin} - A_h \Delta t T_{h1}(i) - A_h \Delta t T_{h2}(i)) \\ (\hat{T}_{h2}(i+1) - (2c_h \Delta t \dot{m}_h T_{h1}(i) - 2c_h \Delta t \dot{m}_h T_{h2}(i) + 2c_h M_h T_{h2}(i) + \\ A_h \Delta t T_{c1}(i) U_{heat} + A_h \Delta t T_{cin} U_{heat} - A_h \Delta t T_{h1}(i) U_{heat} - \\ A_h \Delta t T_{h2}(i) U_{heat}) / (2c_h M_h)) - ((-A_c \Delta t T_{c1}(i) - A_c \Delta t T_{c2}(i) + \\ A_c \Delta t T_{h1}(i) + A_c \Delta t T_{hin})(\hat{T}_{c2}(i+1) - (2c_c \Delta t \dot{m}_c T_{c1}(i) - 2c_c \Delta t \dot{m}_c T_{c2}(i) + \\ 2c_c M_c T_{c2}(i) - A_c \Delta t T_{c1}(i) U_{heat} - A_c \Delta t T_{c2}(i) U_{heat} + A_c \Delta t T_{h1}(i) U_{heat} + \\ A_c \Delta t T_{hin} U_{heat}) / (2c_c M_c))) / c_c M_c \\ = 0 \tag{4.72}$$

(iv) The equality constraint in Equation (4.72) is solved analytically in Mathematica and the solution of U_{heat} is given by:

$$
\begin{aligned}
U_{heat} = -(&2c_c c_h(-A_c c_h \Delta t \dot{m}_c M_h^2 T_{c1}^2(i) - A_c c_h M_c M_h^2 T_{c1}(i) T_{c2}(i) + \\
&A_c c_h \Delta t \dot{m}_c M_h^2 T_{c2}^2(i) - A_c c_h M_c M_h^2 T_{c2}^2(i) + A_c c_h M_c M_h^2 T_{c1}(i) \hat{T}_{c2}(i+1) + \\
&A_c c_h M_c M_h^2 T_{c2}(i) \hat{T}_{c2}(i+1) + A_h c_c \Delta t \dot{m}_h M_c^2 T_{c1}(i) T_{h1}(i) + \\
&A_c c_h \Delta t \dot{m}_c M_h^2 T_{c1}(i) T_{h1}(i) - A_c c_h \Delta t \dot{m}_c M_h^2 T_{c2}(i) T_{h1}(i) + \\
&A_c c_h M_c M_h^2 T_{c2}(k) T_{h1}(i) - A_c c_h M_c M_h^2 \hat{T}_{c2}(i+1) T_{h1}(i) + \\
&A_h c_c \Delta t\, \dot{m}_h M_c^2 T_{cin} T_{h1}(i) - A_h c_c \Delta t \dot{m}_h M_c^2 T_{h1}^2(i) - A_h c_c \Delta t \dot{m}_h M_c^2 T_{c1}(i) T_{h2}(i) + \\
&A_h c_c M_c^2 M_h T_{c1}(i) T_{h2}(i) - A_h c_c \Delta t \dot{m}_h M_c^2 T_{cin} T_{h2}(i) + A_h c_c M_c^2 M_h T_{cin} T_{h2}(i) - \\
&A_h c_c M_c^2 M_h T_{h1}(i) T_{h2}(i) + A_h c_c \Delta t \dot{m}_h M_c^2 T_{h2}^2(i) - A_h c_c M_c^2 M_h T_{h2}^2(i) - \\
&A_h c_c M_c^2 M_h T_{c1}(i) \hat{T}_{h2}(i+1) - A_h c_c M_c^2 M_h T_{cin} \hat{T}_{h2}(i+1) + \\
&A_h c_c M_c^2 M_h T_{h1}(i) \hat{T}_{h2}(i+1) + A_h c_c M_c^2 M_h T_{h2}(i) \hat{T}_{h2}(i+1) + \\
&A_c c_h \Delta t \dot{m}_c M_h^2 T_{c1}(i) T_{hin} - A_c c_h \Delta t \dot{m}_c M_h^2 T_{c2}(i) T_{hin} + A_c c_h M_c M_h^2 T_{c2}(i) T_{hin} - \\
&A_c c_h M_c M_h^2 \hat{T}_{c2}(i+1)\, T_{hin})) / (\Delta t (A_h^2 c_c^2 M_c^2 T_{c1}^2(i) + A_c^2 c_h^2 M_h^2 T_{c1}^2(i) + \\
&2A_c^2 c_h^2 M_h^2 T_{c1}(i) T_{c2}(i) + A_c^2 c_h^2 M_h^2 T_{c2}^2(i) + 2A_h^2 c_c^2 M_c^2 T_{c1}(i) T_{cin} + \\
&A_h^2 c_c^2 M_c^2 T_{cin}^2 - 2A_h^2 c_c^2 M_c^2 T_{c1}(i) T_{h1}(i) - 2A_c^2 c_h^2 M_h^2 T_{c1}(i) T_{h1}(i) - \\
&2A_c^2 c_h^2 M_h^2 T_{c2}(i) T_{h1}(i) - 2A_h^2 c_c^2 M_c^2 T_{cin} T_{h1}(i) + A_h^2 c_c^2 M_c^2 T_{h1}^2(i) + \\
&A_c^2 c_h^2 M_h^2 T_{h1}^2(i) - 2A_h^2 c_c^2 M_c^2 T_{c1}(i) T_{h2}(i) - 2A_h^2 c_c^2 M_c^2 T_{cin} T_{h2}(i) + \\
&2A_h^2 c_c^2 M_c^2 T_{h1}(i) T_{h2}(i) + A_h^2 c_c^2 M_c^2 T_{h2}^2(i) - 2A_c^2 c_h^2 M_h^2 T_{c1}(i) T_{hin} - \\
&2A_c^2 c_h^2 M_h^2 T_{c2}(i) T_{hin} + 2A_c^2 c_h^2 M_h^2 T_{h1}(i) T_{hin} + A_c^2 c_h^2 M_h^2 T_{hin}^2))
\end{aligned}
\tag{4.73}
$$

Note that in this expression T_{h2} and T_{c2} are the output measurements, T_{hin} and T_{cin} are the input measurements, and T_{h1} and T_{c1} are available from state estimation.

(v) The overall heat transfer coefficient, U_{heat}, is calculated using the measurements. The estimates of the model parameter are thus obtained without the need to solve an online optimisation problem. The fouling resistance, R_f, in Equation (4.55) is then computed for FD to monitor the fouling performance and to decide when the heat exchanger needs preventive or corrective maintenance.

4.4.5 Clean Heat Exchanger Scenario

This section focuses on fouling detection of a water-to-water counter-flow heat exchanger. The length of the heat exchanger is 11 m and the inner and outer diameters are 14 mm and 18mm, respectively, for separating the fluids. The outer diameter of the annulus is given as 26 mm. The value of the given parameters is provided in Table 4.5 (Delrot et al., 2012). Two scenarios are considered, which are clean and fouling heat exchangers. For a clean heat exchanger scenario, the inlet hot and cold temperatures, T_{hin} and T_{cin}, are shown in Figure 4.22. The simulated output measurements, T_{h2} and T_{c2}, are shown in Figure 4.23 and the simulated state variables profile, T_{h1} and T_{c1}, for the clean exchanger scenario are shown in Figure 4.24.

The estimate of U_{heat}, is evaluated using the explicit function of measurements, given by Equation (4.73) with the step size, $\Delta t = 1$ s. The estimated U_{heat} is shown in Figure 4.25 and this figure demonstrates that the estimated model parameter value is consistent with the normal values in the clean exchanger. The detection of fault is carried out by monitoring the fouling resistance, R_f, as shown in Figure 4.26. We can see that the fouling resistance for this scenario is less than 0.0001 m^2 K/W. Hence, the heat exchanger is in a clean scenario.

Table 4.5. Parameters of the heat exchanger model

Parameter	**Value**	**Description**
$\dot{m}_h$	0.6 kg s^{-1}	mass flow rate of hot fluid
$\dot{m}_c$	0.55 kg s^{-1}	mass flow rate cold fluid
M_h	0.8382 kg	mass of the hot fluid
M_c	1.5055 kg	mass of the cold fluid
A_h	0.4838 m^2	heat transfer area in hot fluid
A_c	0.2764 m^2	heat transfer area in cold fluid
c_h	4193 J/(kg K)	specific heat in hot fluid
c_c	4193 J/(kg K)	specific heat in cold fluid

Parameter	Value	Description
h_h	1200 W/(m^2 K)	convection heat transfer coefficients for the hot fluid
h_c	1000 W/(m^2 K)	convection heat transfer coefficients for the cold fluid

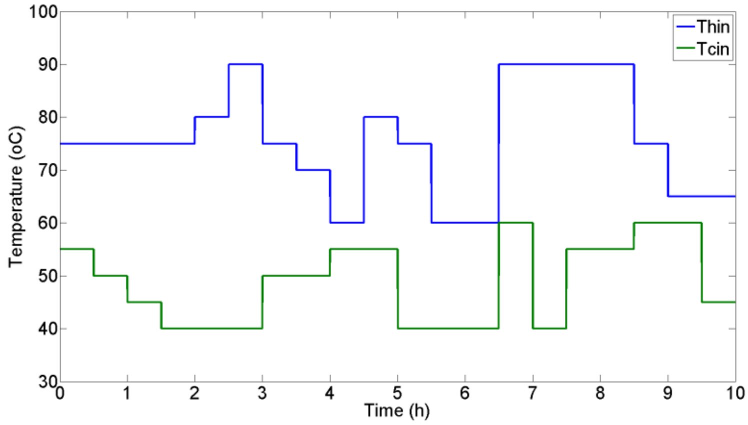

Figure 4.22 Inlet measurements to the heat exchanger

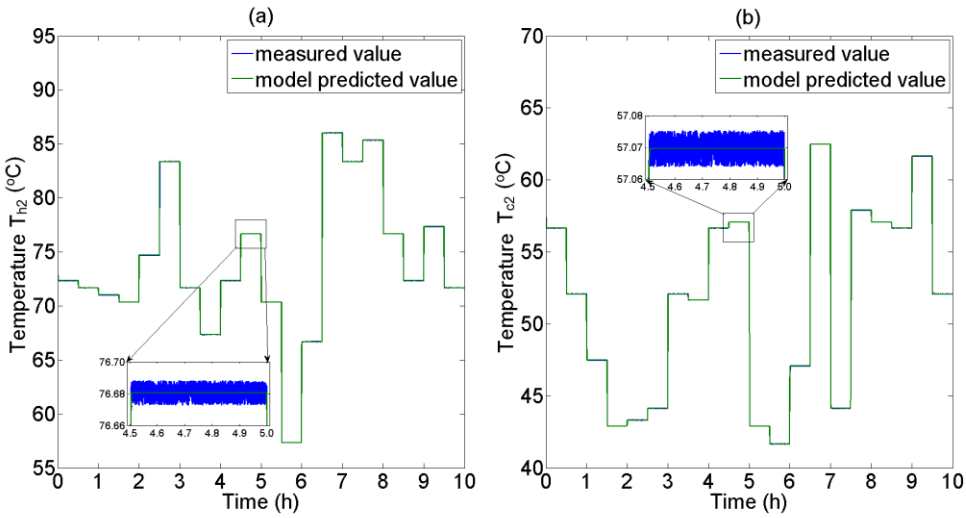

Figure 4.23 Outputs measurements of the clean exchanger (a) T_{h2}, the hot fluid temperature in section 2 (b) T_{c2}, the cold fluid temperature in section 2

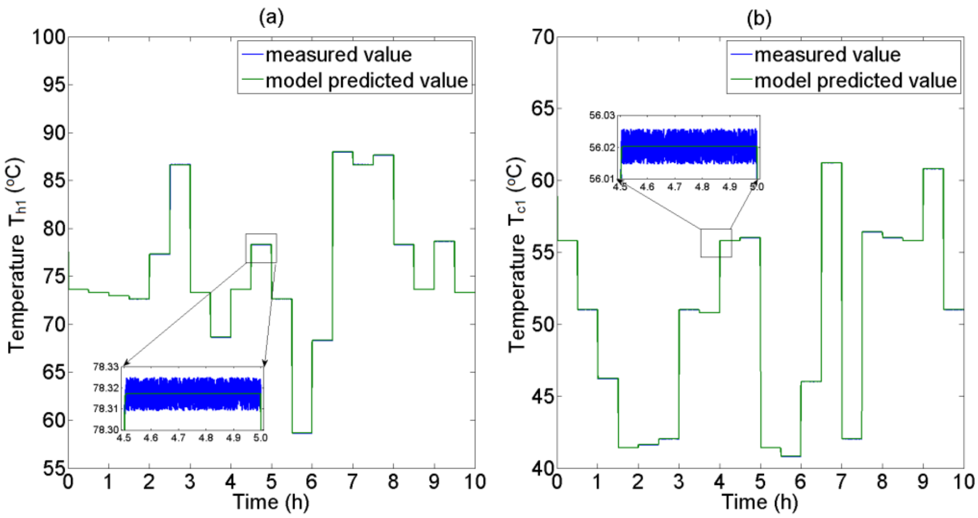

Figure 4.24 State variables profile of the clean exchanger (a) T_{h1}, the hot fluid temperature in section 1 (b) T_{c1}, the cold fluid temperature in section 1

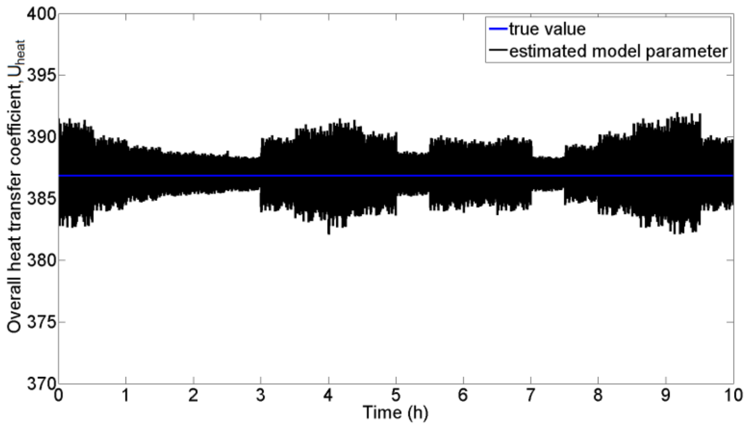

Figure 4.25 Estimated model parameter value for the clean heat exchanger scenario

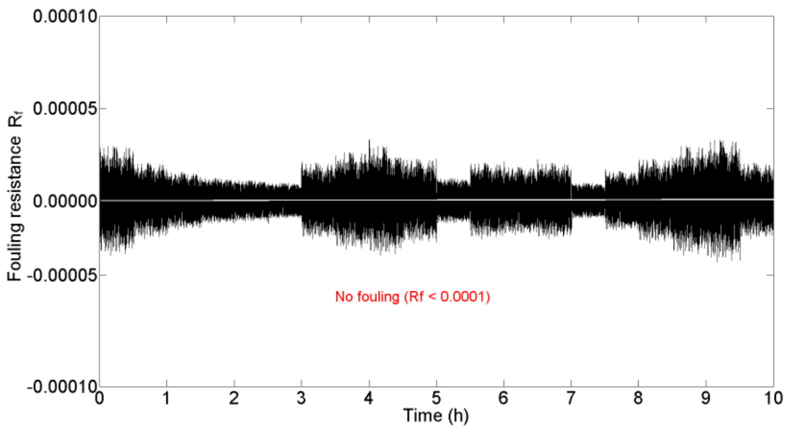

Figure 4.26 Estimated fouling factor, R_f, for the clean heat exchanger scenario

4.4.6 Fouling Heat Exchanger Scenario

An investigation for the faulty scenario was implemented for this case study. In this faulty scenario, the inlet hot and cold temperatures, T_{hin} and T_{cin}, are shown in Figure 4.22. The output measurements, T_{h2} and T_{c2}, and the state variables profile, T_{h1} and T_{c1}, for the fouling exchanger are shown in Figure 4.27 and Figure 4.28, respectively. In this scenario, the evaluation of faulty model parameter, U_{heat}, is calculated with the step size $\Delta t = 1$ s and shown in Figure 4.29. From this figure, we can see that the overall heat transfer coefficient has decreased with time.

The fouling resistance, R_f, is then calculated and monitored for FD to monitor the fouling performance and to decide when the heat exchanger needs preventive or corrective maintenance. For water, the value of the fouling factor is in the range of 0.0001 m^2 K/W, 0.0007 m^2 K/W (Cengel, 2003). Figure 4.30 shows the fouling resistance value of the faulty scenario. In the beginning, the heat exchanger is in the normal condition (clean exchanger), as shown in the figure that the fouling resistance, R_f, is less than 0.0001 m^2 K/W until 6.63 h. After that, the fouling resistance is increased to 0.0007 m^2 K/W until 9.49 hr. At this time, fouling resistance is increased. The condition of the heat exchanger changes and degradation is occurring. Moreover, it indicates that fouling has started to occur in the heat exchanger where maintenance work should be considered to either clean the exchanger or shut down the plant. Over 9.5 hr, the fouling resistance increases drastically and the heat exchanger is in a severe faulty condition and we need faster action for corrective maintenance. Note that the drastically increased in fouling is only to show the applicability of the proposed method in a dynamic state.

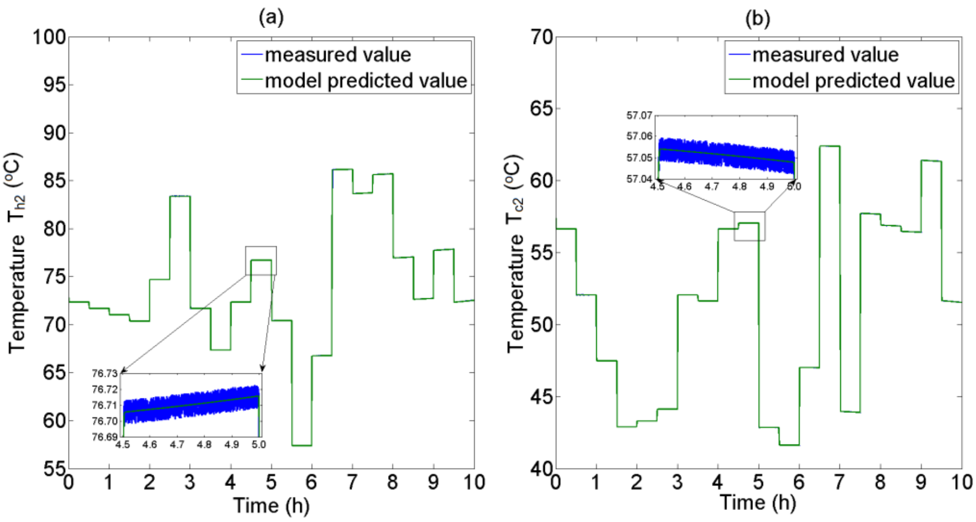

Figure 4.27 Outputs measurements of fouling exchanger (a) T_{h2}, the hot fluid temperature in section 2 (b) T_{c2}, the cold fluid temperature in section 2

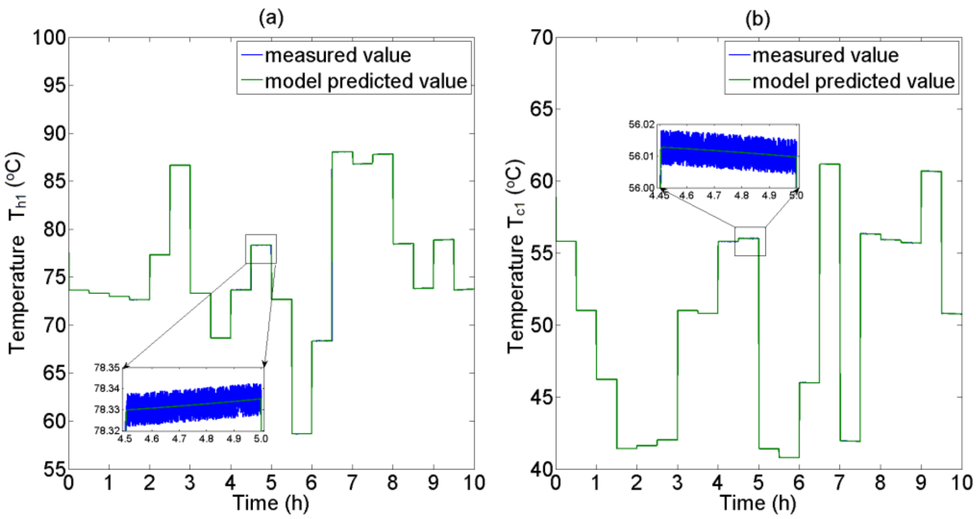

Figure 4.28 State variables profile of fouling exchanger (a) T_{h1}, the hot fluid temperature in section 1 (b) T_{c1}, the cold fluid temperature in section 1

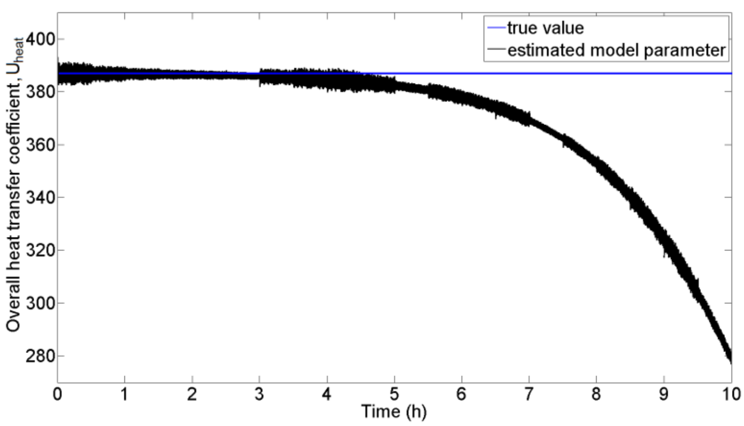

Figure 4.29 Estimated model parameter value for fouling heat exchanger scenario

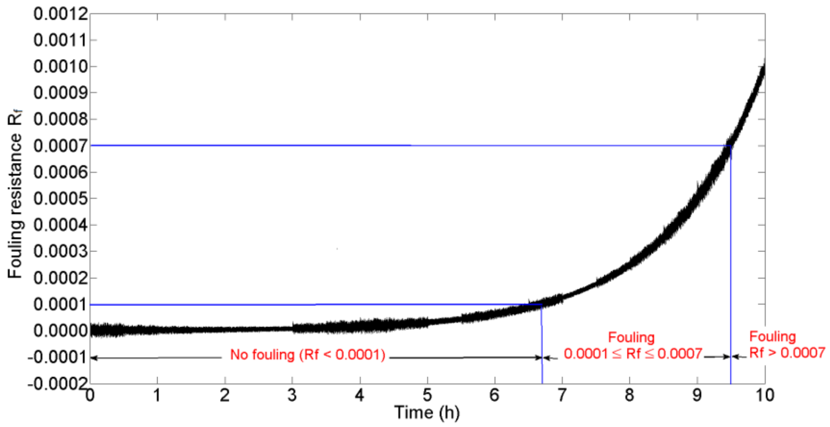

Figure 4.30 Estimated fouling factor, R_f , for fouling heat exchanger scenario

4.5 Glutamic Acid Fermentation Process

Fermentation is a process in which biomass gets converted into products such as alcohol or acid. The fermentation process is highly sensitive to small changes in operating limits that may affect the final product quality if changes happen during crucial stages of the operation. Therefore, the fermentation operation must be maintained within specific limits. The process of detecting and diagnosing a fault in industrial processes thus needs to be implemented early on in operation to maintain the product quality and reduce production cost. Several studies have demonstrated the fault detection in fermentation processes (Çinar et al., 2002, Monroy et al., 2012). For glutamic acid fermentation, the detection has been reported using wavelet analysis (Zhao et al., 1999, Ma et al., 2003), EKF, NN (Liu, 1999) and using SVM (Ma et al., 2007). However, the mentioned approaches are computationally demanding (Liu, 1999) and the diagnosis of fault becomes difficult when more than one fault occurs simultaneously.

In this work, a method to detect faults in batch glutamic acid fermentation processes is proposed. In batch fermentation as shown in Figure 4.31, all ingredients are mixed in a reactor at the beginning of the process and no additional substrate is added during the process. Once the fermentation has finished, the product is removed and the reactor is cleaned, and the fermentation process starts again. In the glutamic acid fermentation process (Ma et al., 2003), the state variables are represented by the concentration of biomass, substrate and product. These state variables cannot be measured online and therefore this methodology cannot be directly applied. Therefore, in this work, a methodology for the cases where the state variables cannot be measured but can be estimated from other measurable quantities such as pH, dissolved oxygen and temperature is presented. By monitoring the estimated kinetic model parameters, process faults can be detected and diagnosed. The estimated kinetic model parameters should be close to observed parameters when no fault is present, and any substantial discrepancy between the estimated and observed parameters indicates changes in the process and can be interpreted as a fault.

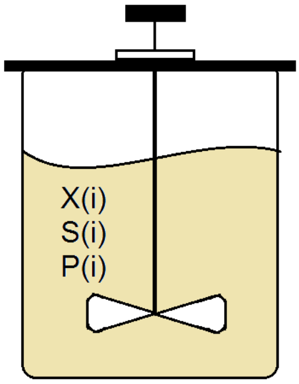

Figure 4.31 Batch fermentation diagram

4.5.1 Mathematical Model

The dynamic model of the glutamic acid fermentation process is as follows (Ma et al., 2003):

$$\frac{dX}{dt} = \mu X \tag{4.74}$$

$$\frac{dP}{dt} = bX\left(\frac{S}{K_s + S}\right) \tag{4.75}$$

$$\frac{dS}{dt} = -\frac{1}{Y_G}\frac{dX}{dt} - \frac{1}{Y_P}\frac{dP}{dt} - mX \tag{4.76}$$

$$\mu = \mu_m (1 - X / x_m) \tag{4.77}$$

where X, P and S are the concentrations of biomass, product and substrate, respectively. These state variables cannot be measured online but can be estimated from other measurable quantities such as pH, dissolved oxygen and temperature. μ is the growth rate of the biomass and is given in Equation (4.77). b is the maximum production rate, K_s is the saturation constant of the substrate, Y_G is the yield coefficient of the biomass, Y_P is the yield coefficient of the product, m is the maintenance coefficient of the biomass, μ_m is the maximum growth rate of the biomass and x_m is the maximum biomass concentration.

Any improper formulation or contamination in the fermentation will change the kinetic model parameters, such as μ_m and Y_P, and lead to a process fault. To ensure that the maximum possible product yield is obtained from the system, it is necessary to make sure that conditions within the fermenter remain closely fixed around a pre-specified ideal trajectory (Lennox et al., 2001). Hence, the kinetic model parameters, μ_m and Y_P, are estimated for FD. The parameter values used for the simulation of the reactor are shown in Table 4.6 (Ma et al., 2003).

Table 4.6. Model parameters for glutamic acid fermentation

Parameter	Value	Description
b	0.358 h^{-1}	maximum production rate
K_s	12.04 g/l	saturation constant of the substrate
Y_G	0.436	yield coefficient of biomass
Y_P	0.645	yield coefficient of the product

Parameter	Value	Description
m	0.105 h^{-1}	maintenance coefficient of the biomass
μ_m	0.767 h^{-1}	maximum growth rate of the biomass
x_m	6.43 g/l	maximum biomass concentration

4.5.2 Fault Detection Problem

In fermentation processes, the objective of this FD problem is to estimate the model parameters, μ_m and Y_P, such that the error, ε_{FD}, between the measurement of $\hat{X}(t_i)$, $\hat{P}(t_i)$ and $\hat{S}(t_i)$, and model predicted value of $X(t_i)$, $P(t_i)$ and $S(t_i)$, is minimised as in Problem 4.5.1. The initial values of state variables are given in equations (4.79) to (4.81).

Problem 4.5.1

$$\varepsilon_{FD} = \min_{\mu_m, Y_P} \sum_{i \in I} \{(\hat{X}(t_i) - X(t_i))^2 + (\hat{P}(t_i) - P(t_i))^2 + (\hat{S}(t_i) - S(t_i))^2\} \qquad (4.78)$$

Subject to:

Equations (4.74) to (4.77)

$$X(0) = 0.03 \text{ g/l} \qquad (4.79)$$

$$P(0) = 0 \text{ g/l} \qquad (4.80)$$

$$S(0) = 101.2 \text{ g/l} \qquad (4.81)$$

$$t \in [0, 15] \qquad (4.82)$$

4.5.3 Parameter Estimate using MPP

In this section, the kinetic model parameters, μ_m and Y_P, are obtained as explicit functions of measurements. The formulation and solution of the parameter estimation are summarised as follows:

(i) The nonlinear ODEs model in equations (4.74) to (4.77) is discretised using Euler's method and reformulated as the following algebraic equations:

$$X(i+1) = X(i) + \Delta t \mu_m \left(1 - \frac{X(i)}{x_m}\right) X(i) \tag{4.83}$$

$$P(i+1) = P(i) + \Delta t b X(i) \left(\frac{S(i)}{K_s + S(i)}\right) \tag{4.84}$$

$$S(i+1) = S(i) + \Delta t \left(-\frac{1}{Y_G} \mu_m \left(1 - \frac{X(i)}{x_m}\right) X(i) - \frac{1}{Y_P} b X(i) \left(\frac{S(i)}{K_s + S(i)}\right) - m X(i)\right) \tag{4.85}$$

(ii) The FD problem is reformulated as the following NLP problem:

Problem 4.5.2

$$\varepsilon_{MPP} = \min_{\mu_m, Y_P} \sum_{i \in I} \{(\hat{X}(i+1) - X(i+1))^2 + (\hat{P}(i+1) - P(i+1))^2 + (\hat{S}(i+1) - S(i+1))^2\} \tag{4.86}$$

Subject to:

$$h_1 = X(i+1) - X(i) - \Delta t \mu_m \left(1 - \frac{X(i)}{x_m}\right) X(i) = 0 \tag{4.87}$$

$$h_2 = P(i+1) - P(i) - \Delta t b X(i) \left(\frac{S(i)}{K_s + S(i)}\right) = 0 \tag{4.88}$$

$$h_3 = S(i+1) - S(i) - \Delta t \left(-\frac{1}{Y_G} \mu_m \left(1 - \frac{X(i)}{x_m}\right) X(i) - \frac{1}{Y_P} b X(i) \left(\frac{S(i)}{K_s + S(i)}\right) - m X(i)\right) = 0 \tag{4.89}$$

Equations (4.79) to (4.82)

(iii) Equations (4.87) to (4.89) are substituted into Equation (4.86) to obtain:

$$G = (\hat{X}(i+1) - (\Delta t \mu_m (1 - \frac{X(i)}{x_m}) X(i) + X(i)))^2 + (\hat{P}(i+1) - (\Delta t b X(i) \\ (\frac{S(i)}{K_s + S(i)}) + P(i)))^2 + (\hat{S}(i+1) - (\Delta t(-\frac{1}{Y_G} \mu_m (1 - \frac{X(i)}{x_m}) X(i) - \frac{1}{Y_P} b X(i) \\ (\frac{S(i)}{K_s + S(i)}) - mX(i)) + S(i)))^2 \tag{4.90}$$

The gradients of G with respect to μ_m and Y_P are given by:

$$\frac{\partial G}{\mu_m} = ((2X(i)(\Delta t X(i) - \Delta t x_m)(\hat{X}(i+1) + (X(i)(\Delta t \mu_m X(i) - x_m - \Delta t \mu_m x_m)) / \\ x_m)) / x_m) + ((2\Delta t X(i)(1 - X(i)/x_m)(\hat{S}(i+1) - \Delta t\,(S(i)/\Delta t - mX(i) - \\ (\mu_m X(i)(1 - X(i)/x_m)) / Y_G - (bS(i)X(i)) / ((K_s + S(i))\,Y_P)))) / Y_G) \\ = 0 \tag{4.91}$$

$$\frac{\partial G}{Y_P} = -(2b\Delta t S(i) X(i)(\hat{S}(i+1) - \Delta t(S(i)/\Delta t - mX(i) - (\mu_m\ X(i)(1 - X(i)/x_m)) \\ /Y_G - (bS(i)X(i)) / ((K_s + S(i))Y_P)))) / (\,(K_s + S)\,{Y_P}^2) \\ = 0 \tag{4.92}$$

(iv) The equality constraints in equations (4.91) and (4.92) are solved analytically in Mathematica, and the solution is given by:

$$\mu_m = \frac{(X(i) - \hat{X}(i+1))x_m}{\Delta t X(i)(X(i) - x_m)} \tag{4.93}$$

$$Y_P = \frac{b\Delta t S(i) X(i) Y_G}{(K_s + S(i))(X(i) - \hat{X}(i+1) + S(i)Y_G - \hat{S}(i+1)Y_G - \Delta t m X(i) Y_G} \tag{4.94}$$

(v) The kinetic model parameters, μ_m and Y_P, are obtained as an explicit function of measurements given in equations (4.93) and (4.94). The residuals of model parameters are monitored for FD.

4.5.4 Fault-free Scenario

In this work, the whole fermentation period is of about 15 hours. The state variables of X, P and S are estimated from other measurable quantities such as pH, dissolved oxygen and temperature using simulated data in Table 4.6. In the fault-free scenario, the simulated measurement value of $\hat{X}$, $\hat{P}$ and $\hat{S}$, and simulated model predicted value of X, P and S, for each concentration are shown in Figure 4.32. The kinetic model parameter values are estimated by equations (4.93) and (4.94) with step size, $\Delta t = 1$ min. The results for the estimated kinetic model parameters, μ_m and Y_p, are shown in Figure 4.33. The figure shows that estimated kinetic model parameters are close to the true value. The FD for this system is continued by monitoring the residual of each estimated model parameter. The results are shown in Figure 4.34. Here, we can see that the residual is less than 5% threshold value for both estimate model parameters, μ_m and Y_p. Hence, no fault was detected.

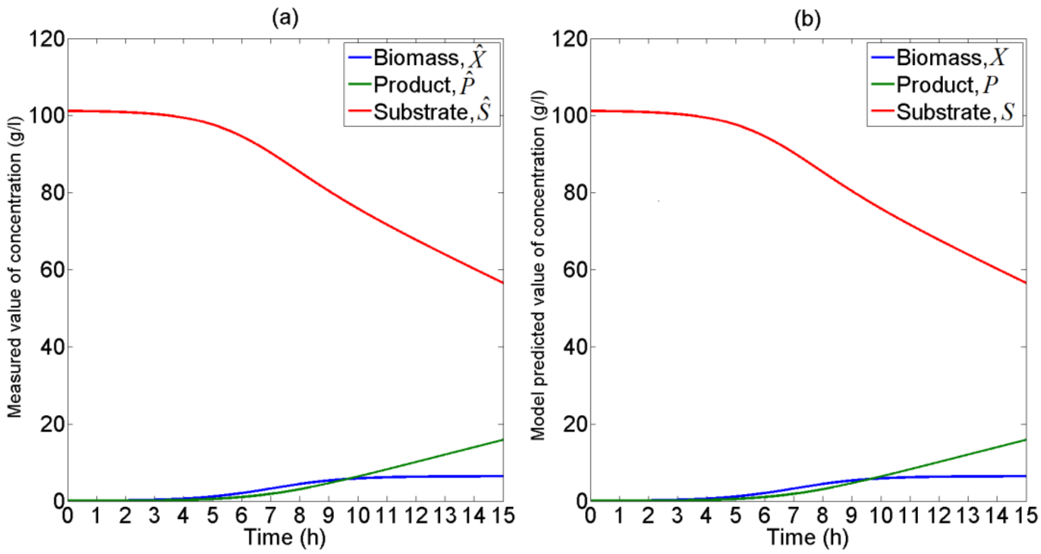

Figure 4.32 State variables profile of concentration in fault-free scenario
(a) Measured value (b) Model predicted value

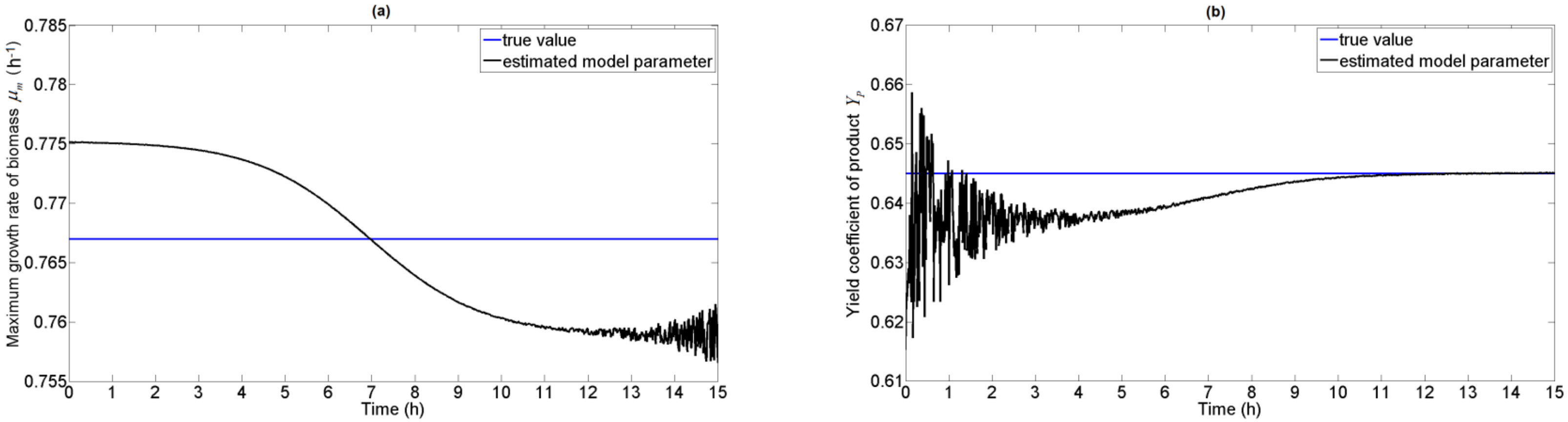

Figure 4.33 Estimated model parameters for fault-free scenario (a) Maximum growth rate of the biomass, μ_m (b) Yield coefficient of product, Y_p

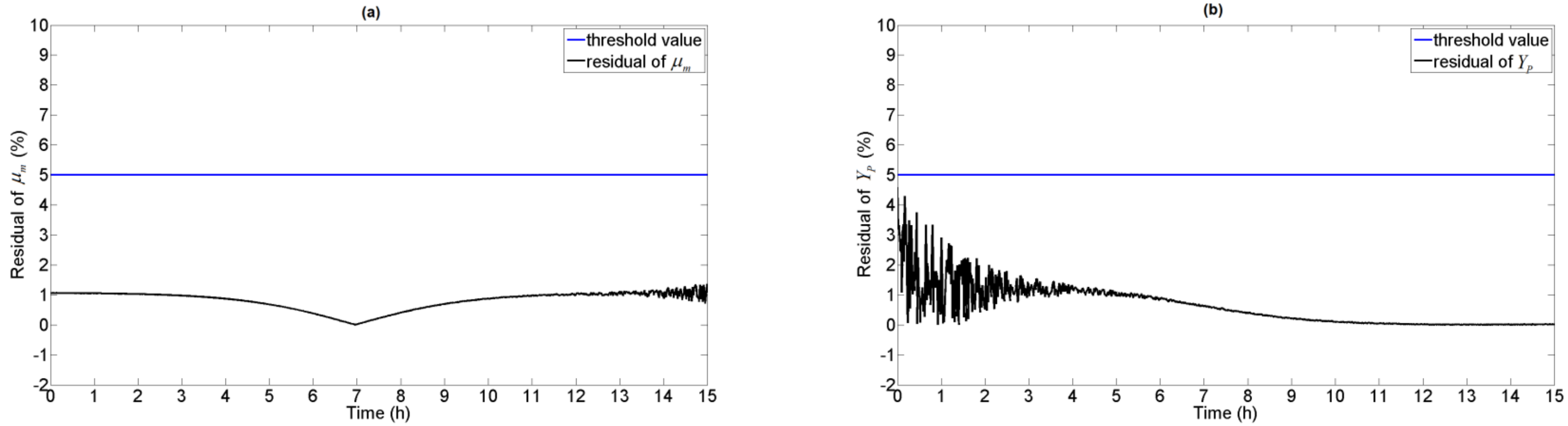

Figure 4.34 Residual evaluation of estimated model parameters for fault-free scenario (a) Maximum growth rate of the biomass, μ_m (b) Yield coefficient of product, Y_p

4.5.5 Faulty Scenario

An investigation for a faulty scenario was implemented for this case study. To demonstrate the application of parameter estimation for faulty processes, the kinetic model parameters are changed as shown in Table 4.7 and the model is simulated to obtain data for parameter estimation. Figure 4.35 shows the measured value and model predicted value of biomass, product and substrate concentrations for a faulty scenario. The estimated maximum growth rate of the biomass, μ_m, and yield coefficient of the product, Y_p, are shown in Figure 4.36 with step size, $\Delta t = 1$ min. From these figures, we can see that, after 5 h, the estimated values of μ_m and Y_p change for each faulty scenario. The detection of fault is carried out by monitoring the value of the residuals of model parameters, and the result is shown in Figure 4.37. These figures show that, at 5 hr of the fermentation processes, the percentage of residual of μ_m and Y_p are increased to 8% and 16%, respectively. It indicates that process faults have started occurring in the fermentation process since the residuals for μ_m and Y_p are more than 5% of the threshold value. The fault is declared in the system after 5h. The MPP based parameter estimation is thus able to accurately and quickly identify the faults in the glutamic acid fermentation system.

Table 4.7 Faulty scenarios for glutamic acid fermentation

Fault kinetic parameter	Fault 1	Fault 2	Fault 3	Fault 4
maximum growth rate of the biomass, μ_m	-10 %	10 %	- 15 %	15 %
yield coefficient of product, Y_p	- 10 %	10 %	- 15 %	15 %
Starting time for change	5 h	5 h	5 h	5 h

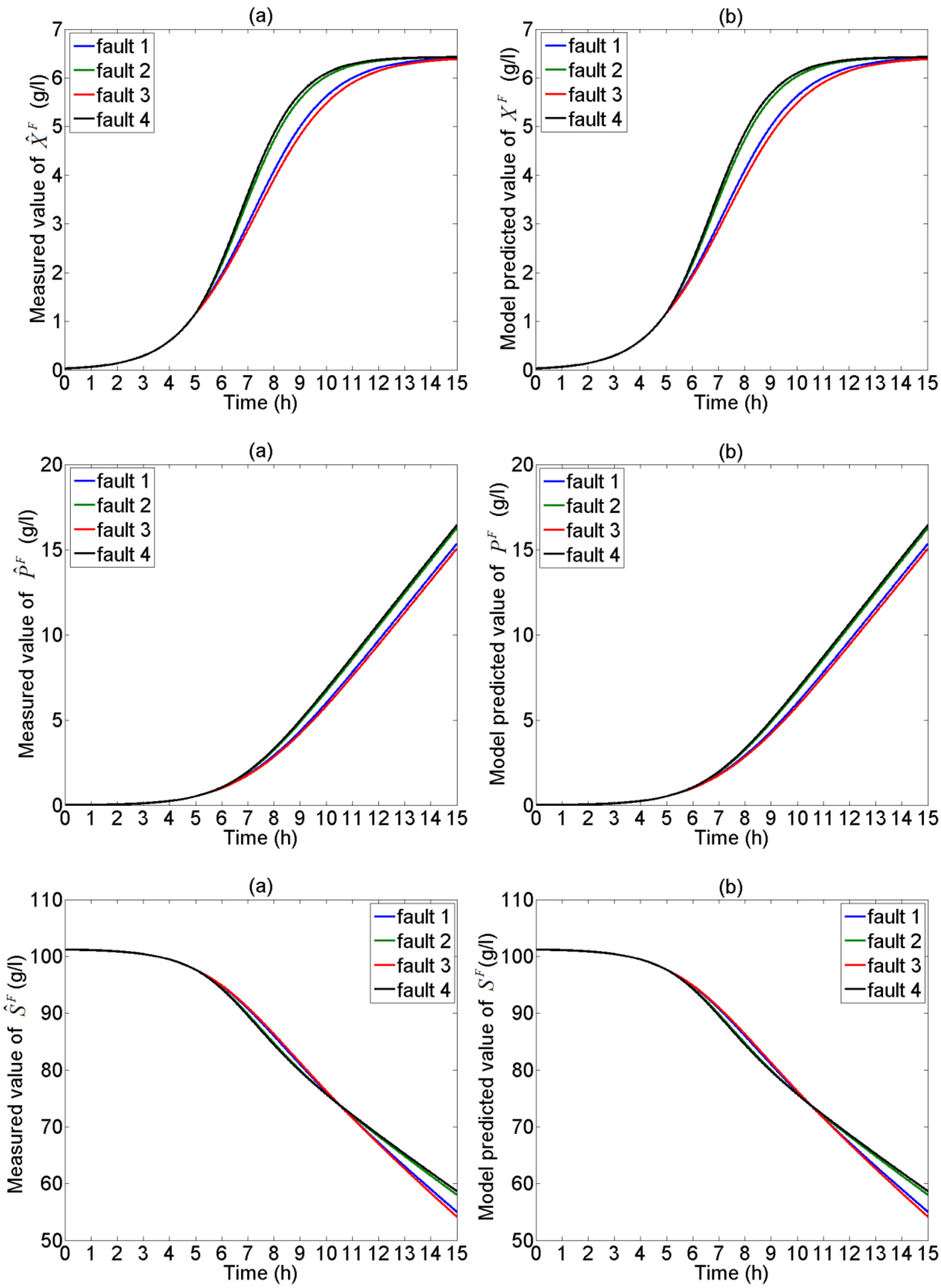

Figure 4.35 State variables profile of concentrations in faulty scenarios
(a) Measured value (b) Model predicted value

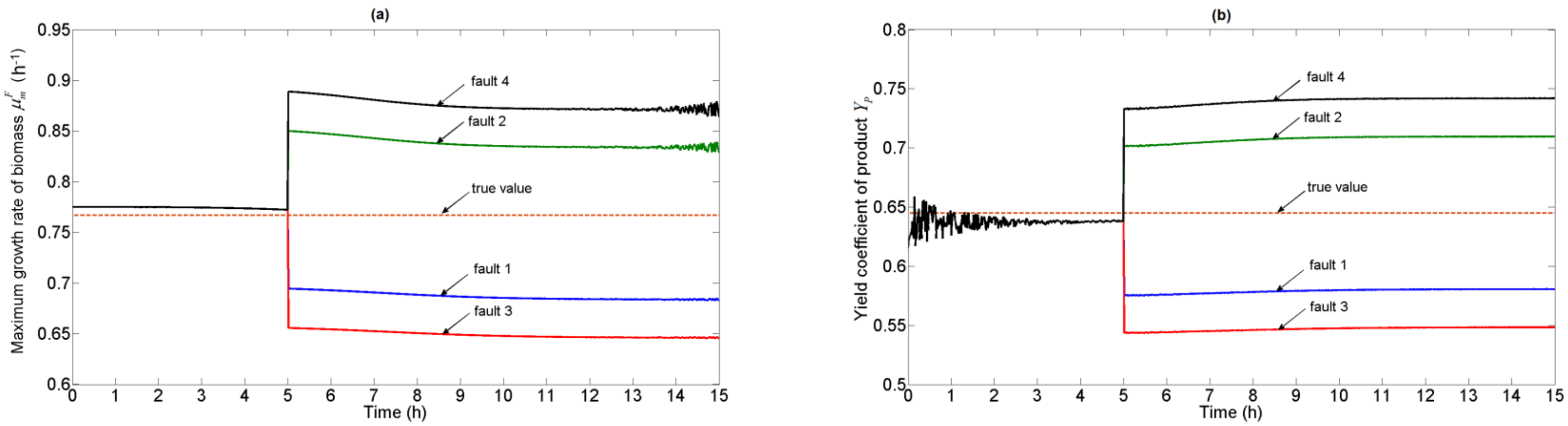

Figure 4.36 Estimated model parameters for faulty scenarios (a) Maximum growth rate of the biomass, μ_m (b) Yield coefficient of product, Y_p

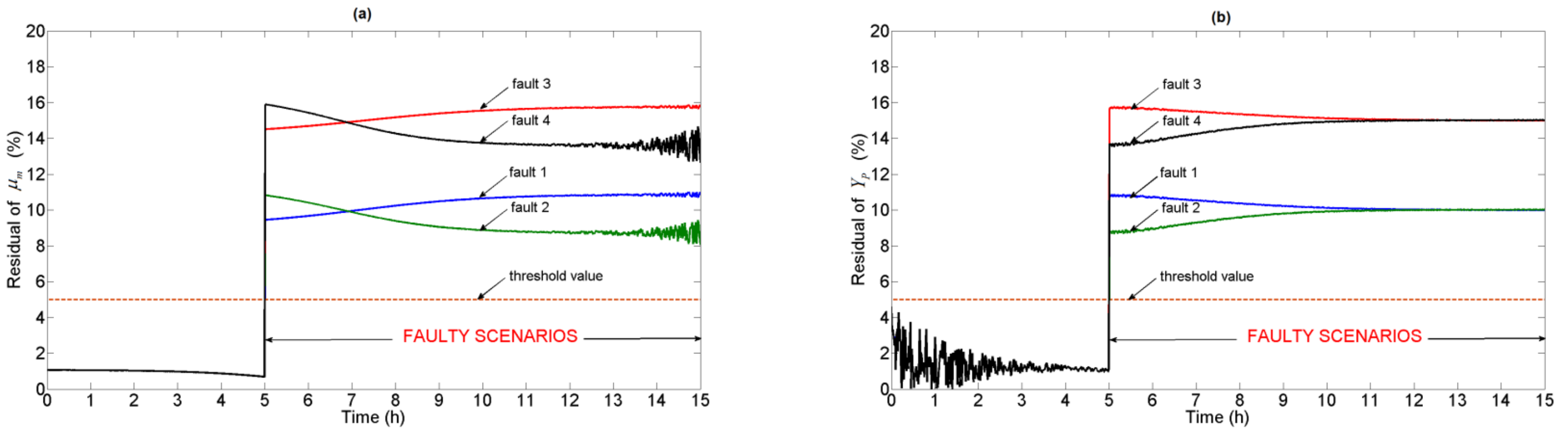

Figure 4.37 Residual evaluation of estimated model parameters for faulty scenarios (a) Maximum growth rate of the biomass, μ_m (b) Yield coefficient of product, Y_p

4.6 Wastewater treatment system

Wastewater treatment (WWT) is a process of converting wastewater into bilge water that can be returned to the environment and used for domestic and industrial applications. The wastewater treatment includes mechanical, biological, sludge and water chemical treatments. To maintain the operation and the quality of the effluent, proper operation and monitoring of wastewater treatment plants are required. FD has become an important step in process monitoring and involving a process of detecting faults and diagnosing their causes and location. This is achieved by continuously monitoring the systems to detect any abnormal conditions, and then evaluating and diagnosing the conditions with faults.

FD methods for sensor faults in a WWT system normally use data-based methods, such as NN and PCA. The NN model is presented in Maier and Dandy (2000) to model a wastewater treatment system. In Caccavale et al. (2010), faults in nitrogen sensors are detected by estimating the concentration of NO and NH by using a NN. Honggui et al. (2014) showed how sensor faults are diagnosed using a fuzzy NN to estimate dissolved oxygen concentration, pH, chemical oxygen demand and total nutrients. In Lee et al. (2004), the kernel PCA is used to extract nonlinear relations in process variables and it shows better performance than linear PCA in process monitoring. Adaptive PCA is used in Baggiani and Marsili-Libelli (2009) to compare the current plant operation with an exact performance based on a reference data set and the sensor outputs. In Sanchez-Fernández et al. (2015), a distributed PCA is applied to detect faults by minimising the communication cost between the blocks in WWTP. The classical PCA is presented using the Benchmark Simulation Model No.1 in Garcia-Alvarez et al. (2009), Chen et al. (2016a) and Carlsson and Zambrano (2016). The combined use of PCA in data pre-processing and ANN has been presented in Gontarski et al. (2000) to improve network performance. Besides, FD in WWT has been discussed using an observer-based method in Fragkoulis et al. (2011), where multiple actuators and sensors fault are detected.

In an aerobic WWT system, respiration rate is used as an indicator of biological activity for monitoring and control (Brouwer et al., 1994, Wimberger and

Verde, 2008). The respiration rate is affected by the initial condition of the biomass, substrate concentration in the inflow and extrinsic growth behaviour of the biomass on inhibitory substrates. In Wimberger and Verde (2008), FD is performed by evaluating the detectability and isolability for analytical- and signal-based methodologies using information from the application of sensitivity theory. However, respiration rate depends on intermittent aeration patterns and the calculation can only be evaluated during air-off periods (Carlsson, 1993, Carlsson et al., 1994, Lindberg and Carlsson, 1996). In this work, we propose FD in a WWT system by detecting and monitoring the kinetic parameters of extrinsic growth behaviour by using MPP. The kinetic parameters of concentration of substrate in the inflow, inhibition coefficient and specific growth rate will be obtained as an explicit function of measurements using MPP and monitored for FD. The kinetic parameters are estimated online repeatedly and, if there is a discrepancy between the estimated parameters and the 'true' parameters, it gives an indication of faults.

4.6.1 Mathematical Model

In this work, an aerobic sequencing batch reactor for a fed-batch reactor is presented. These bioprocesses use activated sludge and provide treatment for wastewater in five stages: Fill, React, Settle, Decant and Idle, as shown in Figure 4.38. During the fill stage, the wastewater is directed into the tank and mixed with the sludge from previous cycles. At the reacting stage, the air is provided as a function of the aeration process that consumes the waste as nutrition and produces carbon dioxide, nitrates and nitrites. After a sufficient amount of reaction time, the aeration process is stopped and the sludge is allowed to settle. At the decanting stage, the treated wastewater is removed from the reactor and the sludge that remains is reused for the next cycle. The reactor then enters the idle stage, which is used to prepare the SBR for the next cycle.

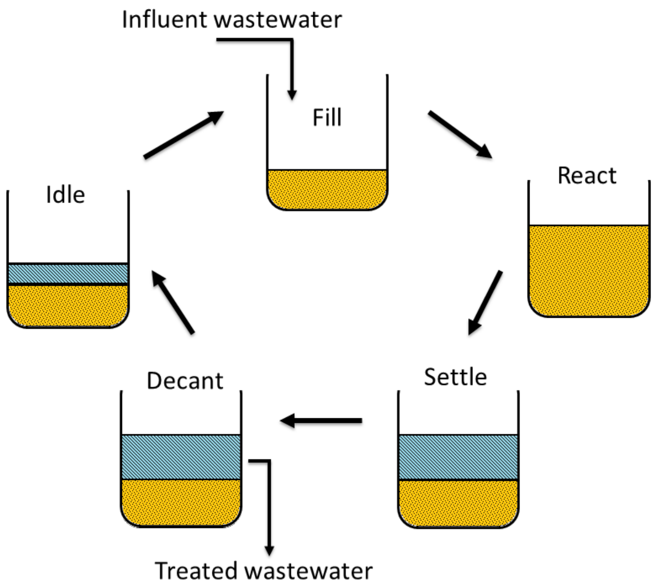

Figure 4.38 The sequencing batch reactor stages

The aerobic sequencing batch reactor system involves aerobic growth and endogenous respiration reactions given by:

$$\text{Growth: } S_c + S_o \rightarrow X \tag{4.95}$$

$$\text{Endogenous respiration: } S_c + X \rightarrow X \tag{4.96}$$

where S_c represents the concentrations of organic matter, S_o is the concentration of dissolved oxygen and X represents the concentrations of biomass. The mathematical model of the process is given by the following equations (Fibrianto et al., 2008):

$$\frac{dX}{dt} = \mu X - \frac{q_{in}}{V} X \tag{4.97}$$

$$\frac{dS_c}{dt} = -k_1 \mu X + \frac{q_{in}}{V}\left(S_{c_{in}} - S_c\right) \tag{4.98}$$

$$\frac{dS_o}{dt} = -k_2 \mu X - bX + \frac{q_{in}}{V}\left(S_{o_{in}} - S_o\right) + k_{La}\left(S_{o_s} - S_o\right) \tag{4.99}$$

$$\frac{dV}{dt} = q_{in} \tag{4.100}$$

$$\mu = \frac{\mu_o S_c}{K_s + S_c + \frac{S_c^{\,2}}{K_i}} \tag{4.101}$$

where μ is growth rate, q_{in} is inlet flow rate, V is volume, k_1 is yield coefficients of the substrate to biomass, k_2 is yield coefficients of oxygen to biomass, b is endogenous respiration coefficient, $S_{c_{in}}$ is concentration of substrate in the inflow, $S_{o_{in}}$ is concentration of dissolved oxygen in the inflow, S_{o_s} is dissolved oxygen mass at saturation and k_{La} is oxygen mass transfer coefficient. The growth rate is represented by the Haldane model and is given by Equation (4.101). In this model, the fed-batch process operation constantly maintains the growth rate around its maximum because the growth rate of microorganisms is inhibited by the substrate. The parameter values for the wastewater treatment process reaction are shown in Table 4.8 (Fibrianto et al., 2008).

Table 4.8. Model parameters for wastewater treatment process reaction

Parameter	Value	Description
$S_{c_{in}}$	168 mg/l	concentration of substrate in the inflow
$S_{o_{in}}$	0 mg/l	concentration of dissolved oxygen in the inflow
q_{in}	14.8mg/l	inflow rate
S_{o_s}	6 mg/l	dissolved oxygen mass at saturation
k_1	3.7	conversion coefficient of the substrate to biomass
k_2	1.0363	conversion coefficient of oxygen to biomass
b	0.0059 h^{-1}	endogenous respiration coefficient
k_{La}	16.8 h^{-1}	oxygen mass transfer coefficient
K_i	3.753 mg/l	inhibition coefficient
K_s	60 mg/l	half-saturation coefficient
μ_o	0.1916 h^{-1}	specific growth rate

4.6.2 Fault Detection Problem

In this work, a method to estimate and detect faults in wastewater treatment is presented. The related kinetic parameters for the faulty process to be investigated are the concentration of substrate in the inflow, $S_{c_{in}}$, inhibition coefficient, K_i, and specific growth rate, μ_o, which affect the respiration rate. Thus, these kinetic parameters will be obtained as an explicit function of measurements using MPP and monitored for FD. The objective of this FD problem is to estimate the model parameters such that the error, ε_{FD}, between the measurement $\hat{X}(t_i)$, $\hat{S}_c(t_i)$ and $\hat{S}_o(t_i)$ and model predicted value of $X(t_i)$, $S_c(t_i)$ and $S_o(t_i)$ is minimised as shown in Problem 4.6.1. The initial values of state variables are given in equations (4.103) to (4.106).

Problem 4.6.1

$$\varepsilon_{FD} = \min_{Sc_{in}, K_i, \mu_o} \sum_{i \in I} \{(\hat{X}(t_i) - X(t_i))^2 + (\hat{S}_c(t_i) - S_c(t_i))^2 + (\hat{S}_o(t_i) - S_o(t_i))^2 + (\hat{V}(t_i) - V(t_i))^2\} \tag{4.102}$$

Subject to:

Equations (4.97) to (4.101)

$$X(0) = 4734 \text{ mg/l} \tag{4.103}$$

$$S_c(0) = 0 \text{ mg/l} \tag{4.104}$$

$$S_o(0) = 6 \text{ mg/l} \tag{4.105}$$

$$V(0) = 3 \text{ l} \tag{4.106}$$

$$t \in [0, 6] \tag{4.107}$$

4.6.3 Parameter Estimate using MPP

The formulation and solution of the parameter estimation problem using MPP are summarised as follows:

i) The nonlinear ODEs model equations (4.97) to (4.101) is discretised using Euler's method and reformulated as the following algebraic equations:

$$X(i+1) = \Delta t\left(\frac{X(i)}{\Delta t} + \frac{S_c(i)\mu_o X(i)}{K_s + S_c(i) + \dfrac{S_c(i)^2}{K_i}} - \frac{q_{in}}{V(i)}\right) \tag{4.108}$$

$$S_c(i+1) = \Delta t\left(\frac{S_c(i)}{\Delta t} + \frac{q_{in}\,(-S_c(i) + S_{c_{in}})}{V(i)} - \frac{k_1 S_c(i)\mu_o X(i)}{K_s + S_c(k) + \dfrac{S_c(i)^2}{K_i}}\right) \tag{4.109}$$

$$\begin{aligned} S_o(i+1) = \Delta t\Bigg(&\frac{S_o(i)}{\Delta t} + k_{la}(-S_o(i) + S_{o_s}) + \\ &\frac{q_{in}\,(-S_o(i) + S_{o_{in}})}{V(i)} - bX(i) - \frac{k_2 S_c(i)\mu_o X(i)}{K_s + S_c(i) + \dfrac{S_c(i)^2}{K_i}}\Bigg) \end{aligned} \tag{4.110}$$

$$V(i+1) = \Delta t q_{in} + V(i) \tag{4.111}$$

(ii) The FD problem is reformulated as the following NLP problem:

Problem 4.6.2

$$\begin{aligned} \varepsilon_{MPP} = \min_{Sc_{in}, K_i, \mu_o} \sum_{i\in I} \{ &(\hat{X}(i+1) - X(i+1))^2 + (\hat{S}_c(i+1) - S_c(i+1))^2 + \\ &(\hat{S}_o(i+1) - S_o(i+1))^2 + (\hat{V}(i+1) - V(i+1))^2 \} \end{aligned} \tag{4.112}$$

Subject to:

$$\begin{aligned} h_1 &= X(i+1) - X(i) - (\Delta t S_c(i)\mu_o X(i)) / (K_s + S_c(i) + (S_c(i)^2)/K_i) + \\ &\quad (\Delta t q_{in})/V(i) \\ &= 0 \end{aligned} \tag{4.113}$$

$$\begin{aligned} h_2 &= S_c(i+1) - \Delta t(S_c(i) - (\Delta t q_{in}(-S_c(i) + S_{c_{in}}))/V(i)) + \\ &\quad (\Delta t k_1 S_c(i)\mu_o X(i)) \; / (K_s + S_c(i) + S_c(i)^2 / K_i) \\ &= 0 \end{aligned} \tag{4.114}$$

$$h_3 = S_o(i+1) - S_o(i) - \Delta t k_{la}(-S_o(i) + S_{o_s}) - (\Delta t q_{in}(-S_o(i) + S_{o_{in}}))/V(i) + \Delta t b X(i) + (\Delta t k_2 S_c(i)\mu_o X(i))/(K_s + S_c(i) + S_c(i)^2/K_i) = 0 \quad (4.115)$$

$$h_4 = V(i+1) - \Delta t q_{in} - V(i) = 0 \quad (4.116)$$

Equations (4.103) to (4.107)

(iii) Equations (4.113) to (4.116) are substituted into Equation (4.112) to obtain:

$$G = (\hat{X}(i+1) - (X(i) + (\Delta t S_c(i)\mu_o X(i))/(K_s + S_c(i) + (S_c(i)^2)/K_i) - (\Delta t q_{in})/V(i)))^2 + (\hat{S}_c(i+1) - (\Delta t(S_c(i) + (\Delta t q_{in}(-S_c(i) + S_{c_{in}}))/V(i)) - (\Delta t k_1 S_c(i)\mu_o X(i))/(K_s + S_c(i) + S_c(i)^2/K_i)))^2 + (\hat{S}_o(i+1) - (S_o(i) + \Delta t k_{la}(-S_o(i) + S_{o_s}) + (\Delta t q_{in}(-S_o(i) + S_{o_{in}}))/V(i) - \Delta t b X(i) - (\Delta t k_2 S_c(i)\mu_o X(i))/(K_s + S_c(i) + S_c(i)^2/K_i)))^2 + (\hat{V}(i+1) - (\Delta t q_{in} + V(i)))^2 \quad (4.117)$$

The gradients of G with respect to estimate model parameters, $S_{c_{in}}$, K_i and μ_o, are given by:

$$\frac{\partial G}{\partial S_{c_{in}}} = -((2\Delta t q_{in}(\hat{S}_c(i+1) - \Delta t(S_c(i)/\Delta t + (q_{in}(-S_c(i) + S_{c_{in}}))/V(i) - (k_1 S_c(i) u_o X(i))/(K_s + S_c(i) + S_c(i)^2/K_i))))/V) = 0 \quad (4.118)$$

$$\frac{\partial G}{\partial K_i} = (2\Delta t k_1 S_c(i)^3 u_o X(i)(\hat{S}_c(i+1) - \Delta t(S_c(i)/\Delta t + (q_{in}(-S_c(i) + S_{c_{in}}))/V(i) - (k_1 S_c(i) u_o X(i))/(K_s + S_c(i) + S_c(i)^2/K_i))))/(K_i^2(K_s + S_c(i) + S_c(i)^2/K_i)^2) + (2\Delta t k_2 S_c(i)^3 u_o X(i)(\hat{S}_o(i+1) - \Delta t(S_o(i)/\Delta t + k_{la}(-S_o(i) + S_{o_s}) + (q_{in}(-S_o(i) + S_{o_{in}}))/V(i) - bX(i) - (k_2 S_c(i) u_o X(i))/(K_s + S_c(i) + S_c(i)^2/K_i))))/(K_i^2(K_s + S_c(i) + S_c(i)^2/K_i)^2) - (2\Delta t S_c(i)^3 u_o X(i)(-\Delta t(X(i)/\Delta t + (S_c(i) u_o X(i))/(K_s + S_c(i) + S_c(i)^2/K_i) - (q_{in} X(i))/V(i)) + \hat{X}(i+1)))/(K_i^2(K_s + S_c(i) + S_c(i)^2/K_i)^2) = 0 \quad (4.119)$$

$$\frac{\partial G}{\partial \mu_o} = (2\Delta t k_1 S_c(i) X(i)(\hat{S}_c(i+1) - \Delta t(S_c(i)/\Delta t + (q_{in}(-S_c(i) + S_{c_{in}}))/$$
$$V(i) - (k_1 S_c(i) u_o X(i))/(K_s + S_c(i) + S_c(i)^2/K_i))))/$$
$$(K_s + S_c(i) + S_c(i)^2/K_i) + (2\Delta t k_2 S_c(i) X(i)(\hat{S}_o(i+1) - \Delta t(S_o(i)/\Delta t +$$
$$k_{la}(-S_o(i) + S_{o_s}) + (q_{in}(-S_o(i) + S_{o_{in}}))/V(i) - bX(i) -$$
$$(k_2 S_c(i) u_o X(i))/(K_s + S_c(i) + S_c(i)^2/K_i))))/$$
$$(K_s + S_c(i) + S_c(i)^2/K_i) - (2\Delta t S_c(i) X(i)$$
$$(-\Delta t(X(i)/\Delta t + (S_c(i) u_o X(i))/(K_s + S_c(i) + S_c(i)^2/K_i) -$$
$$(q_{in} X(i))/V(i)) + \hat{X}(i+1)))/(K_s + S_c(i) + S_c(i)^2/K_i)$$
$$= 0 \tag{4.120}$$

(iv) The equality constraints in equations (4.118) to (4.120) are solved analytically in Mathematica, and the solution is given by:

$$S_{c_{in}} = (\Delta t^2 K_i K_s q_{in}{}^2 S_c(i) + \Delta t^2 K_i q_{in}{}^2 S_c(i)^2 + \Delta t^2 q_{in}{}^2 S_c(i)^3 -$$
$$\Delta t K_i K_s q_{in} S_c(i) V(i) - \Delta t K_i q_{in} S_c(i)^2 V(i) - \Delta t q_{in} S_c(i)^3 V(i) +$$
$$\Delta t K_i K_s q_{in} \hat{S}_c(i+1) V(i) + \Delta t K_i q_{in} S_c(i) \hat{S}_c(i+1) V(i) +$$
$$\Delta t(i) q_{in} S_c(i)^2 \hat{S}_c(i+1) V(i) + \Delta t^2 k_1 K_i q_{in} S_c(i) u_o V(i) X(i))/$$
$$(\Delta t^2 q_{in}{}^2 (K_i K_s + K_i S_c(i) + S_c(i)^2)) \tag{4.121}$$

$$K_i = -(S_c(i)^2 (\Delta t k_1 q_{in} S_c(i) - \Delta t k_1 q_{in} S_{c_{in}} + \Delta t k_2 q_{in} S_o(i) - \Delta t k_2 q_{in} S_{o_{in}} -$$
$$k_1 S_c(i) V(i) + k_1 \hat{S}_c(i+1) V(i) - k_2 S_o(i) V(i) + \Delta t k_2 k_{la} S_o(i) V(i) +$$
$$k_2 \hat{S}_o(i+1) V(i) - \Delta t k_2 k_{la} S_{o_s} V(i) - \Delta t q_{in} X(i) + V(i) X(i) +$$
$$b\Delta t k_2 V(i) X(i) - V(i) \hat{X}(i+1))) \ / (\Delta t k_1 K_s q_{in} S_c(i) + \Delta t k_1 q_{in} S_c(i)^2 -$$
$$\Delta t k_1 K_s q_{in} S_{c_{in}} - \Delta t k_1 q_{in} S_c(i) S_{c_{in}} + \Delta t k_2 K_s q_{in} S_o(i) + \Delta t k_2 q_{in} S_c(i) S_o(i) -$$
$$\Delta t k_2 K_s q_{in} S_{o_{in}} - \Delta t k_2 q_{in} S_c(i) S_{o_{in}} - k_1 K_s S_c(i) V(i) - k_1 S_c(i)^2 V(i) +$$
$$k_1 K_s \hat{S}_c(i+1) V(i) + k_1 S_c(i) \hat{S}_c(i+1) V(i) - k_2 K_s S_o(i) V(i) +$$
$$\Delta t k_2 k_{la} K_s S_o(i) V(i) - k_2 S_c(i) S_o(i) V(i) + \Delta t k_2 k_{la} S_c(i) S_o(i) V(i) +$$
$$k_2 K_s \hat{S}_o(i+1) V(i) + k_2 S_c(i) \hat{S}_o(i+1) V(i) - \Delta t k_2 k_{la} K_s S_{o_s} V(i) -$$
$$\Delta t k_2 k_{la} S_c(i) S_{o_s} V(i) - \Delta t K_s q_{in} X(i) - \Delta t q_{in} S_c(i) X(i) +$$
$$K_s V(i) X(i) + b\Delta t k_2 K_s V(i) X(i) + S_c(i) V(i) X(i) + b\Delta t k_2 S_c(i) V(i) X(i) +$$
$$\Delta t S_c(i) u_o V(i) + \Delta t k_1{}^2 S_c(i) u_o V(i) X(i) + \Delta t k_2{}^2 S_c(i) u_o V(i) X(i) -$$
$$K_s V(i) \hat{X}(i+1) - S_c(i) V(i) \hat{X}(i+1)) \tag{4.122}$$

$$
\begin{aligned}
\mu_o = {} & ((2\Delta t k_1 S_c(i)^2 X(i))/(K_s + S_c(i) + S_c(i)^2/K_i) - \\
& (2\Delta t k_1 S_c(i)\hat{S}_c(i+1)X(i))/(K_s + S_c(i) + S_c(i)^2/K_i) + \\
& (2\Delta t k_2 S_c(i)S_o(i)X(i))/(K_s + S_c(i) + S_c(i)^2/K_i) - \\
& (2\Delta t k_2 S_c(i)\hat{S}_o(i+1)X(i))/(K_s + S_c(i) + S_c(i)^2/K_i) + \\
& (2\Delta t^2 k_2 k_{la} S_c(i)(-S_o(i) + S_{o_s})X(i))/(K_s + S_c(i) + S_c(i)^2/K_i) + \\
& (2\Delta t^2 k_1 q_{in} S_c(i)(-S_c(i) + S_{c_{in}})X(i))/((K_s + S_c(i) + S_c(i)^2 / \\
& K_i)V(i)) + (2\Delta t^2 k_2 q_{in} S_c(i)(-S_o(i) + S_{o_{in}})X(i))/((K_s + S_c(i) + \\
& S_c(i)^2/K_i)V(i)) - (2\Delta t S_c(i)X(i)^2)/(K_s + S_c(i) + S_c(i)^2/K_i) - \\
& (2b\Delta t^2 k_2 S_c(i)X(i)^2)/(K_s + S_c(i) + S_c(i)^2/K_i) + (2\Delta t^2 q_{in} S_c(i)X^2)/ \\
& ((K_s + S_c(i) + S_c(i)^2/K_i)V(i)) + (2\Delta t S_c(i)X(i)\hat{X}(i+1))/ \\
& (K_s + S_c(i) + S_c(i)^2/K_i))/((2\Delta t^2 S_c(i)^2 X(i)^2)/(K_s + S_c(i) + \\
& S_c(i)^2/K_i)^2 + (2\Delta t^2 k_1{}^2 S_c(i)^2 X(i)^2)/(K_s + S_c(i) + S_c(i)^2/K_i)^2 + \\
& (2\Delta t^2 k_2{}^2 S_c(i)^2 X(i)^2)/(K_s + S_c(i) + S_c(i)^2/K_i)^2)
\end{aligned} \tag{4.123}
$$

(v) In this case study, only single fault was assumed to occur at any time to solve the problem for the non-square system of ODEs model. Hence, as an example in Equation (4.121), the symbolic solution $S_{c_{in}}$ was obtained in terms of model parameters, K_i and μ_o, and state variables, X, S_c, and V. In Equation (4.122), the symbolic solution K_i was obtained in terms of model parameters, $S_{c_{in}}$ and μ_o, and state variables, X, S_c, S_o, and V. The solution μ_o was obtained in terms of model parameters, $S_{c_{in}}$ and K_i, and state variables, X, S_c, S_o, and V, as shown in Equation (4.123).

4.6.4 Fault-free Scenario

In the fault-free scenario, the simulated measured values and model predicted values for concentrations are shown in Figure 4.39 using simulated data from Table 4.8. The estimated model parameters, $S_{c_{in}}$, K_i and μ_o, are calculated using equations (4.121) to (4.123) with step size, $\Delta t = 0.001$ h. The estimated model parameters are shown in Figure 4.40. The result shows that the estimated model parameter is close to true model parameters. The detection of fault is carried out by monitoring the value of the residual of model parameters and shown in Figure 4.41. We can see that no fault was detected in any of the parameters since the residual is less than the threshold. The threshold is chosen as 10% from the nominal system.

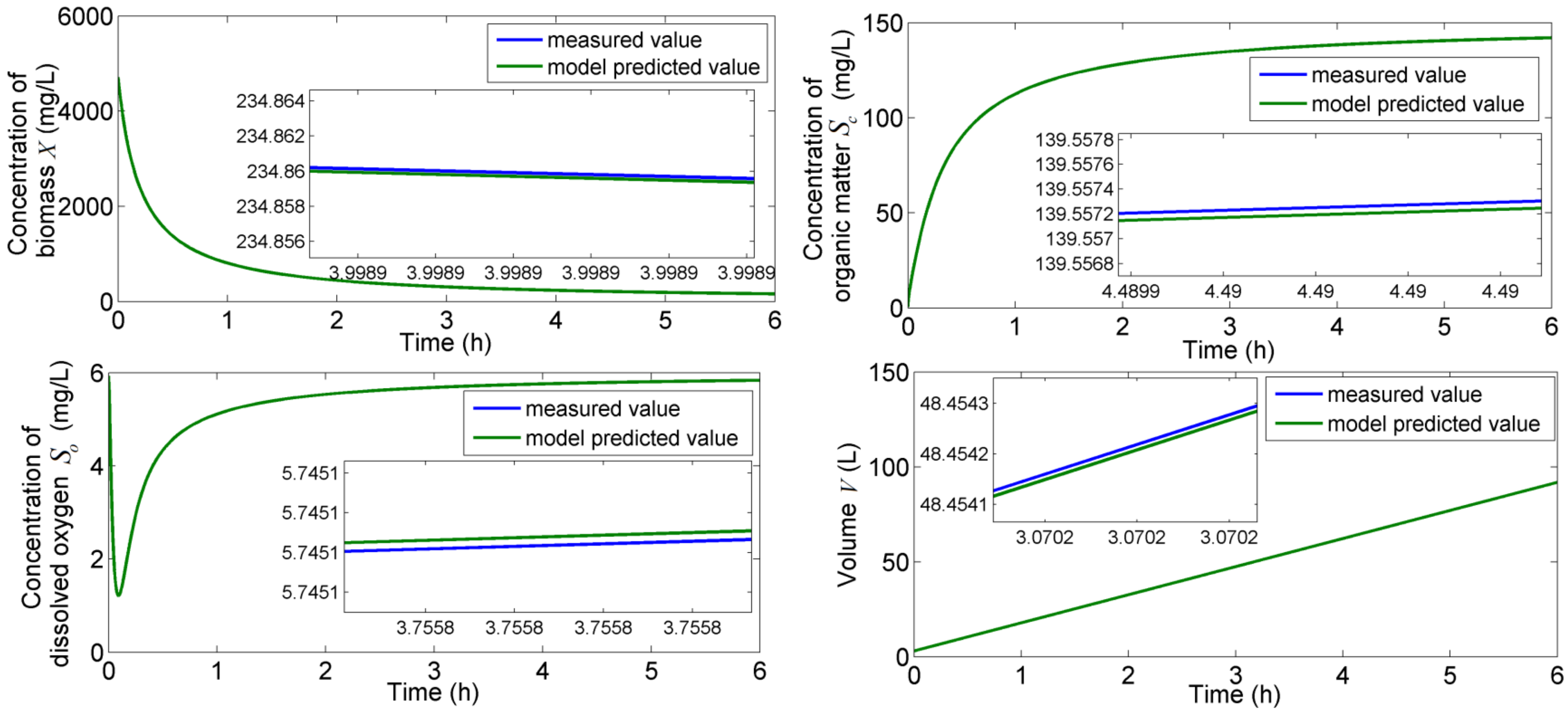

Figure 4.39 State variables profile for fault-free scenario

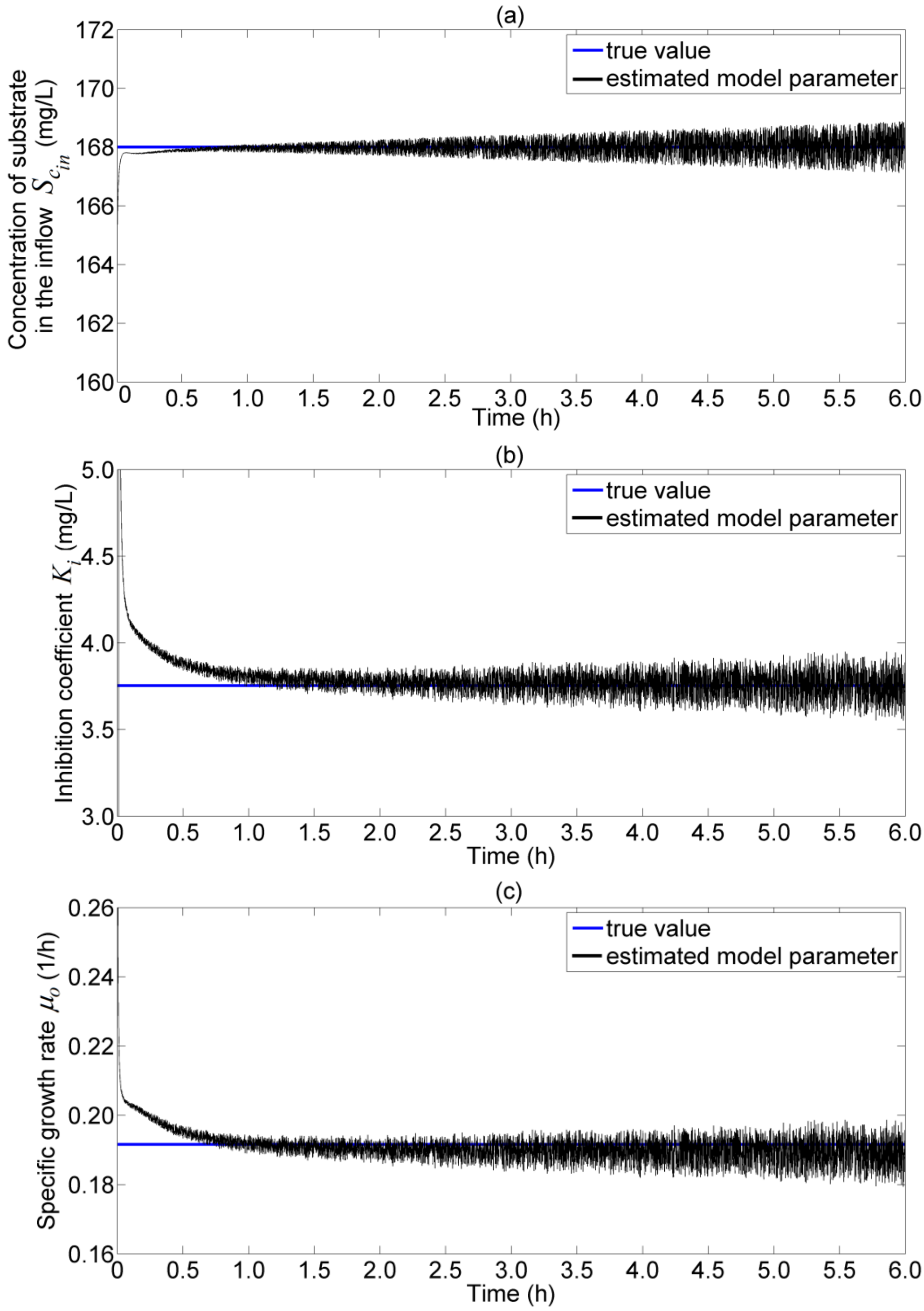

Figure 4.40 Estimated model parameters for fault-free scenario (a) Concentration of substrate in the inflow, $S_{c_{in}}$, (b) Inhibition coefficient, K_i, and (c) Specific growth rate, μ_o

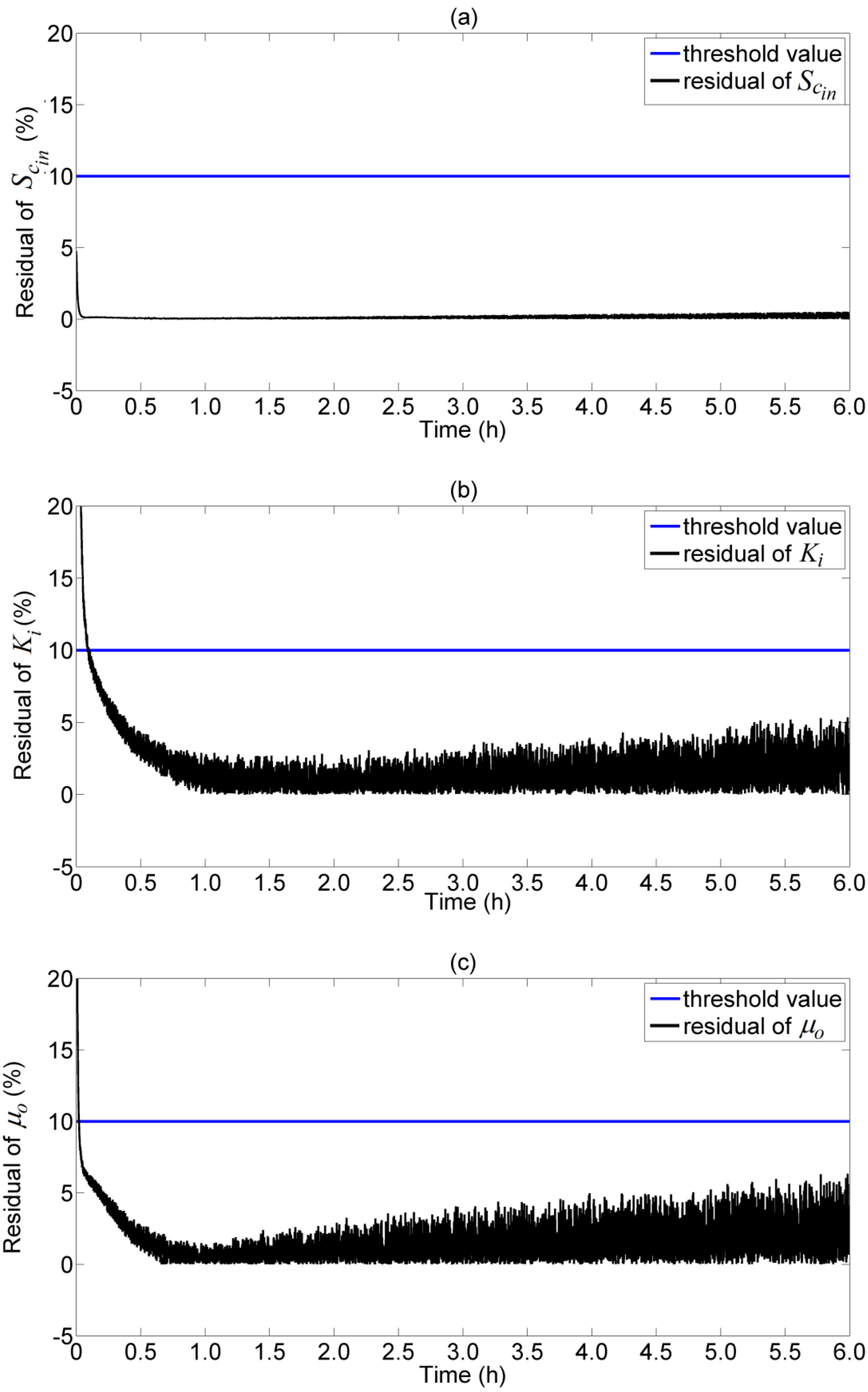

Figure 4.41 Residual of estimated model parameters for fault-free scenario (a) Concentration of substrate in the inflow, $S_{c_{in}}$, (b) Inhibition coefficient, K_i, and (c) Specific growth rate, μ_o

4.6.5 Faulty Scenario

Investigation for the faulty scenarios was implemented where the percentages of changes in kinetic parameters are given in Table 4.9. In this case study, a single fault is assumed to occur at any time. The step size is given as $\Delta t = 0.001$ h. For faulty scenario 1, only fault in $S_{c_{in}}$ is affected in the system for a 30% decrease. We can see that the estimated parameter, $S_{c_{in}}$, in Figure 4.42 has decreased from 168 mg/l to 118 mg/l after 3 h. The residual of $S_{c_{in}}$ is shown in Figure 4.43 and monitored for FD. This result indicates that the fault occurs at 3 h as the residual of $S_{c_{in}}$ is more than a threshold value of 10%. In faulty scenario 2, the fault in K_i increases 20% at 3h, but no fault was introduced in $S_{c_{in}}$ and μ_o. Using the symbolic solution of K_i, the estimated parameters of K_i is calculated and the result is shown in Figure 4.44. We can see that the estimated parameter, K_i, has increased from 3.753 mg/l to 4.878 mg/l after 3 h and the residual of K_i is monitored for FD. Figure 4.45 shows that, after 3 h, the residual of K_i is more than 10% of the threshold and therefore the fault is declared in the system related to inhibition coefficient. In fault scenario 3, only parameter fault of μ_o is assumed to occur in the system. Hence, the estimated parameter using the symbolic solution of μ_o is evaluated and calculated as shown in Figure 4.46. This result shows that the estimated model parameter is decreased from 0.1916 h^{-1} to 0.1341 h^{-1} at 3 h. The residual of μ_o is monitored for FD and the result is shown in Figure 4.47. The system has been declared as faulty scenario at 3 h where the fault is occurred in μ_o.

Table 4.9. Faulty scenario for the wastewater treatment system

Fault kinetic model parameter	Scenario 1	Scenario 2	Scenario 3
Concentration of substrate in the inflow, $S_{c_{in}}$	- 30%	-	-
Inhibition coefficient, K_i	-	+ 30 %	-
Specific growth rate, μ_o	-	-	- 30%

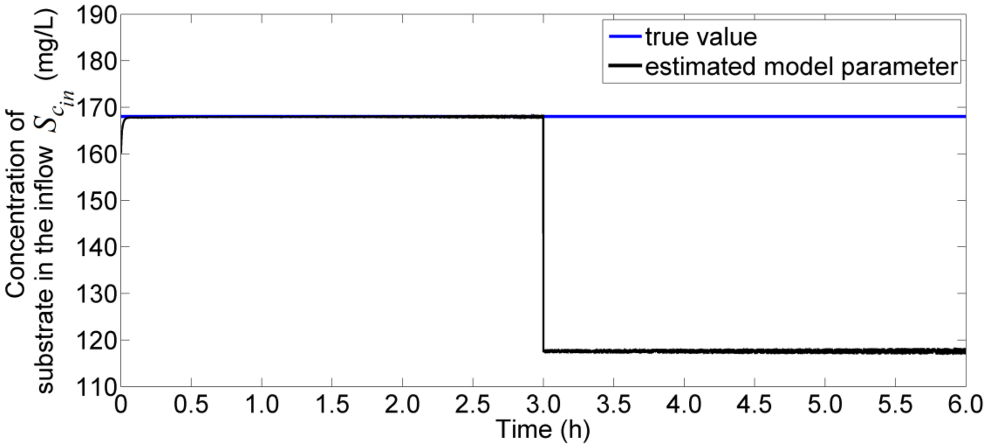

Figure 4.42 Estimated model parameter, $S_{c_{in}}$, for faulty scenario 1

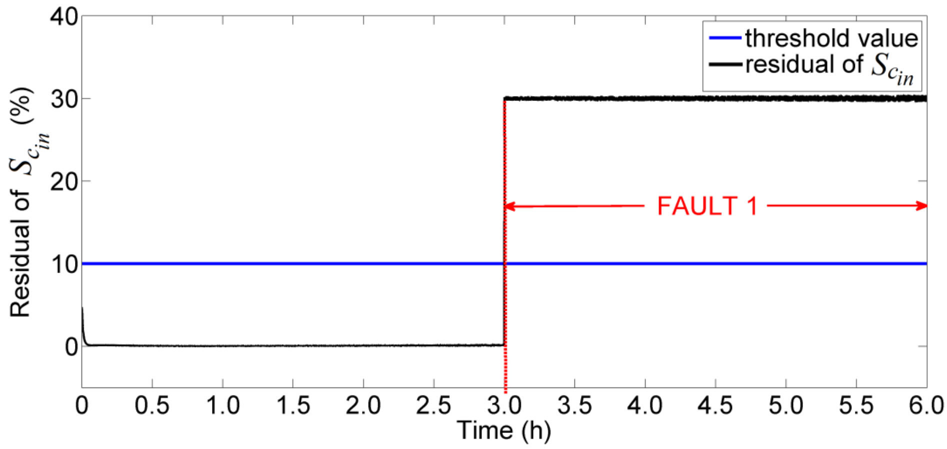

Figure 4.43 Residual of the estimated model parameter, $S_{c_{in}}$, for faulty scenario 1

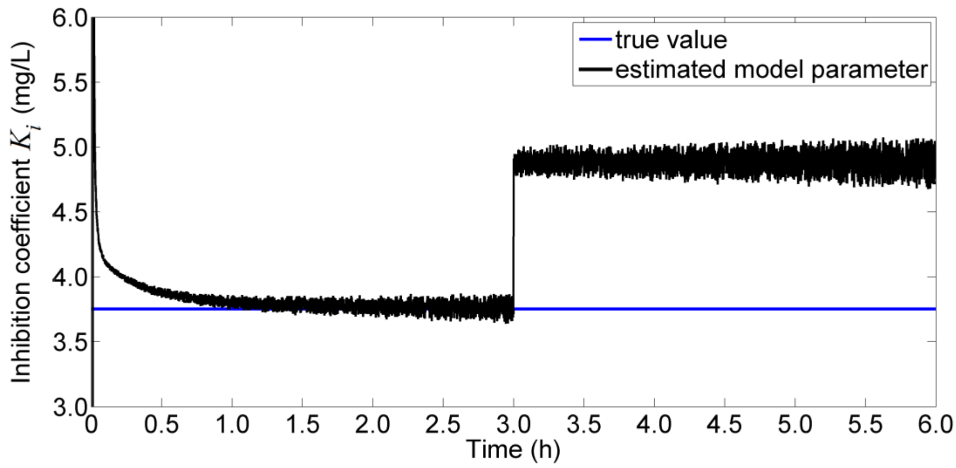

Figure 4.44 Estimated model parameter, K_i, for faulty scenario 2

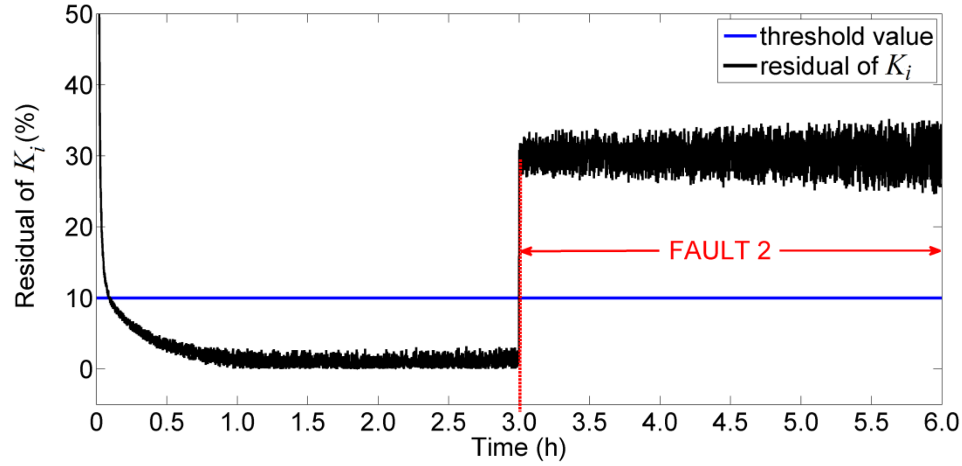

Figure 4.45 Residual of the estimated model parameter, K_i, for faulty scenario 2

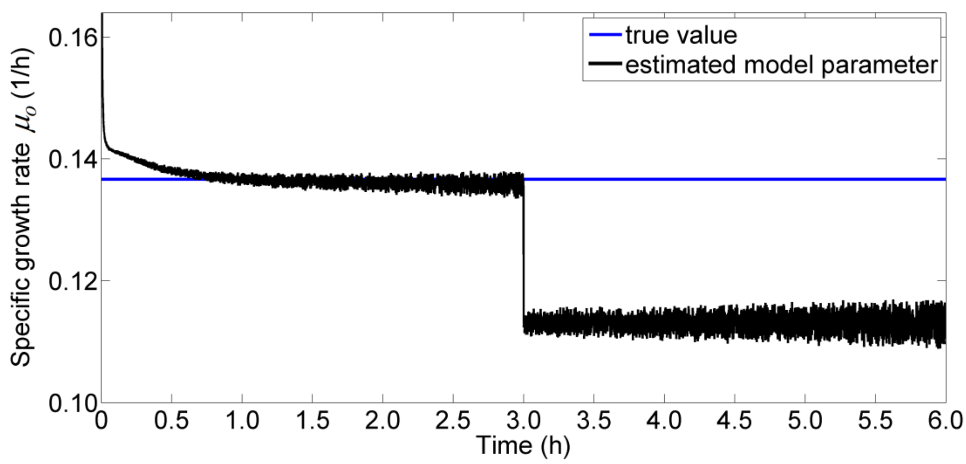

Figure 4.46 Estimated model parameter, μ_o, for faulty scenario 3

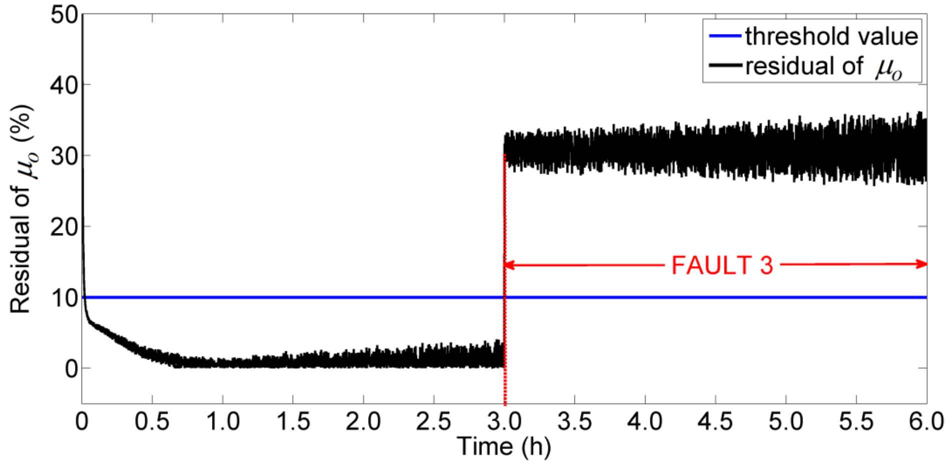

Figure 4.47 Residual of the estimated model parameter, μ_o, for faulty scenario 3

4.7 Concluding Remarks

(i) The objective of this chapter is to demonstrate the applicability of the proposed method of parameter estimation using MPP towards application for model-based FD. The applicability of FD is presented in five case studies of process systems which are evaporator, tank, heat exchanger, fermentation and wastewater treatment systems.

(ii) The mathematical model and related parameter faults have been explained in this chapter. The formulation for fault detection problem and KKT condition for each case is derived systematically. The KKT condition is solved using Mathematica to obtain the parametric function. Two scenarios in FD application, fault and fault-free scenarios, are examined to evaluate the performance of the parametric function.

(iii) The findings suggest that a methodology for FD based on MPP is successfully able to obtain the model parameters as an explicit function of the measurements for the square system of ODEs model. However, for a case where a non-square system of ODEs model is involved, the proposed method can only estimate for a single fault at one time as presented in the heat exchanger and wastewater treatment systems.

(iv) The proposed work has successfully demonstrated the advantages of MPP for FD using parameter estimation. Simple function evaluations replace the online computational burden in the optimisation problem of FD. The proposed method is also able to estimate the model parameters accurately using symbolic solution at a dynamic state. Hence, the faults in the system are quickly identified by monitoring the residual of model parameters as each parameters faults are related to the physical fault interpretation in the system.

CHAPTER 5 PARAMETER ESTIMATION FOR SYSTEM DISCRETISATION USING IMPLICIT EULER'S METHOD

5.1 Introduction

An implicit Euler's method is proposed for another discretisation method for nonlinear ODEs. The advantages of the implicit method which are provide more numerically stable for solving stiff differential equations and more accurate approximate solutions (Koch et al., 2000, Acary and Brogliato, 2009, Benko et al., 2009, Acary and Brogliato, 2010, Hasan et al., 2014, Sun et al., 2014). In this chapter, the objective of this study is to study the influence of the discretisation of nonlinear ODEs in the MPP algorithm. Hence, the complexity of implicit parametric functions, the accuracy of parameter estimates and the effect of step size will be discussed with comparison to explicit Euler's method.

5.2 Discretisation of Ordinary Differential Equation

The discretisation of an ODE model in equations (3.2) to (3.3) using an implicit Euler's method is given by:

$$x_j(i+1) = x_j(i) + \Delta t f_j\left(\mathbf{x}(i+1), \mathbf{u}(i), \boldsymbol{\theta}\right), i \in I, \ j \in J \tag{5.1}$$

where the step size is given by Δt. Equation (5.1) represents the prediction of x_j at time step $i+1$ where $x_j(i)$ is a state variables values at time step i and $f_j\left(\mathbf{x}(i+1), \mathbf{u}(i), \boldsymbol{\theta}\right)$ is a vector of functions evaluated at step $i+1$.

5.3 Parameter Estimation using Multiparametric Programming

The algorithm to obtain the model parameters as an explicit function of measurements using MPP, as discussed in Chapter 3 is summarised in Table 5.1 with the discretisation of ODE using implicit Euler's method.

Table 5.1. Parameter estimation using MPP algorithm

Step 1.	Discretise nonlinear ODE model in Equation (3.2) to algebraic equations as given in Equation (5.1) using implicit Euler's method
Step 2.	Formulate FD optimisation problem as an NLP problem as given in equations (3.6) to (3.8)
Step 3.	Formulate KKT conditions for equations (3.6) to (3.8) as given in equations (3.9) to (3.13)
Step 4.	Solve the equality constraints in equations (3.12) and (3.13) of the KKT conditions parametrically to obtain Lagrange multipliers and model parameters, $\boldsymbol{\theta}(\hat{\mathbf{x}})$, as a function of measurements, $\hat{\mathbf{x}}$
Step 5.	Screen the solutions obtained in the previous step and ignore solutions with imaginary parts
Step 6.	Calculate the estimated model parameters, $\boldsymbol{\theta}$, using the measurement, $\hat{\mathbf{x}}$, by a simple evaluation of $\boldsymbol{\theta}(\hat{\mathbf{x}})$

5.4 Illustrated examples of the proposed method

In this section, three examples are presented using the implicit Euler's method for discretising the nonlinear ODEs for parameter estimation using MPP. The comparison results between discretisation using implicit Euler's and explicit Euler's method in Section 3.2.1 are discussed.

5.4.1 Example 1: First-order irreversible chain reaction

In example 1, the first-order irreversible chain reactions model has been discussed in Section 3.5.1 where the nonlinear ODE model is given in equations (3.18) and (3.19) as below:

$$\frac{dz_1}{dt} = \theta_1 z_1 \tag{3.18}$$

$$\frac{dz_2}{dt} = \theta_1 z_1 - \theta_2 z_2 \tag{3.19}$$

where z_1 and z_2 are the state variables of concentrations of A and B respectively and θ_1 and θ_2 are the reaction rate constants of n_1 and n_2.

(a) Discretisation of Ordinary Differential Equations

The nonlinear ODE model in equations (3.18) and (3.19) is discretised using the implicit Euler's method and reformulated as the following algebraic equations:

$$z_1(i+1) = \frac{z_1(i)}{1+\Delta t\theta_1} \tag{5.2}$$

$$z_2(i+1) = \frac{\Delta t\theta_1 z_1(i+1) + z_2(i)}{1+\Delta t\theta_2} \tag{5.3}$$

(b) Parameter Estimation Problem

The parameter estimation problem is reformulated as the following NLP problem for the discretisation method to estimate the model parameters, θ_1 and θ_2, such that the error, ε_{MPP}, between the measurement of state variables, $\hat{z}_i(i+1)$, and model predicted value of state variables, $z_i(i+1)$, is minimised as follows:

Problem 5.1

$$\varepsilon_{MPP} = \min_{\theta_1,\theta_2} \sum_{i\in I} \left\{ (\hat{z}_1(i+1) - z_1(i+1))^2 + (\hat{z}_2(i+1) - z_2(i+1))^2 \right\} \tag{5.4}$$

Subject to:

$$h_1 = z_1(i+1) - \frac{z_1(i)}{1+\Delta t\theta_1} = 0 \tag{5.5}$$

$$h_2 = z_2(i+1) - \frac{\Delta t\theta_1 z_1(i+1) + z_2(i)}{1+\Delta t\theta_2} = 0 \tag{5.6}$$

Equations (3.21) to (3.23)

Equations (5.5) and (5.6) are substituted into Equation (5.4) to obtain:

$$g = \left(\hat{z}_1(i+1) - \frac{z_1(i)}{1+\Delta t\theta_1} \right)^2 + \left(\hat{z}_2(i+1) - \frac{\Delta t\theta_1 z_1(i+1) + z_2(i)}{1+\Delta t\theta_2} \right)^2 \tag{5.7}$$

The gradients of g with respect to θ_1 and θ_2 equal to zero are given by:

$$\begin{aligned} \frac{\partial g}{\theta_1} &= (2\Delta t\, z_1(i)(-(z_1(i)/(1+\Delta t\theta_1)) + \hat{z}_1(i+1)))/(1+\Delta t\theta_1)^2 - (2(-((\Delta t^2\theta_1\, z_1(i))/ \\ &\quad (1+\Delta t\theta_1)^2) + (\Delta t\, z_1(i))/(1+\Delta t\theta_1))(-(((\Delta t\theta_1\, z_1(i))/(1+\Delta t\theta_1) + z_2(i))/ \\ &\quad (1+\Delta t\theta_2)) + \hat{z}_2(i+1)))/(1+\Delta t\theta_2) \\ &= 0 \end{aligned} \tag{5.8}$$

$$\begin{aligned} \frac{\partial g}{\theta_2} &= (2\Delta t((\Delta t\theta_1 z_1(i))/(1+\Delta t\theta_1) + z_2(i))(-(((\Delta t\theta_1 z_1(i))/(1+\Delta t\theta_1) + z_2(i))/ \\ &\quad (1+\Delta t\theta_2)) + \hat{z}_2(i+1)))/(1+\Delta t\theta_1)^2 \\ &= 0 \end{aligned} \tag{5.9}$$

The equality constraints of KKT conditions in equations (5.8) and (5.9) are solved analytically in Mathematica, and the solution for Example 1 with discretisation using implicit Euler's method is given by:

(i) Solution 1

$$\theta_1 = -\frac{z_2(i)}{\Delta t\,(z_1(i)+z_2(i))} \tag{5.10}$$

$$\theta_2 = \frac{-z_1(i)+\hat{z}_1(i+1)-z_2(i)-\hat{z}_2(i+1)}{\Delta t\,(z_1(i)-\hat{z}_1(i+1)+z_2(i))} \tag{5.11}$$

(ii) Solution 2

$$\theta_1 = \frac{z_1(i)-\hat{z}_1(i+1)}{\Delta \mathrm{t}\,\hat{z}_1(i+1)} \tag{5.12}$$

$$\theta_2 = \frac{x_1(i)-\hat{x}_1(i+1)+x_2(i)-\hat{x}_2(i+1)}{\Delta \mathrm{t}\,\hat{x}_2(i+1)} \tag{5.13}$$

The discretisation of nonlinear ODEs using implicit Euler's method for parameter estimation using MPP provides the parameter estimates as given in solutions 1 and 2. Considering the positive values of reaction rate parameters in this example, $\theta_1 \geq 0$ and $\theta_2 \geq 0$; solution 1 is ignored because it implies that the concentration of B, $z_2(i)$ is negative, which is not true. Hence, model parameters are estimated using solution 2.

In Section 3.5.1, the solution model parameters for Example 1 with the discretisation of ODEs model using explicit Euler's method is given by equations (3.32) and (3.33) as follows:

$$\theta_1 = -\frac{-z_1(i)+\hat{z}_1(i+1)}{\Delta t\, z_1(i)} \tag{3.32}$$

$$\theta_2 = -\frac{-z_1(i)+\hat{z}_1(i+1)-z_2(i)+\hat{z}_2(i+1)}{\Delta t\, z_2(i)} \tag{3.33}$$

Next, a comparison between solution in equations (5.12), (5.13), (3.32) and (3.33) is carried out for analysing the accuracy of parameter estimates and effect of step size.

(c) Result for Example 1

The simulated data for state variables profile, z_1 and z_2, generated at $t = t_i$ with initial values given by $z_1(0) = 1$ and $z_2(0) = 0$ is shown in Figure 3.1 (Chapter 3, Section 3.5.1). In Example 1, three different step sizes are used to estimate model parameters. The model parameters, θ_1 and θ_2, obtained in equations (5.12), (5.13), (3.32) and (3.33) are calculated and compared for effectiveness and accuracy between the two discretisation methods of ODEs. The comparison of model parameters for different step sizes, $\Delta t = [0.10, 0.05, 0.01]$, is shown in figures 5.1 and 5.2 for θ_1 and θ_2, respectively. From these figures, we can see that, for the smallest step size, $\Delta t = 0.01$, the estimated model parameters, θ_1 and θ_2, are close to the actual true values of the model parameters ($\hat{\theta}_1 = 5$ and $\hat{\theta}_2 = 1$). Tables 5.2 and 5.3 show that percentage error (%) of the implicit Euler's method is smaller than that obtained by explicit Euler's method for $\Delta t = 0.01$. This figure indicates that the present method provides better results than those obtained by the explicit Euler method. (Note: the time (t_i) in tables 5.2 and 5.3 only shows the selected time for the purpose of presenting the percentage error results.)

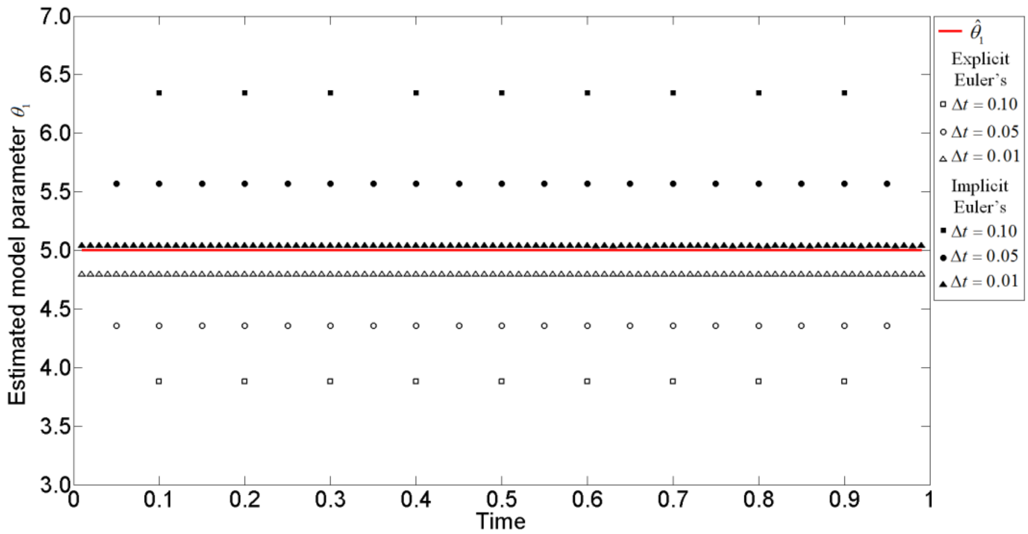

Figure 5.1 Estimated model parameter, θ_1, for different step sizes, Δt

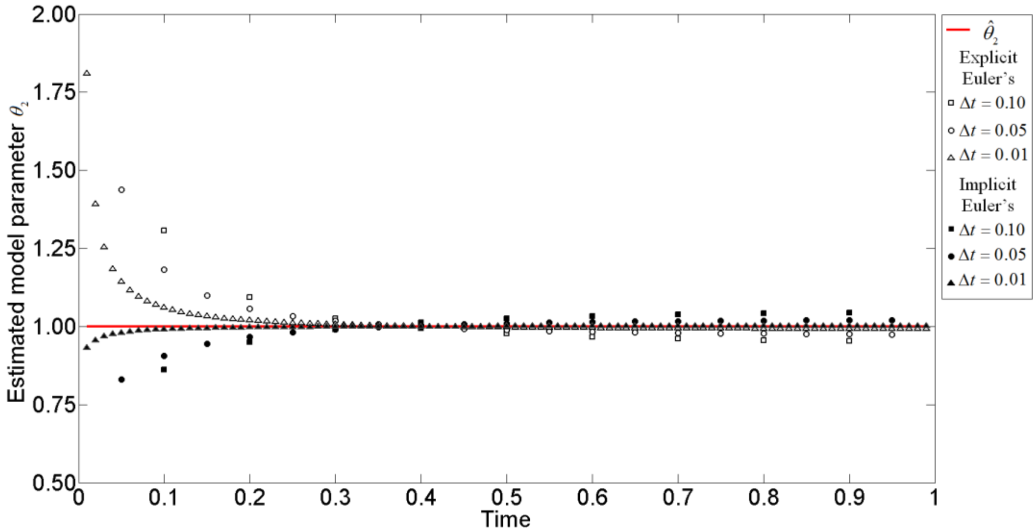

Figure 5.2 Estimated model parameter, θ_2, for different step sizes, Δt

Table 5.2. Comparison of the estimated model parameters, θ_1 for step size $\Delta t = 0.01$

Time (t_i)	Implicit Euler θ_1	Explicit Euler θ_1	Implicit Euler % Error	Explicit Euler % Error
0.10	5.03682	4.79529	0.7364	4.0942
0.20	5.03682	4.79529	0.7364	4.0942
0.30	5.03682	4.79529	0.7364	4.0942
0.40	5.03682	4.79529	0.7364	4.0942
0.50	5.03682	4.79529	0.7364	4.0942
0.60	5.03682	4.79529	0.7364	4.0942
0.70	5.03681	4.79528	0.7362	4.0944
0.80	5.03679	4.79526	0.7358	4.0948
0.90	5.03682	4.79529	0.7364	4.0942

Table 5.3. Comparison of the estimated model parameters, θ_2 for step size $\Delta t = 0.01$

Time (t_i)	Implicit Euler θ_2	Explicit Euler θ_2	Implicit Euler % Error	Explicit Euler % Error
0.10	0.99098	1.05976	0.9020	5.9760
0.20	0.99714	1.01915	0.2860	1.9150
0.30	0.99921	1.00628	0.0790	0.6280
0.40	1.00019	1.0003	0.0190	0.0300
0.50	1.00073	0.99706	0.0730	0.2940
0.60	1.00105	0.99514	0.1050	0.4860
0.70	1.00125	0.99394	0.1250	0.6060
0.80	1.00138	0.99318	0.1380	0.6820
0.90	1.00146	0.99269	0.1460	0.7310

5.4.2 Example 2: Lotka–Volterra model

The Lotka–Volterra model (Esposito and Floudas, 2000, Dua, 2011, Dua and Dua, 2011) has been discussed in Section 3.5.2 where the nonlinear ODE model is given as below:

$$\frac{dz_1}{dt} = \theta_1 z_1 (1 - z_2) \tag{3.34}$$

$$\frac{dz_2}{dt} = \theta_2 z_2 (z_1 - 1) \tag{3.35}$$

where z_1 and z_2 are state variables of prey and predator. The model parameters, θ_1 and θ_2, represents parameters describing the ecological interaction system to be estimated using MPP.

(a) Discretisation of Ordinary Differential Equations

The nonlinear ODE model in equations (3.34) and (3.35) is discretised using implicit Euler's method and reformulated as the following algebraic equations:

$$z_1(i+1) = \frac{z_1(i)}{1 - \Delta t\theta_1 + \Delta t\theta_1 z_2(i+1)} \tag{5.14}$$

$$z_2(i+1) = \frac{z_2(i)}{-1 - \Delta t\theta_2 + \Delta t\theta_2 z_1(i+1)} \tag{5.15}$$

(b) Parameter Estimation Problem

The parameter estimation problem is reformulated as the following NLP problem for the discretisation method to estimate the model parameters, θ_1 and θ_2, such that the error, ε_{MPP}, between the measurement of state variables, $\hat{z}_i(i+1)$, and model predicted value of state variables, $z_i(i+1)$, is minimised as follows:

Problem 5.2

$$\varepsilon_{MPP} = \min_{\theta_1,\theta_2} \sum_{i \in I} \left\{ (\hat{z}_1(i+1) - z_1(i+1))^2 + (\hat{z}_2(i+1) - z_2(i+1))^2 \right\} \tag{5.16}$$

Subject to:

$$h_1 = z_1(i+1) - \frac{z_1(i)}{1 - \Delta t\theta_1 + \Delta t\theta_1 z_2(i+1)} = 0 \tag{5.17}$$

$$h_2 = z_2(i+1) - \frac{z_2(i)}{-1 - \Delta t\theta_2 + \Delta t\theta_2 z_1(i+1)} = 0 \tag{5.18}$$

Equations (3.37) – (3.39)

Equations (5.17) and (5.18) are substituted into Equation (5.16) to obtain:

$$\begin{aligned} g &= (\hat{z}_1(i+1) - z_1(i) / (1 - \Delta t\theta_1 + \Delta t\theta_1 z_2(i+1)))^2 + ((\hat{z}_2(i+1) - z_2(i) / \\ &\quad (-1 - \Delta t\theta_2 + \Delta t\theta_2 (z_1(i) / (1 - \Delta t\theta_1 + \Delta t\theta_1 z_2(i+1)))))^2 \end{aligned} \tag{5.19}$$

The gradients of g with respect to θ_1 and θ_2 equal to zero are given by:

$$\frac{\partial g}{\theta_1} = (2z_1(i)(-\Delta t + \Delta t z_2(i+1))(\hat{z}_1(i+1) - z_1(i) / (1 - \Delta t\theta_1 + \Delta t\theta_1 z_2(i+1)))) / \tag{5.20}$$

$$(1 - \Delta t\theta_1 + \Delta t\theta_1 z_2(i+1))^2 + (2\Delta t\theta_2 z_1(i) z_2(i)(-\Delta t + \Delta t z_2(i+1))(\hat{z}_2(i+1) +$$
$$z_2(i) / (-1 - \Delta t\theta_2 + (\Delta t\theta_2 z_1(i)) / (1 - \Delta t\theta_1 + \Delta t\theta_1 z_2(i+1))))) / ((1 - \Delta t\theta_1 +$$
$$\Delta t\theta_1 z_2(i+1))^2 (-1 - \Delta t\theta_2 + (\Delta t\theta_2 z_1(i)) / (1 - \Delta t\theta_1 + \Delta t\theta_1 z_2(i+1)))^2)$$
$$= 0$$

$$\frac{\partial g}{\theta_2} = -((2z_2(i)(-\Delta t + (\Delta t\ z_1(i)) / (1 - \Delta t\theta_1 + \Delta t\theta_1 z_2(i+1)))(\hat{z}_2(i+1) + z_2(i) / \tag{5.21}$$

$$(-1 - \Delta t\theta_2 + (\Delta t\theta_2 z_1(i)) / (1 - \Delta t\theta_1 + \Delta t\theta_1 z_2(i+1))))) / (-1 - \Delta t\theta_2 +$$
$$(\Delta t\theta_2 z_1(i)) / (1 - \Delta t\theta_1 + \Delta t\theta_1 z_2(i+1)))^2)$$
$$= 0$$

The equality constraints of KKT conditions in equations (5.20) and (5.21) are solved analytically in Mathematica, and the solution for Example 2 with discretisation using implicit Euler's method is given by:

(i) Solution 1

$$\theta_1 = \frac{-1 - z_1(i)}{\Delta t\,(-1 + z_2(i+1))} \tag{5.22}$$

$$\theta_2 = \frac{-1 + \hat{z}_1(i+1)}{\Delta t z_2(i)\,(z_2(i) - \hat{z}_2(i+1))} \tag{5.23}$$

(ii) Solution 2

$$\theta_1 = \frac{z_1(i) - \hat{z}_1(i+1)}{\Delta \mathrm{t}\ \hat{z}_1(i+1)(-1 + z_2(i+1))} \tag{5.24}$$

$$\theta_2 = \frac{-z_2(i) + \hat{z}_2(i+1)}{\Delta t\,(-1 + \hat{z}_1(i+1))\ \hat{z}_2(i+1)} \tag{5.25}$$

The solution for Example 2 using implicit Euler's method gives two sets of model parameters as an explicit function of measurements, as given in solution 1 and solution 2. Considering the positive values of model parameters in this example, $\theta_1 \geq 0$ and $\theta_2 \geq 0$, solution 1 is ignored because it implies that the state variable of prey, $z_1(i)$ is a negative value which is not true. Hence, model parameters are evaluated using solution 2.

In Section 3.5.2, the solution model parameters for Example 2 with the discretisation of ODEs model using explicit Euler's method is given by equations (3.48) and (3.49) as below:

$$\theta_1 = \frac{z_1(i) - \hat{z}_1(i+1)}{\Delta t\, z_1(i)(-1 + z_2(i))} \tag{3.48}$$

$$\theta_2 = \frac{-z_2(i) + \hat{z}_2(i+1)}{\Delta t(-1 + z_1(i))z_2(i)} \tag{3.49}$$

The comparison between solutions from equations (5.24), (5.25), (3.48) and (3.49) is carried out for investigating the accuracy of parameter estimates and effect of step size.

(c) Result for Example 2

The simulated data for state variables profile, z_1 and z_2, was generated at $t = t_i$ with initial values given by $z_1(0) = 1.2$ and $z_2(0) = 1.1$ as shown in Figure 3.4 (Chapter 3, Section 3.5.2). In this example, the model parameters are estimated using the explicit function as given in equations (5.24), (5.25), (3.48) and (3.49). Three different step sizes are used to estimate model parameters, $\Delta t = [0.10, 0.05, 0.01]$. The estimated model parameters, θ_1 and θ_2, for different step sizes, Δt, are shown in Figures 5.3 and 5.4. As the step size decreased, the estimated model parameter values, θ_1 and θ_2 , became closer to the true values of the model parameters ($\hat{\theta}_1 = 3$ and $\hat{\theta}_2 = 1$). Tables 5.4 and 5.5 show that percentage error of the implicit Euler's method is smaller than that obtained by explicit Euler method for $\Delta t = 0.01$. Thus, the discretisation using implicit Euler's method gave more accurate model parameters compared to explicit Euler's method, where the estimated model parameters are close to the true values. (Note: the time (t_i) in tables 5.4 and 5.5 only shows the selected time to present the percentage error results.)

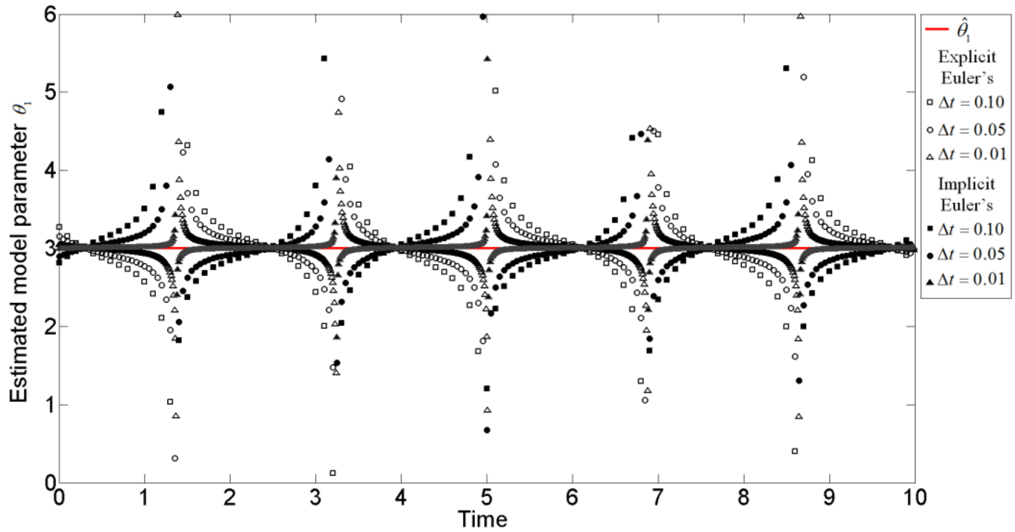

Figure 5.3 Estimated model parameter, θ_1, for different step sizes, Δt

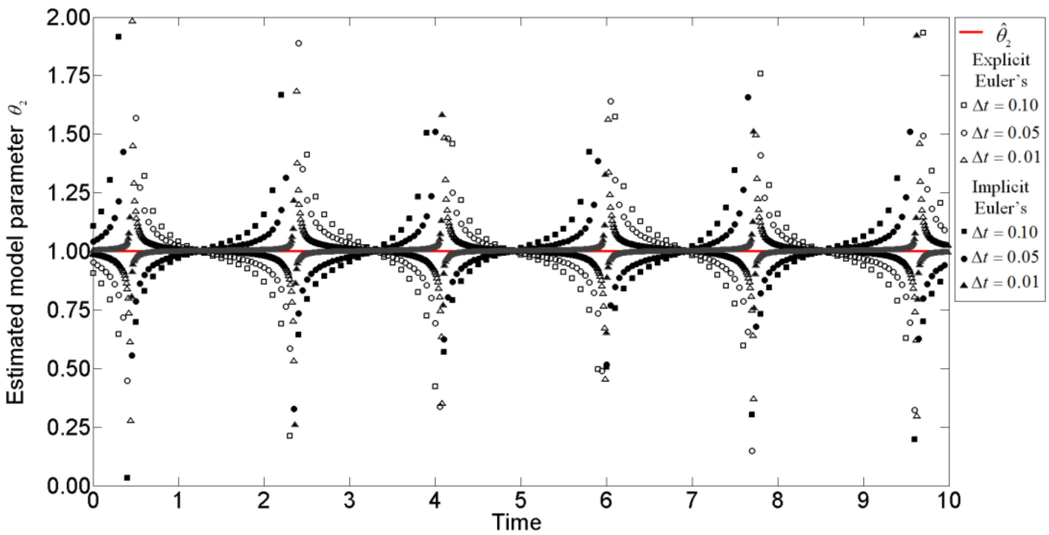

Figure 5.4 Estimated model parameter, θ_2, for different step sizes, Δt

Table 5.4. Comparison of the estimated model parameters, θ_1 for step size $\Delta t = 0.01$

Time (t_i)	Implicit Euler θ_1	Explicit Euler θ_1	Implicit Euler % Error	Explicit Euler % Error
0.00	2.99132	3.04693	0.289	1.564
0.01	2.99174	3.04472	0.275	1.491
0.02	2.99216	3.04259	0.261	1.420
0.03	2.99255	3.04055	0.248	1.352
0.04	2.99294	3.03857	0.235	1.286
0.05	2.99331	3.03667	0.223	1.222
0.06	2.99367	3.03482	0.211	1.161
0.07	2.99402	3.03304	0.199	1.101
0.08	2.99435	3.03130	0.188	1.043
0.09	2.99468	3.02963	0.177	0.988
0.10	2.99500	3.02800	0.167	0.933

Table 5.5. Comparison of the estimated model parameters, θ_2 for step size $\Delta t = 0.01$

Time (t_i)	Implicit Euler θ_2	Explicit Euler θ_2	Implicit Euler % Error	Explicit Euler % Error
0.00	1.00291	0.98652	0.291	1.348
0.01	1.00303	0.98593	0.303	1.407
0.02	1.00316	0.98531	0.316	1.469
0.03	1.00329	0.98468	0.329	1.532
0.04	1.00342	0.98403	0.342	1.597
0.05	1.00356	0.98335	0.356	1.665
0.06	1.0037	0.98265	0.370	1.735
0.07	1.00385	0.98192	0.385	1.808
0.08	1.00401	0.98116	0.401	1.884
0.09	1.00417	0.98037	0.417	1.963
0.10	1.00434	0.97955	0.434	2.045

5.4.3 Example 3: Single-stage evaporator

A mathematical model of a single-stage evaporator system (Dalle Molle and Himmelblau, 1987) as described in Section 4.2.1 is given as:

$$\frac{dW}{dt} = F - \left(\delta W + E_c\right) - V \tag{4.1}$$

$$\frac{dT}{dt} = \frac{\beta F x_F + (V-F)(T-T_B)}{W} \tag{4.2}$$

Where

$$V = \left(\frac{UA(T_S - T) - FC_p(T - T_F) - Q_L}{\Delta H_V}\right) \tag{4.3}$$

(a) Discretisation of Ordinary Differential Equations

The nonlinear ODE model in equations (4.1) to (4.3) is discretised using implicit Euler's method and reformulated as the following algebraic equations:

$$\begin{aligned} W(i+1) = (&-(F - E_c - ((UA(T_S - T(i+1) - FC_p(T(i+1) - T_F) - Q_L)/ \\ &\Delta H_V)\Delta t - W(i))/(-\delta\Delta t - 1) \end{aligned} \tag{5.26}$$

$$\begin{aligned} T(i+1) = \frac{1}{2}\frac{1}{\Delta t(C_p F + UA)}(&C_p F T_B \Delta t - C_p F T_F \Delta t - F\Delta H_V \Delta t + T_B UA\Delta t + \\ &T_S UA\Delta t - Q_L \Delta t - \Delta H_V W(i+1) - (C_p^2 F^2 T_B^2 \Delta t^2 - 2C_p^2 F^2 T_B T_F \Delta t^2 + \\ &C_p^2 F^2 T_F^2 \Delta t^2 + 4C_p F^2 \beta \Delta H_V \Delta t^2 x_F + 2C_p F^2 T_B \Delta H_V \Delta t^2 - \\ &2C_p F^2 T_F \Delta H_V \Delta t^2 + 2C_p F T_B^2 UA\Delta t^2 - 2C_p F T_B T_F UA\Delta t^2 - \\ &2C_p F T_B T_S UA\Delta t^2 + 2C_p F T_F T_S UA\Delta t^2 + 4FUA\beta\Delta H_V \Delta t^2 x_F + \\ &2C_p F Q_L T_B \Delta t^2 - 2C_p F Q_L T_F \Delta t^2 + 4C_p F T(i) W(i+1)\Delta H_V \Delta t - \\ &2C_p F T_B W(i+1)\Delta H_V \Delta t - 2C_p F T_F W(i+1)\Delta H_V \Delta t + F^2 \Delta H_V{}^2 \Delta t^2 + \\ &2FT_B UA\Delta H_V \Delta t^2 + 2FT_S UA\Delta H_V \Delta t^2 + T_B{}^2 UA^2 \Delta t^2 - 2T_B T_S UA^2 \Delta t^2 - \\ &T_S{}^2 UA^2 \Delta t^2 + 2FQ_L \Delta H_V \Delta t^2 + 2FW(i+1)\Delta H_V{}^2 \Delta t + 2Q_L T_B UA\Delta t^2 - \\ &2Q_L T_S UA\Delta t^2 + 4T(i) UAW(i+1)\Delta H_V \Delta t - 2T_B UAW(i+1)\Delta H_V \Delta t - \\ &2T_S UAW(i+1)\Delta H_V \Delta t + Q_L{}^2 \Delta t^2 + 2Q_L W(i+1)\Delta H_V \Delta t + \\ &W(i+1)^2 \Delta H_V{}^2)^{1/2}) \end{aligned} \tag{5.27}$$

(b) Parameter Estimation Problem

The parameter estimation problem is reformulated as the following NLP problem for the discretisation method to estimate the model parameters, UA and x_F, such that the error, ε_{MPP}, between the measurement of state variables, $\hat{W}(i+1)$ and $\hat{T}(i+1)$, and model predicted value of state variables, $W(i+1)$ and $T(i+1)$, is minimised as follows:

Problem 5.3

$$\varepsilon_{MPP} = \min_{UA, x_f} \sum_{i \in I} \{(\hat{W}(i+1) - W(i+1))^2 + (\hat{T}(i+1) - T(i+1))^2\} \tag{5.28}$$

Subject to:

$$\begin{aligned} h_1 &= W(i+1) - (-(F - E_c - ((UA(T_S - T(i+1) - FC_p(T(i+1) - T_F) - \\ &\quad Q_L) / \Delta H_V)\Delta t - W(i)) / (-\delta\Delta t - 1) \\ &= 0 \end{aligned} \tag{5.29}$$

$$\begin{aligned} h_2 &= T(i+1) - (\frac{1}{2}\frac{1}{\Delta t(C_p F + UA)}(C_p F T_B \Delta t - C_p F T_F \Delta t - F\Delta H_V \Delta t + \\ &\quad T_B UA\Delta t + T_S UA\Delta t - Q_L \Delta t - \Delta H_V W(i+1) - (C_p^2 F^2 T_B^2 \Delta t^2 - \\ &\quad 2C_p^2 F^2 T_B T_F \Delta t^2 + C_p^2 F^2 T_F^2 \Delta t^2 + 4C_p F^2 \beta \Delta H_V \Delta t^2 x_F + \\ &\quad 2C_p F^2 T_B \Delta H_V \Delta t^2 - 2C_p F^2 T_F \Delta H_V \Delta t^2 + 2C_p F T_B^2 UA\Delta t^2 - \\ &\quad 2C_p F T_B T_F UA\Delta t^2 - 2C_p F T_B T_S UA\Delta t^2 + 2C_p F T_F T_S UA\Delta t^2 + \\ &\quad 4FUA\beta\Delta H_V \Delta t^2 x_F + 2C_p F Q_L T_B \Delta t^2 - 2C_p F Q_L T_F \Delta t^2 + \\ &\quad 4C_p F T(i) W(i+1)\Delta H_V \Delta t - 2C_p F T_B W(i+1)\Delta H_V \Delta t - \\ &\quad 2C_p F T_F W(i+1)\Delta H_V \Delta t + F^2 \Delta H_V{}^2 \Delta t^2 + 2F T_B UA\Delta H_V \Delta t^2 + \\ &\quad 2F T_S UA\Delta H_V \Delta t^2 + T_B{}^2 UA^2 \Delta t^2 - 2T_B T_S UA^2 \Delta t^2 - T_S{}^2 UA^2 \Delta t^2 + \\ &\quad 2F Q_L \Delta H_V \Delta t^2 + 2F W(i+1)\Delta H_V{}^2 \Delta t + 2Q_L T_B UA\Delta t^2 - \\ &\quad 2Q_L T_S UA\Delta t^2 + 4T(i) UA W(i+1)\Delta H_V \Delta t - 2T_B UA W(i+1)\Delta H_V \Delta t - \\ &\quad 2T_S UA W(i+1)\Delta H_V \Delta t + Q_L{}^2 \Delta t^2 + 2Q_L W(i+1)\Delta H_V \Delta t + \\ &\quad W(i+1)^2 \Delta H_V{}^2)^{1/2})) \\ &= 0 \end{aligned} \tag{5.30}$$

Equations (4.5) to (4.7)

Equations (5.29) and (5.30) are substituted into Equation (5.28) to obtain:

$$
\begin{aligned}
g = {} & (\hat{W}(i+1) - ((-(F - E_c - ((UA(T_S - T(i+1) - FC_p(T(i+1) - T_F) - Q_L)/ \\
& \Delta H_V)\Delta t - W(i))/(-\delta\Delta t - 1)))^2 + (\hat{T}(i+1) - (\frac{1}{2}\frac{1}{\Delta t(C_p F + UA)}(C_p F T_B \Delta t \\
& - C_p F T_F \Delta t - F\Delta H_V \Delta t + T_B UA\Delta t + T_S UA\Delta t - Q_L \Delta t - \Delta H_V W(i+1) - \\
& (C_p^2 F^2 T_B^2 \Delta t^2 - 2C_p^2 F^2 T_B T_F \Delta t^2 + C_p^2 F^2 T_F^2 \Delta t^2 + 4C_p F^2 \beta \Delta H_V \Delta t^2 x_F + \\
& 2C_p F^2 T_B \Delta H_V \Delta t^2 - 2C_p F^2 T_F \Delta H_V \Delta t^2 + 2C_p F T_B^2 UA\Delta t^2 - 2C_p F T_B T_F UA\Delta t^2 \\
& - 2C_p F T_B T_S UA\Delta t^2 + 2C_p F T_F T_S UA\Delta t^2 + 4FUA\beta\Delta H_V \Delta t^2 x_F + \\
& 2C_p F Q_L T_B \Delta t^2 - 2C_p F Q_L T_F \Delta t^2 + 4C_p F T(i) W(i+1)\Delta H_V \Delta t - \\
& 2C_p F T_B W(i+1)\Delta H_V \Delta t - 2C_p F T_F W(i+1)\Delta H_V \Delta t + F^2 \Delta H_V{}^2 \Delta t^2 + \\
& 2F T_B UA\Delta H_V \Delta t^2 + 2F T_S UA\Delta H_V \Delta t^2 + T_B{}^2 UA^2 \Delta t^2 - 2T_B T_S UA^2 \Delta t^2 - \\
& T_S{}^2 UA^2 \Delta t^2 + 2FQ_L \Delta H_V \Delta t^2 + 2FW(i+1)\Delta H_V{}^2 \Delta t + 2Q_L T_B UA\Delta t^2 - \\
& 2Q_L T_S UA\Delta t^2 + 4T(i) UAW(i+1)\Delta H_V \Delta t - 2T_B UAW(i+1)\Delta H_V \Delta t - \\
& 2T_S UAW(i+1)\Delta H_V \Delta t + Q_L{}^2 \Delta t^2 + 2Q_L W(i+1)\Delta H_V \Delta t + \\
& W(i+1)^2 \Delta H_V{}^2)^{1/2})))^2
\end{aligned}
\tag{5.31}
$$

The gradients of g with respect to UA and x_F are given by:

$$
\begin{aligned}
\frac{\partial g}{UA} = &-(1/2)T_B\Delta t + T_S\Delta t - (1/2)(2C_PFT_B{}^2\Delta t^2 - 2C_PFT_BT_F\Delta t^2 - \\
&2C_PFT_BT_S\Delta t^2 + 2C_PFT_FT_S\Delta t^2 + 4F\beta\Delta H_V\Delta t^2 x_F + 2FT_B\Delta H_V\Delta t^2 - \\
&2FT_S\Delta H_V\Delta t^2 + 2T_B{}^2UA\Delta t^2 - 4T_BT_SUA\Delta t^2 + 2T_S{}^2UA\Delta t^2 + 2Q_LT_B\Delta t^2 - \\
&2Q_LT_S\Delta t^2 + 4T(i)W(i+1)\Delta H_V\Delta t - 2T_BW(i+1)\Delta H_V\Delta t - \\
&2T_SW(i+1)\Delta H_V\Delta t)/sqrt(C_P{}^2F^2T_B{}^2\Delta t^2 - 2C_P{}^2F^2T_BT_F\Delta t^2 + \\
&C_P{}^2F^2T_F{}^2\Delta t^2 + 4C_PF^2\beta\Delta H_V\Delta t^2 x_F + 2C_PF^2T_B\Delta H_V\Delta t^2 - \\
&2C_PF^2T_F\Delta H_V\Delta t^2 + 2C_PFT_B{}^2UA\Delta t^2 - 2C_PFT_BT_FUA\Delta t^2 - \\
&2C_PFT_BT_SUA\Delta t^2 + 2C_PFT_FT_SUA\Delta t^2 + 4FUA\beta\Delta H_V\Delta t^2 x_F + \\
&2C_PFQ_LT_B\Delta t^2 - 2C_PFQ_LT_F\Delta t^2 + 4C_PFT(i)W(i+1)\Delta H_V\Delta t - \\
&2C_PFT_BW(i+1)\Delta H_V\Delta t - 2C_PFT_FW(i+1)\Delta H_V\Delta t + F^2\Delta H_V{}^2\Delta t^2 + \\
&2FT_BUA\Delta H_V\Delta t^2 - 2FT_SUA\Delta H_V\Delta t^2 + T_B{}^2UA^2\Delta t^2 - 2T_BT_SUA^2\Delta t^2 + \\
&T_S{}^2UA^2\Delta t^2 + 2FQ_L\Delta H_V\Delta t^2 + 2FW(i+1)\Delta H_V{}^2\Delta t + 2Q_LT_BUA\Delta t^2 - \\
&2Q_LT_SUA*\Delta t^2 + 4T(i)UAW(i+1)\Delta H_V\Delta t - 2T_BUAW(i+1)\Delta H_V\Delta t - \\
&2T_SUAW(i+1)\Delta H_V\Delta t + Q_L{}^2\Delta t^2 + Q_LW(i+1)\Delta H_V\Delta t + \\
&W(i+1)^2\Delta H_V{}^2))/(\Delta t(C_PF + UA)) + (1/2)(C_PFT_B\Delta t + C_PFT_F\Delta t - \\
&F\Delta H_V\Delta t + T_BUA\Delta t + T_SUA\Delta t - Q_L\Delta t - \Delta H_VW(i+1) - \\
&sqrt(C_P{}^2F^2T_B{}^2\Delta t^2 - 2C_P{}^2F^2T_BT_F\Delta t^2 + C_P{}^2F^2T_F{}^2\Delta t^2 + \\
&4C_PF^2\beta\Delta H_V\Delta t^2 x_F + 2C_PF^2T_B\Delta H_V\Delta t^2 - 2C_PF^2T_F\Delta H_V\Delta t^2 + \\
&2C_PFT_B{}^2UA\Delta t^2 - 2C_PFT_BT_FUA\Delta t^2 - 2C_PFT_BT_SUA\Delta t^2 + \\
&2C_PFT_FT_SUA\Delta t^2 + 4FUA\beta\Delta H_V\Delta t^2 x_F + 2C_PFQ_LT_B\Delta t^2 - \\
&2C_PFQ_LT_F\Delta t^2 + 4C_PFTW(i+1)\Delta H_V\Delta t - 2C_PFT_BW(i+1)\Delta H_V\Delta t - \\
&2C_PFT_FW(i+1)\Delta H_V\Delta t + F^2\Delta H_V{}^2\Delta t^2 + 2FT_BUA\Delta H_V\Delta t^2 - \\
&2FT_SUA\Delta H_V\Delta t^2 + T_B{}^2UA^2\Delta t^2 - 2T_BT_SUA^2\Delta t^2 + T_S{}^2UA^2\Delta t^2 + \\
&2FQ_L\Delta H_V\Delta t^2 + 2FW(i+1)\Delta H_V{}^2\Delta t + 2Q_LT_BUA\Delta t^2 - 2Q_LTsUA\Delta t^2 + \\
&4T(i)UAW(i+1)\Delta H_V\Delta t - 2T_BUAW(i+)\Delta H_V\Delta t - \\
&2T_SUAW(i+1)\Delta H_V\Delta t + Q_L{}^2\Delta t^2 + 2Q_LW(i+1)\Delta H_V\Delta t + \\
&W(i+1)^2\Delta H_V{}^2))/(\Delta t(C_PF + UA)^2) \\
= &\,0
\end{aligned}
\tag{5.32}
$$

$$\frac{\partial g}{x_F} = (1/2)(\hat{T}(i+1) - (1/2)(C_P F T_B \Delta t + C_P F T_F \Delta t - F * \Delta H_V * \Delta t + \tag{5.33}$$
$$T_B UA\Delta t + T_S UA\Delta t - Q_L \Delta t - \Delta H_V W(i+1) - sqrt(C_P{}^2 F^2 T_B{}^2 \Delta t^2 -$$
$$2C_P{}^2 F^2 T_B T_F \Delta t^2 + C_P{}^2 F^2 T_F{}^2 \Delta t^2 + 4C_P F^2 \beta \Delta H_V \Delta t^2 x_F +$$
$$2C_P F^2 T_B \Delta H_V \Delta t^2 - 2C_P F^2 T_F \Delta H_V \Delta t^2 + 2C_P F T_B{}^2 UA\Delta t^2 -$$
$$2C_P F T_B T_F UA\Delta t^2 - 2C_P F T_B T_S UA\Delta t^2 + 2C_P F T_F T_S UA\Delta t^2 +$$
$$4FUA\beta \Delta H_V \Delta t^2 x_F + 2C_P F Q_L T_B \Delta t^2 - 2C_P F Q_L T_F \Delta t^2 +$$
$$4C_P F T(i) W(i+1) \Delta H_V \Delta t - 2C_P F T_B W(i+1) \Delta H_V \Delta t -$$
$$2C_P F T_F W(i+1) \Delta H_V \Delta t + F^2 \Delta H_V{}^2 \Delta t^2 + 2F T_B UA\Delta H_V \Delta t^2 -$$
$$2F T_S UA\Delta H_V \Delta t^2 + T_B{}^2 UA^2 \Delta t^2 - 2T_B T_S UA^2 \Delta t^2 + T_S{}^2 UA^2 \Delta t^2 +$$
$$2F Q_L \Delta H_V \Delta t^2 + 2FW(i+1) \Delta H_V{}^2 \Delta t + 2Q_L T_B UA\Delta t^2 - 2Q_L T_S UA\Delta t^2 +$$
$$4T(i) UAW(i+1) \Delta H_V \Delta t - 2T_B UAW(i+1) \Delta H_V \Delta t -$$
$$2T_S UAW(i+1) \Delta H_V \Delta t + Q_L{}^2 \Delta t^2 + 2Q_L W(i+1) \Delta H_V \Delta t +$$
$$W(i+1)^2 \Delta H_V{}^2)) / (\Delta t(C_P F + UA)))(4C_P F^2 \beta \Delta H_V \Delta t^2 +$$
$$4FUA\beta \Delta H_V \Delta t^2) / (sqrt(C_P{}^2 F^2 T_B{}^2 \Delta t^2 - 2C_P{}^2 F^2 T_B T_F \Delta t^2 +$$
$$C_P{}^2 F^2 T_F{}^2 \Delta t^2 + 4C_P F^2 \beta \Delta H_V \Delta t^2 x_F + 2C_P F^2 T_B \Delta H_V \Delta t^2 -$$
$$2C_P F^2 T_F \Delta H_V \Delta t^2 + 2C_P F T_B{}^2 UA\Delta t^2 - 2C_P F T_B T_F UA\Delta t^2 -$$
$$2C_P F T_B T_S UA\Delta t^2 + 2C_P F T_F T_S UA\Delta t^2 + 4FUA\beta \Delta H_V \Delta t^2 x_F +$$
$$2C_P F Q_L T_B \Delta t^2 - 2C_P F Q_L T_F \Delta t^2 + 4C_P FTW(i+1) \Delta H_V \Delta t -$$
$$2C_P F T_B W(i+1) \Delta H_V \Delta t - 2C_P F T_F W(i+1) \Delta H_V \Delta t + F^2 \Delta H_V{}^2 \Delta t^2 +$$
$$2F T_B UA\Delta H_V \Delta t^2 - 2F T_S UA\Delta H_V \Delta t^2 + T_B{}^2 UA^2 \Delta t^2 - 2T_B T_S UA^2 \Delta t^2 +$$
$$T_S{}^2 UA^2 \Delta t^2 + 2F Q_L \Delta H_V \Delta t^2 + 2FW(i+1) \Delta H_V{}^2 \Delta t + 2Q_L T_B UA\Delta t^2 -$$
$$2Q_L T_S UA\Delta t^2 + 4T(i) UAW(i+1) \Delta H_V \Delta t - 2T_B UAW(i+1) \Delta H_V \Delta t -$$
$$2T_S UAW(i+1) \Delta H_V \Delta t + Q_L{}^2 \Delta t^2 + 2Q_L W(i+1) \Delta H_V \Delta t +$$
$$W(i+1)^2 \Delta H_V{}^2) \Delta t(C_P F + UA))$$
$$= 0$$

The equality constraints in equations (5.32) and (5.33) are solved analytically in Mathematica, and the solution for Example 3 with discretisation using implicit Euler's method is given by:

$$UA = (C_P F T_F \Delta t - C_P F T(i+1) \Delta t + \hat{W}(i+1) \Delta H_V \delta \Delta t + E_C \Delta H_V \Delta t - \tag{5.34}$$
$$F \Delta H_V \Delta t - Ql \Delta t - W(i) \Delta H_V + \hat{W}(i+1) \Delta H_V) / (\Delta t(T(i+1) - T_S))$$

$$x_F = -(C_P F T_B T_F \hat{T}(i+1)\Delta t - C_P F T_B T_F T(i+1)\Delta t - C_P F T_B \hat{T}(i+1) T_S \Delta t + \\
C_P F T_B T(i+1) T_S \Delta t - C_P F T_F \hat{T}(i+1)^2 \Delta t + C_P F T_F \hat{T}(i+1) T(i+1)\Delta t + \\
C_P F \hat{T}(i+1)^2 T_S \Delta t - C_P F \hat{T}(i+1) T(i+1) T_S \Delta t + \\
T_B \hat{T}(i+1) \hat{W}(i+1) \Delta H_V \delta \Delta t - T_B T_S \hat{W}(i+1) \Delta H_V \delta \Delta t - \\
\hat{T}(i+1)^2 \hat{W}(i+1) \Delta H_V \delta \Delta t + \hat{T}(i+1) T_S \hat{W}(i+1) \Delta H_V \delta \Delta t + \\
E_C T_B \hat{T}(i+1) \Delta H_V \Delta t - E_C T_B T_S \Delta H_V \Delta t - E_C \hat{T}(i+1)^2 \Delta H_V \Delta t + \\
E_C \hat{T}(i+1) T_S \Delta H_V \Delta t - F T_B \hat{T}(i+1) \Delta H_V \Delta t + F T_B T(i+1) \Delta H_V \Delta t + \\
F \hat{T}(i+1)^2 \Delta H_V \Delta t - F \hat{T}(i+1) T(i+1) \Delta H_V \Delta t - Q_L T_B \hat{T}(i+1) \Delta t + \\
Q_L T_B T(i+1) \Delta t + Q_L \hat{T}(i+1)^2 \Delta t - Q_L \hat{T}(i+1) T(i+1) \Delta t + \\
T(i) T(i+1) W(i+1) \Delta H_V - T(i) T_S W(i+1) \Delta H_V - T_B \hat{T}(i+1) W(i) \Delta H_V + \\
T_B \hat{T}(i+1) \hat{W}(i+1) \Delta H_V + T_B T_S W(i) \Delta H_V - T_B T_S \hat{W}(i+1) \Delta H_V + \\
\hat{T}(i+1)^2 W(i) \Delta H_V - \hat{T}(i+1)^2 \hat{W}(i+1) \Delta H_V - \hat{T}(i+1) T(i+1) W(i+1) \Delta H_V \\
-\hat{T}(i+1) T_S W(i) \Delta H_V + \hat{T}(i+1) T_S \hat{W}(i+1) \Delta H_V + \hat{T}(i+1) T_S W(i+1) \Delta H_V) / \\
((T(i+1) - T_S) F \beta \Delta H_V \Delta t) \tag{5.35}$$

In Section 4.2, the solution model parameters for a single-stage evaporator system with the discretisation of the ODEs model using explicit Euler's method are given by equations (4.17) and (4.18) as below:

$$UA = -(1/(\Delta t\,(T(i) - T_S)))(-\Delta H_V \Delta t E_c + \Delta H_V \Delta t F + \Delta t Q_L + C_P \Delta t F T(i) - \\
C_P \Delta t F T_F + \Delta H_V W(i) - \delta \Delta H_V \Delta t W(i) - \Delta H_V \hat{W}(i+1)) \tag{4.17}$$

$$x_F = -(1/(\beta \Delta t F))(-\Delta t E_c T(i) + \Delta t E_c T_B + 2T(i) W(i) - \delta \Delta t T(i) W(i) - \\
T_B W(i) + \delta \Delta t T_B W(i) - \hat{T}(i+1) W(i) - T(i) \hat{W}(i+1) + T_B \hat{W}(i+1)) \tag{4.18}$$

The comparison between solutions from equations (5.34), (5.35), (4.17) and (4.18) is carried out for investigating the accuracy of parameter estimates and the effect of step size.

(c) Result for Example 3

The simulated data for state variables profile, W and T, was generated at $t = t_i$ with initial values given by $W(0) = 13.8$ kg and $T(0) = 107\,^{\circ}$C as shown in Figures 5.5

and 5.6. Two step sizes, $\Delta t = [0.10, 0.05]$, are used to estimate model parameters and the estimated model parameters, UA and x_F, are shown in figures 5.7 and 5.8. As the step size decreased to 0.05, the estimated model parameter values for UA and x_F became closer to the true values of the model parameters ($U\hat{A} = 40.548$ and $\hat{x}_F = 0.032$). Tables 5.6 and 5.7 show that percentage error of the implicit Euler's method is smaller than that obtained by explicit Euler's method for $\Delta t = 0.05$. Thus, the discretisation using implicit Euler's method gave more accurate model parameters compared to explicit Euler's method, where the estimated model parameters are close to the true values. (Note: the time, t_i, in tables 5.6 and 5.7 only shows the selected time to present the percentage error results.)

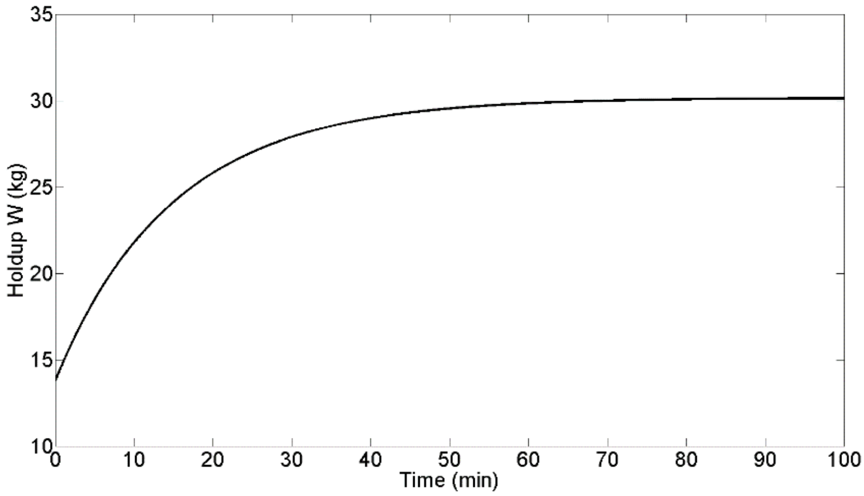

Figure 5.5 State variables profile for holdup, W

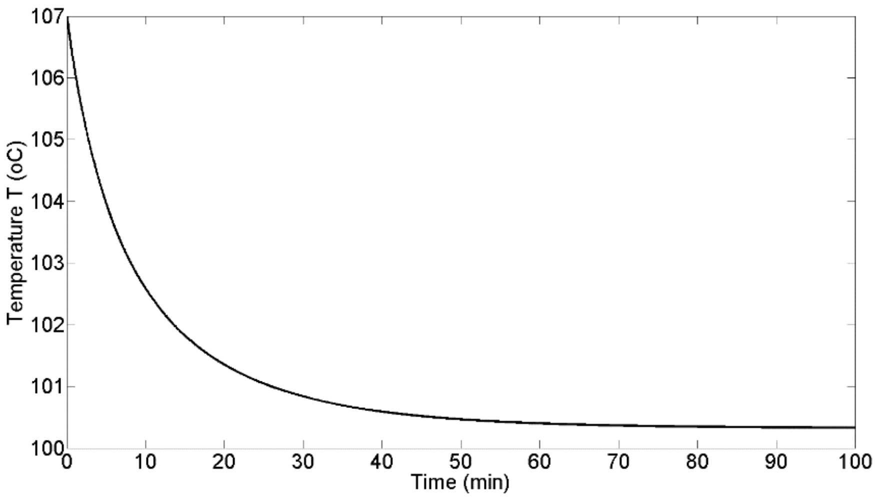

Figure 5.6 State variables profile for temperature, T

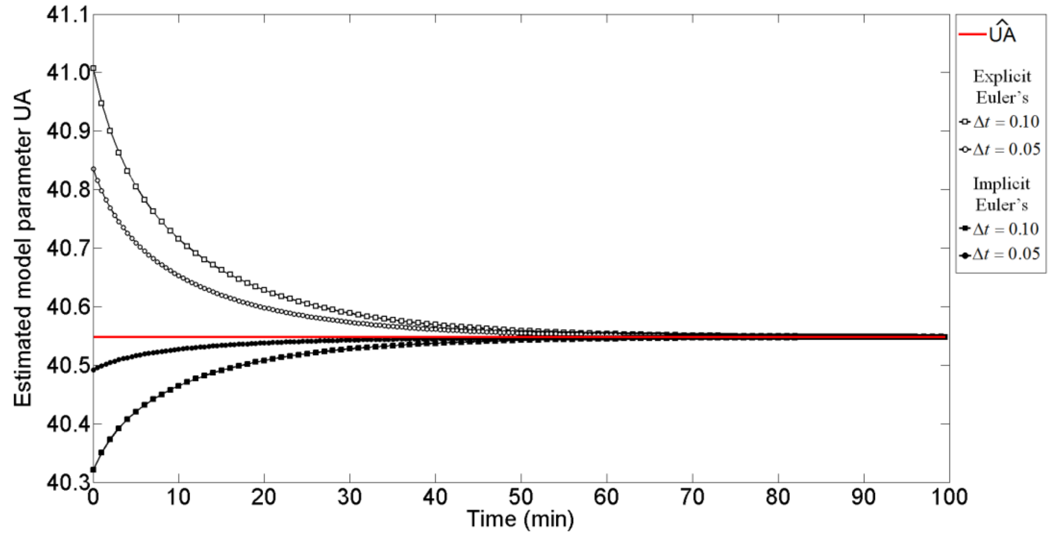

Figure 5.7 Estimated model parameter, UA, for different step sizes, Δt

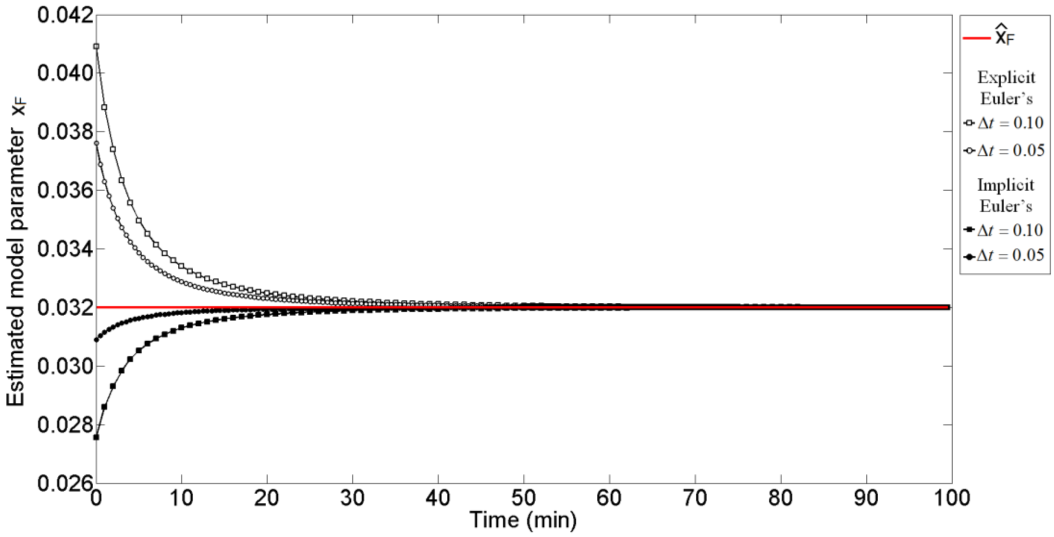

Figure 5.8 Estimated model parameter, x_F , for different step sizes, Δt

Table 5.6. Comparison of the estimated model parameters, UA for step size $\Delta t = 0.05$

Time (t_i)	Implicit Euler UA	Explicit Euler UA	Implicit Euler % Error	Explicit Euler % Error
0.00	40.4915	40.8357	0.138	0.704
0.50	40.4954	40.8155	0.129	0.655
1.00	40.4988	40.7979	0.120	0.612
1.50	40.5019	40.7825	0.113	0.575
2.00	40.5045	40.7687	0.107	0.541
2.50	40.507	40.7563	0.101	0.511
3.00	40.5091	40.7451	0.095	0.484
3.50	40.5111	40.7349	0.090	0.459
4.00	40.513	40.7256	0.086	0.436
4.50	40.5146	40.717	0.082	0.415
5.00	40.5162	40.709	0.078	0.395
5.50	40.5176	40.7017	0.074	0.377
6.00	40.519	40.6948	0.071	0.360
6.50	40.5203	40.6884	0.068	0.345
7.00	40.5214	40.6823	0.065	0.330
7.50	40.5226	40.6767	0.062	0.316
8.00	40.5236	40.6713	0.060	0.303
8.50	40.5246	40.6663	0.057	0.291
9.00	40.5255	40.6616	0.055	0.279
9.50	40.5264	40.6571	0.053	0.268
10.00	40.5273	40.6528	0.051	0.257

Table 5.7. Comparison of the estimated model parameters, x_F for step size $\Delta t = 0.05$

Time (t_i)	Implicit Euler x_F	Explicit Euler x_F	Implicit Euler % Error	Explicit Euler % Error
0.00	0.03089	0.03761	3.416	17.296
0.50	0.03103	0.0369	2.983	15.095
1.00	0.03115	0.0363	2.623	13.276
1.50	0.03125	0.03581	2.323	11.754
2.00	0.03133	0.03539	2.069	10.471
2.50	0.0314	0.03503	1.853	9.378
3.00	0.03146	0.03473	1.668	8.441
3.50	0.03151	0.03447	1.509	7.632
4.00	0.03156	0.03424	1.370	6.929
4.50	0.0316	0.03404	1.249	6.315
5.00	0.03163	0.03386	1.142	5.776
5.50	0.03166	0.03371	1.048	5.299
6.00	0.03169	0.03357	0.964	4.878
6.50	0.03171	0.03345	0.890	4.501
7.00	0.03173	0.03334	0.824	4.164
7.50	0.03175	0.03325	0.764	3.863
8.00	0.03177	0.03316	0.711	3.590
8.50	0.03179	0.03308	0.662	3.344
9.00	0.0318	0.03301	0.617	3.122
9.50	0.03181	0.03294	0.578	2.919
10.00	0.03183	0.03288	0.541	2.734

5.5 Concluding Remarks

In this chapter, the influence of discretisation the nonlinear ODEs in parameter estimation using MPP is discussed. The implicit Euler's method is proposed in the discretisation method and demonstrated through three examples. The results show that the implementation of MPP using implicit Euler's method successfully obtained model parameters as an explicit function of measurements. However, the parametric expressions obtained for the implicit Euler's method were more complex than has been obtained using the explicit Euler's method. Compared with the explicit discretisation, the implicit Euler's gave more accurate parameter estimates. A small step size also influences the estimated values of model parameters.

CHAPTER 6 CONCLUDING REMARKS AND FUTURE DIRECTIONS

6.1 Concluding Remarks

An improvement and comprehensive method considering the effect of accuracy and complexity for parameter estimation FD has been derived and develop using MPP; which is useful for solving the optimisation problem. The proposed MPP approach can be applied to the parameter estimation problem to obtained explicit parametric function. The formulation of parameter estimation for FD utilising MPP is presented. The nonlinear ODEs are discretised to algebraic equations using Euler's method. Then, the FD problem is formulated as a NLP problem. The KKT conditions for this FD problem are then written down. This results in a square system of parametric nonlinear algebraic equations. These equations are then solved symbolically to obtain model parameters as an explicit function of measurements is obtained. The detection of fault is carried out by monitoring the changes in the model parameters.

To demonstrate the evaluation and availability of the proposed method in FD application, five case studies involving nonlinear ODEs model have been investigated. In the evaporator system, the two parameters of interest for faulty operation are examined, the heat transfer coefficient and the composition of feed. These two parameter faults are useful in determining the condition of the evaporator and examine the efficiency of the process. In the quadruple-tank system, leakage is assumed to be produced by a hole at the bottom of the tanks which is related to cross-section of the outlet holes. Fouling in heat exchanger is evaluated from fouling resistance where examined from overall heat transfer coefficient. For the fermentation process and wastewater treatment system, any improper formulation or contamination in the fermentation will change the kinetic model parameters. A small change in operating conditions or a mis-operation during critical stages may impact the final product quality and even lead to a chemical disaster.

The FD problem for all case studies is derived, and the MPP algorithm solves the optimisation problem to obtain an explicit parametric function. In these five cases, faulty and fault-free scenarios have been analysed. The analytical results of estimated model parameters showed excellent performance for the accuracy of the parameter estimation for both scenarios.

In the proposed method of parameter estimation using MPP, the discretisation of nonlinear ODEs to algebraic equations is required. In this work, the influence of the discretisation method has been investigated. The implicit Euler's method is proposed to evaluate the complexity and accuracy of the parametric function. The results indicate that the parametric expressions obtained for the implicit Euler's method were more complex than that obtained for the explicit Euler's method. Moreover, the implicit Euler's gave more accurate parameter estimates for the same step size.

In conclusion, the set of objectives are fulfilled satisfactorily in developing and demonstrating a new parameter estimation algorithm for FD using an MPP approach. However, a limitation of the proposed approach is observed, where the symbolic solution of the parametric nonlinear algebraic equations may not always be possible or maybe too complex.

6.2 Contribution to Knowledge

The main contributions of this work are as follows:

(i) The development of the parameter estimation algorithm using MPP method is successfully proposed for FD. In this development, the model parameter is obtained as an explicit function of measurement. This explicit parametric function represents the significant development in parameter estimation where online computation burden is replaced by simple function evaluation.

(ii) The demonstration of parameter estimation using MPP for model-based fault detection applications is successfully implemented into process systems. The parameter estimation algorithm using MPP is demonstrated into evaporator, tank, heat exchanger, fermentation and wastewater treatment systems. In each case, the related parameter fault to the physical interpretation is determined. Faults are detected through a simple function evaluation obtained using MPP. The symbolic solution of parameter estimate gives advantages of MPP for FD application using parameter estimation to detect faults quickly and accurately.

(iii) The influence of discretisation of nonlinear ordinary differential equations using implicit Euler's method for parameter estimation is investigated. The parametric expression obtained using implicit Euler's method gave more accurate parameter estimates compare to explicit Euler's method. However, the explicit parametric function becomes complicated and not available for some cases. Hence, the discretisation of nonlinear ODEs method gives an impact into the development of MPP for complexity and accuracy of parameter estimation.

6.3 Future Directions

The research presented in this work has raised several research questions, thus opening up a variety of potential research directions which could be pursued in the future.

(i) Investigation of parameter estimation algorithm for robustness issues in fault detection

Another issue in the FD problem is modelling the errors and noise (robustness). When the model of a process system is subject to model uncertainty or noise, to achieve effective FD, the effect of the noise has to be de-coupled from the residual signal to avoid 'false alarms' in detection. Hence, the next consideration is to develop robust FD algorithms. However, it should be noted that future work will not only include improvement of robustness in FD, but will also need to demonstrate how to improve system performance, not only when all components are functioning normally, but also in cases when there are malfunctions in sensors, actuators or other system components.

(ii) Demonstrate the parameter estimation approach for application with large-scale process systems

The capability of the proposed method for use with large-scale process systems can be considered and investigated. Large-scale process systems present a more challenging and difficult task in parameter estimation using model-based FD due to the large size of the mathematical model required.

(iii) Real-time implementation of fault detection using the MPP **approach**

FD using the MPP approach can also be extended for real-time implementation using a microcontroller. A microcontroller is a system on a chip that contains processor cores (CPU) with memory and programmable input/output peripherals and which is designed for embedded application. The function of model parameters is programmed and uploaded into the microcontroller. Thus, the estimation of model parameters can be performed online and in real-time systems.

(iv) Implementation of a fault-tolerant control system using the model predictive control approach

Once the faults have been identified using an FD method, an implementation of a fault tolerant control system is required through a reconfiguration of the control system to cancel the effects of the faults or to attenuate them. In this method, MPC as control reconfiguration can be considered. The MPC uses the explicit model to predict the future behaviour of the plant and solves a constrained optimisation problem online to obtain optimal control.

REFERENCES

ACARY, V. & BROGLIATO, B. 2009. Implicit Euler numerical simulations of sliding mode systems. *Research Report RR-6886***,** 17-20.

ACARY, V. & BROGLIATO, B. 2010. Implicit Euler numerical scheme and chattering-free implementation of sliding mode systems. *Systems & Control Letters,* 59**,** 284-293.

ACOSTA DÍAZ, C., CAMPS ECHEVARRÍA, L., PRIETO-MORENO, A., SILVA NETO, A. J. & LLANES-SANTIAGO, O. 2016. A model-based fault diagnosis in a nonlinear bioreactor using an inverse problem approach and evolutionary algorithms. *Chemical Engineering Research and Design,* 114**,** 18-29.

ALCORTA GARCÍA, E. & FRANK, P. M. 1997. Deterministic nonlinear observer-based approaches to fault diagnosis: A survey. *Control Engineering Practice,* 5**,** 663-670.

ASTORGA-ZARAGOZA, C.-M., ALVARADO-MARTÍNEZ, V.-M., ZAVALA-RÍO, A., MÉNDEZ-OCAÑA, R.-M. & GUERRERO-RAMÍREZ, G.-V. 2008. Observer-based monitoring of heat exchangers. *ISA Transactions,* 47**,** 15-24.

ASTORGA-ZARAGOZA, C. M., ZAVALA-RÍO, A., ALVARADO, V. M., MÉNDEZ, R. M. & REYES-REYES, J. 2007. Performance monitoring of heat exchangers via adaptive observers. *Measurement,* 40**,** 392-405.

BAGGIANI, F. & MARSILI-LIBELLI, S. 2009. Real-time fault detection and isolation in biological wastewater treatment plants. *Water Science and Technology,* 60**,** 2949-2961.

BATUR, C., ZHOU, L. & CHAN, C. C. Support vector machines for fault detection. 41st IEEE Conference on Decision and Control, 2002. 1355-1356.

BENKO, D., BILES, D. C., ROBINSON, M. P. & SPRAKER, J. S. 2009. Numerical approximation for singular second order differential equations. *Mathematical and Computer Modelling,* 49**,** 1109-1114.

BENKOUIDER, A. M., BUVAT, J. C., COSMAO, J. M. & SABONI, A. 2009. Fault detection in semi-batch reactor using the EKF and statistical method. *Journal of Loss Prevention in the Process Industries,* 22**,** 153-161.

BILARDELLO, P., JOULIA, X., LE LANN, J. M., DELMAS, H. & KOEHRET, B. 1993. A general strategy for parameter estimation in differential-algebraic systems. *Computers and Chemical Engineering,* 17**,** 517-525.

BROUWER, H., KLAPWIJK, A. & KEESMAN, K. J. 1994. Modelling and Control of Activated Sludge Plants on the Basis of Respirometry. *Water Science and Technology,* 30**,** 265-274.

BUCIAKOWSKI, M., DE ROZPRZA FAYGEL, M., OCHALEK, J. & WITCZAK, M. 2014. Actuator fault diagnosis and fault-tolerant control: Application to the quadruple-tank process. *11th European Workshop on Advanced Control and Diagnosis - ACD 2014***,** 93-102.

CACCAVALE, F., DIGIULIO, P., IAMARINO, M., MASI, S. & PIERRI, F. 2010. A neural network approach for on-line fault detection of nitrogen sensors in alternated active sludge treatment plants. *Water Science and Technology,* 62**,** 2760-2768.

CARLSSON, B. 1993. On-line estimation of the respiration rate in an activated sludge process. *Water Science and Technology,* 28**,** 427-434.

CARLSSON, B., LINDBERG, C., HASSELBLAD, S. & XU, S. 1994. On-line estimation of the respiration rate and the oxygen transfer rate at kungsangen wastewater treatment plant in uppsala. *Water Science and Technology,* 30**,** 255-263.

CARLSSON, B. & ZAMBRANO, J. 2016. Fault detection and isolation of sensors in aeration control systems. *Water Science and Technology,* 73**,** 648-653.

CENGEL, Y. A. 2003. Heat Transfer: A Practical Approach. *Mc Graw-Hill***,** 785-841.

CHANG, J.-S., DENG, J.-H. & WANG, G.-B. 2016. Estimation of kinetic parameters for glycerol/alcohol dehydration reaction systems with incomplete chromatography data sets. *Journal of the Taiwan Institute of Chemical Engineers,* 60**,** 185-198.

CHANG, J. S., LI C.C., W.L., L. & DENG, J. H. 2015. Two-stage parameter estimation applied to ordinary differential equation models. *Journal of the Taiwan Institute of Chemical Engineers,* 57**,** 26-35.

CHAPRA, S. C. & CANALE, R. P. 2009. *Numerical methods for engineers,* McGraw-Hill.

CHARITOPOULOS, V. M. & DUA, V. 2016. Explicit model predictive control of hybrid systems and multiparametric mixed integer polynomial programming. *AIChE Journal,* 62**,** 3441-3460.

CHEN, A., ZHOU, H., AN, Y. & SUN, W. 2016a. PCA and PLS monitoring approaches for fault detection of wastewater treatment process. *IEEE International Symposium on Industrial Electronics***,** 1022-1027.

CHEN, J. & PATTON, R. J. 1999. *Robust Model-Based Fault Diagnosis for Dynamic Systems*, Kluwer.

CHEN, J., PATTON, R. J. & ZHANG, H. Y. 1996. Design of unknown input observers and robust fault detection filters. *International Journal of Control,* 63**,** 85-105.

CHEN, W., BIEGLER, L. T. & MUÑOZ, S. G. 2016b. An approach for simultaneous estimation of reaction kinetics and curve resolution from process and spectral data. *Journal of Chemometrics,* 30**,** 506-522.

CHEN, X. D., LI, D. X. Y., LIN, S. X. Q. & ÖZKAN., N. 2004. On-line fouling/cleaning detection by measuring electric resistance-equipment development and application to milk fouling detection and chemical cleaning monitoring. *Journal of Food Engineering,* 61**,** 181-189.

CHOW, E. Y. & WILLSKY, A. S. 1984. Analytical redundancy and the design of robust failure detection systems. *IEEE Transaction on Automatic Control,* 29**,** 603-614.

CIMPOESU, E. M., CIUBOTARU, B. D. & STEFANOIU, D. Fault Detection and Diagnosis Using Parameter Estimation with Recursive Least Squares. 2013 19th International Conference on Control Systems and Computer Science, 29-31 May 2013 2013. 18-23.

ÇINAR, A., BIROL, G. & ÜNDEY, C. 2002. A modular simulation package for fed-batch fermentation: Penicillin production. *Computers and Chemical Engineering,* 26**,** 1553-1565.

DAI, X. & GAO, Z. 2013. From model, signal to knowledge: A data-driven perspective of fault detection and diagnosis. *IEEE Transactions on Industrial Informatics,* 9**,** 2226-2238.

DALLE MOLLE, D. T. & HIMMELBLAU, D. M. 1987. Fault Detection in a Single-Stage Evaporator via Parameter Estimation Using the Kalman Filter. *Industrial and Engineering Chemistry Research,* 26**,** 2482-2489.

DE, S., NORTHROP, P. W. C., RAMADESIGAN, V. & SUBRAMANIAN, V. R. 2013. Model-based simultaneous optimization of multiple design parameters for lithium-ion batteries for maximization of energy density. *Journal of Power Sources,* 227**,** 161-170.

DELMOTTE, F., DAMBRINE, M., DELROT, S. & LALOT, S. 2013. Fouling detection in a heat exchanger: A polynomial fuzzy observer approach. *Control Engineering Practice,* 21**,** 1386-1395.

DELROT, S., GUERRA, T. M., DAMBRINE, M. & DELMOTTE, F. 2012. Fouling detection in a heat exchanger by observer of Takagi-Sugeno type for systems with unknown polynomial inputs. *Engineering Applications of Artificial Intelligence,* 25**,** 1558-1566.

DING, S. X. 2008. *Model-Based Fault Diagnosis Techniques: Design Schemes, Algorithms, and Tools,* Berlin, Germany, Springer-Verlag.

DU, M. & MHASKAR, P. 2013. Active fault isolation of nonlinear process systems. *AIChE Journal,* 59**,** 2435-2453.

DU, M. & MHASKAR, P. 2014. Isolation and handling of sensor faults in nonlinear systems. *Automatica,* 50**,** 1066-1074.

DUA, V. 2011. An Artificial Neural Network approximation based decomposition approach for parameter estimation of system of ordinary differential equations. *Computers & Chemical Engineering,* 35**,** 545-553.

DUA, V. 2015. Mixed integer polynomial programming. *Computers and Chemical Engineering,* 72**,** 387-394.

DUA, V. & DUA, P. 2011. A Simultaneous Approach for Parameter Estimation of a System of Ordinary Differential Equations, Using Artificial Neural Network Approximation. *Industrial & Engineering Chemistry Research,* 51**,** 1809-1814.

DUA, V. & PISTIKOPOULOS, E. N. 1999. Algorithms for the Solution of Multiparametric Mixed-Integer Nonlinear Optimization Problems. *Industrial & Engineering Chemistry Research,* 38**,** 3976-3987.

ENGLEZOS, P. & KALOGERAKIS, N. 2001. *Applied Parameter Estimation for Chemical Engineers,* New York, Marcel Dekker.

ESCOBAR, R. F., ASTORGA-ZARAGOZA, C. M., HERNÁNDEZ, J. A., JUÁREZ-ROMERO, D. & GARCÍA-BELTRÁN, C. D. 2015. Sensor fault compensation via software sensors: Application in a heat pump's helical evaporator. *Chemical Engineering Research and Design,* 93**,** 473-482.

ESCOBET, T. & TRAVÉ-MASSUYÈS, L. 2001. Parameter estimation methods for fault detection and isolation. *12th International Workshop on Principles of Diagnosis***,** 1-11.

ESPOSITO, W. R. & FLOUDAS, C. A. 2000. Global optimization for the parameter estimation of differential-algebraic systems. *Industrial and Engineering Chemistry Research,* 39**,** 1291-1310.

FIBRIANTO, H., MAZOUNI, D., IGNATOVA, M., HERVEAU, M., HARMAND, J. & DOCHAIN, D. 2008. Dynamical modelling, identification and software sensors for SBRs. *Mathematical and Computer Modelling of Dynamical Systems,* 14**,** 17-26.

FILBERT, D., SCHNEIDER, C. & SPANNHAKE, S. 1991. Model Equation and Fault Detection of Electric Motors. *IFAC Proceedings Volumes,* 24**,** 457-460.

FONOD, R., HENRY, D., CHARBONNEL, C. & BOMSCHLEGL, E. A class of nonlinear unknown input observer for fault diagnosis: Application to fault tolerant control of an autonomous spacecraft. 2014 UKACC International Conference on Control (CONTROL), 9-11 July 2014 2014. 13-18.

FRAGKOULIS, D., ROUX, G. & DAHHOU, B. 2011. Detection, isolation and identification of multiple actuator and sensor faults in nonlinear dynamic systems: Application to a waste water treatment process. *Applied Mathematical Modelling,* 35**,** 522-543.

FRANK, P. M. 1996. Analytical and Qualitative Model-based Fault Diagnosis – A Survey and Some New Results. *European Journal of Control,* 2**,** 6-28.

FRANK, P. M. & DING, X. 1997. Survey of robust residual generation and evaluation methods in observer-based fault detection systems. *Journal of Process Control,* 7**,** 403-424.

GANESH, C., BALLAL, P., BHUSHAN, M. & PATWARDHAN, S. C. Leak Identification using Extended Kitanidis-Kalman Filter. 12th International Symposium on Process Systems Engineering and 25th European Symposium on Computer Aided Process Engineering, 2015. 1817-1822.

GAO, Z., CECATI, C. & DING, S. X. 2015. A Survey of Fault Diagnosis and Fault-Tolerant Techniques Part I: Fault Diagnosis. *IEEE Transactions On Industrial Electronics,* 62**,** 3768 - 3774.

GARATTI, S. & BITTANTI, S. 2012. A new paradigm for parameter estimation in system modeling. *International Journal of Adaptive Control and Signal Processing,* 27**,** 667-687.

GARCIA-ALVAREZ, D., FUENTE, M. J., VEGA, P. & SAINZ, G. 2009. Fault Detection and Diagnosis using Multivariate Statistical Techniques in a Wastewater Treatment Plant. *IFAC Proceedings Volumes,* 42**,** 952-957.

GERTLER, J. 1988. Survey of model-based failure detection and isolation in complex plants. *IEEE Control Systems Magazine,* 3**,** 3-11.

GERTLER, J. 1997. Fault detection and isolation using parity relations. *Control Engineering Practice,* 5**,** 653-661.

GONTARSKI, C. A., RODRIGUES, P. R., MORI, M. & PRENEM, L. F. 2000. Simulation of an industrial wastewater treatment plant using artificial neural networks. *Computers & Chemical Engineering,* 24**,** 1719-1723.

GUDMUNDSSON, O., PALSSON, O. P., PALSSON, H. & LALOT, S. 2008. Method to Detect Fouling in Heat Exchangers. *The 11th International symposium on District Heating and Cooling*.

HASAN, M. K., AHAMED, M. S., HUQ, M. A., ALAM, M. S. & HOSSAIN, M. B. 2014. A new implicit method for numerical solution of singular initial value problems. *The Open Mathematics Journal,* 2**,** 1-5.

HONGGUI, H., YING, L. & JUNFEI, Q. 2014. A fuzzy neural network approach for online fault detection in waste water treatment process. *Computers and Electrical Engineering,* 40**,** 2216-2226.

HSOUMI, A., HARABI, R. E., ALI, S. B. H. & ABDELKRIM, M. N. Diagnosis of a Continous Stirred Tank Reactor Using Kalman Filter. 2009 International Conference on Computational Intelligence, Modelling and Simulation, 7-9 Sept. 2009 2009. 153-158.

HUANG, B. 2001. Detection of abrupt changes of total least squares models and application in fault detection. *IEEE Transactions on Control Systems Technology,* 9**,** 357-367.

HWANG, I., KIM, S., KIM, Y. & SEAH, C. E. 2010. A Survey of Fault Detection, Isolation, and Reconfiguration Methods. *IEEE Transactions on Control Systems Technology,* 18**,** 636-653.

HWANG, M. & SEINFELD, J. H. 1972. A New Algorithm for the Estimation of Parameters in Ordinary Differential Equations. *AIChE Journal,* 18**,** 90-93.

HWANG, W. & HUH, K. 2014. Fault Detection and Estimation for Electromechanical Brake Systems Using Parity Space Approach. *Journal of Dynamic Systems, Measurement, and Control,* 137**,** 014504.

ISERMANN, R. 1984. Process Fault Detection Based on Modeling and Estimation Methods - A Survey. *Automatica,* 20**,** 387-404.

ISERMANN, R. 1993. Fault diagnosis of machines via parameter estimation and knowledge processing—Tutorial paper. *Automatica,* 29**,** 815-835.

ISERMANN, R. 1997. Supervision, fault-detection and fault-diagnosis methods - An introduction. *Control Engineering Practice,* 5**,** 639-652.

ISERMANN, R. 2005. Model-based fault-detection and diagnosis - Status and applications. *Annual Reviews in Control,* 29**,** 71-85.

ISERMANN, R. 2006. Fault-diagnosis systems: An introduction from fault detection to fault tolerance. *Springer*.

ISERMANN, R. & BALLÉ, P. 1997. Trends in the application of model based fault detection and diagnosis of technical processes. *Control Engineering Practice,* 5**,** 709-719.

JOHANSSON, K. H. 2000. The quadruple-tank process: a multivariable laboratory process with an adjustable zero. *IEEE Transactions on Control Systems Technology,* 8**,** 456-465.

JONSSON, G. R., LALOT, S., PALSSON, O. P. & DESMET, B. 2007. Use of extended Kalman filtering in detecting fouling in heat exchangers. *International Journal of Heat and Mass Transfer,* 50**,** 2643-2655.

JONSSON, G. R. & PALSSON, O. P. 1991. Use of empirical relations in the parameters of heat exchanger models. *Industrial and Engineering Chemistry Research***,** 1193-1199.

JONSSON, G. R. & PALSSON, O. P. 1994. An Application of Extended Kalman Filtering to Heat Exchanger Models. *Journal of Dynamic Systems, Measurement and Control,* 116**,** 257.

KABBAJ, N., POLIT, M., DAHHOU, B. & ROUX, G. Adaptive observers based fault detection and isolation for an alcoholic fermentation process. ETFA 2001. 8th International Conference on Emerging Technologies and Factory Automation. Proceedings (Cat. No.01TH8597), 15-18 Oct. 2001 2001. 669-673 vol.2.

KAMEL, M., CHADLI, M., CHAABANE, M., HAJJAJI, A. E. & CHAARI, A. 2009. Fault detection and isolation for a Lipschitz nonlinear system: Application to a bank of tanks. *17th Mediterranean Conference on Control and Automation*, 377-382.

KARAMI, F., POSHTAN, J. & POSHTAN, M. 2010. Detection of broken rotor bars in induction motors using nonlinear Kalman filters. *ISA Transactions,* 49**,** 189-195.

KIM, I. W., EDGAR, T. F. & LIEBMAN, M. J. 1991. A Sequential Error-in-Variables Method for Nonlinear Dynamic Systems. *Computers & Chemical Engineering,* 15**,** 663-670.

KIM, M. & KIM, M. S. 2005. Performance investigation of a variable speed vapor compression system for fault detection and diagnosis. *International Journal of Refrigeration,* 28**,** 481-488.

KOCH, O., KOFLER, P. & WEINMÜLLER, E. B. 2000. The implicit Euler method for the numerical solution of singular initial value problems. *Applied Numerical Mathematics,* 34**,** 231-252.

LAKHMANI, P., VALIUM, J., CHANDRASEKARAN, G. & PATWARDHAN, S. C. 2016. Application of a moving window parameter estimator for leak identification in the quadruple tank system. *IFAC-PapersOnLine,* 49**,** 629-634.

LALOT, S. & LECOEUCHE, S. 2003. Online fouling detection in electrical circulation heaters using neural networks. *International Journal of Heat and Mass Transfer,* 46**,** 2445-2457.

LALOT, S., PALSSON, O. P., JONSSON, G. R. & DESMET, B. 2007. Comparison of neural networks and Kalman filters performances for fouling detection in a heat exchanger. *International Journal of Heat Exchangers,* 8**,** 151-168.

LECOEUCHE, S., LALOT, S. & DESMET, B. 2005. Modelling a non-stationary single tube heat exchanger using multiple coupled local neural networks. *International Communications in Heat and Mass Transfer,* 32**,** 913-922.

LEE, J.-M., YOO, C., CHOI, S. W., VANROLLEGHEM, P. A. & LEE, I.-B. 2004. Nonlinear process monitoring using kernel principal component analysis. *Chemical Engineering Science,* 59**,** 223-234.

LENNOX, B., MONTAGUE, G. A., HIDEN, H. G., GOULDING, P. R. & KORNFELD, G. 2001. Process monitoring of an industrial fed-batch fermentation. *Biotechnology and Bioengineering,* 74**,** 125-135.

LIANG, Z., PARLIKAD, A. K., SRINIVASAN, R. & RASMEKOMEN, N. 2017. On fault propagation in deterioration of multi-component systems. *Reliability Engineering and System Safety,* 162**,** 72-80.

LINDBERG, C.-F. & CARLSSON, B. 1996. Estimation of the respiration rate and oxygen transfer function utilizing a slow DO sensor. *Water Science and Technology,* 33**,** 325-333.

LIU, W. 1999. An extended Kalman filter and neural network cascade fault diagnosis strategy for the glutamic acid fermentation process. *Artificial Intelligence in Engineering,* 13**,** 131-140.

LIU, X., XIAO, L., LV, L., LIU, P., XU, G., ZHENG, Z. & WANG, S. 2019. Analytical sensitivity computation using collocation method with non-uniform mesh discretisation for numerical solutions of optimal control problems. *International Journal of Control***,** 1-11.

MA, L., WANG, F., JIANG, Y. & GAO, F. 2003. A Fault Diagnosis Method for Fermentation Process. *IFAC Proceedings,* 37**,** 661-665.

MA, L., WANG, J. & LIU, Z. 2007. A Fault Diagnosis Method Based on Composite Model and SVM for Fermentation Process. *2007 IEEE International Conference on Control and Automation***,** 3107-3110.

MAIER, H. R. & DANDY, G. C. 2000. Neural networks for the prediction and forecasting of water resources variables: a review of modelling issues and applications. *Environmental Modelling & Software,* 15**,** 101-124.

MARQUARDT, D. W. 1963. An algorithm for least-squares estimation of nonlinears parameters. 11**,** 431-441.

MEHRKANOON, S., MEHRKANOON, S. & SUYKENS, J. A. K. 2014. Parameter estimation of delay differential equations: An integration-free LS-SVM approach. *Communications in Nonlinear Science and Numerical Simulation,* 19**,** 830-841.

MHASKAR, P., GANI, A., EL-FARRA, N. H., MCFALL, C., CHRISTOFIDES, P. D. & DAVIS, J. F. 2006. Integrated Fault-Detection and Fault-Tolerant Control of Process Systems. *AIChE Jurnal,* 52**,** 2129-2148.

MHASKAR, P., MCFALL, C., GANI, A., CHRISTOFIDES, P. D. & DAVIS, J. F. 2008. Isolation and handling of actuator faults in nonlinear systems. *Automatica,* 44**,** 53-62.

MOHANRAJ, M., JAYARAJ, S. & MURALEEDHARAN, C. 2015. Applications of artificial neural networks for thermal analysis of heat exchangers - A review. *International Journal of Thermal Sciences,* 90**,** 150-172.

MONROY, I., VILLEZ, K., GRAELLS, M. & VENKATASUBRAMANIAN, V. 2012. Fault diagnosis of a benchmark fermentation process: A comparative study of feature extraction and classification techniques. *Bioprocess and Biosystems Engineering,* 35**,** 689-704.

NGUANG, S. K., ZHANG, P. & DING, S. X. 2007. Parity relation based fault estimation for nonlinear systems: An LMI approach. *International Journal of Automation and Computing,* 4**,** 164-168.

OBERDIECK, R., DIANGELAKIS, N. A., PAPATHANASIOU, M. M., NASCU, I. & PISTIKOPOULOS, E. N. 2016. POP - Parametric Optimization Toolbox. *Industrial and Engineering Chemistry Research,* 55**,** 8979-8991.

ODENDAAL, H. M. & JONES, T. 2014. Actuator fault detection and isolation: An optimised parity space approach. *Control Engineering Practice,* 26**,** 222-232.

PAPAMICHAIL, I. & ADJIMAN, C. S. 2002. A rigorous global optimization algorithm for problems with ordinary differential equations. *Journal of Global Optimization,* 24**,** 1-33.

PAPAMICHAIL, I. & ADJIMAN, C. S. 2004. Global optimization of dynamic systems. *Computers and Chemical Engineering,* 28**,** 403-415.

PATTON, R. J. & CHEN, J. 1991. A review of parity space approaches to fault diagnosis. *IFAC Symposium on Fault Detection, Supervision and Safety for Technical Processes,* 24**,** 65-81.

PATTON, R. J. & CHEN, J. 1997. Observer-based fault detection and isolation: Robustness and applications. *Control Engineering Practice,* 5**,** 671-682.

PATTON, R. J. & CHEN, J. 2000. Uncertainty modelling and robust fault diagnosis for dynamic systems. *Issues of Fault Diagnosis for Dynamic Systems.* Springer London.

PATTON, R. J., CHEN, J. & NIELSEN, S. B. 1995. Model-based methods for fault diagnosis: Some guide-lines. *Transactions of the Institute of Measurement and Control,* 17**,** 73-83.

PATTON, R. J., FRANK, P. M. & CLARK, R. N. 2000. *Issues of Fault Diagnosis for Dynamic Systems*, Springer.

PHATAK, M. S. & VISWANADHAM, N. 1988. Actuator fault detection and isolation in linear systems. *International Journal of Systems Science,* 19**,** 1590-1594.

PISTIKOPOULOS, E. N. 2009. Perspectives in Multiparametric Programming and Explicit Model Predictive Control. *AIChE Jurnal,* 55**,** 1918-1925.

PISTIKOPOULOS, E. N., DUA, V., BOZINIS, N. A., BEMPORAD, A. & MORARI, M. 2002. On-line optimization via off-line parametric optimization tools. *Computers and Chemical Engineering,* 26**,** 175-185.

PISTIKOPOULOS, E. N., GEORGIADIS, M. & DUA, V. 2007a. *Multi-parametric Model-Based Control: Theory and Applications, Volume 2*, Wiley-VCH,Weinheim.

PISTIKOPOULOS, E. N., GEORGIADIS, M. & DUA, V. 2007b. *Multi-Parametric Programming: Theory, Algorithms, and Applications, Volume 1*, Wiley-VCH,Weinheim.

POULIEZOS, A. D. & STAVRAKAKIS, G. S. 1994. *Parameter Estimation Methods for Fault Monitoring*, Springer, Dordrecht.

POYTON, A. A., VARZIRI, M. S., MCAULEY, K. B., MCLELLAN, P. J. & RAMSAY, J. O. 2006. Parameter estimation in continuous-time dynamic models using principal differential analysis. *Computers and Chemical Engineering,* 30**,** 698-708.

PROGOVAC, D., WANG, L. Y. & YIN, G. 2014. Parameter estimation and reliable fault detection of electric motors. *Control Theory and Technology,* 12**,** 110-121.

SAKIZLIS, V., PERKINS, J. D. & PISTIKOPOULOS, E. N. 2003. Parametric controllers in simultaneous process and control design. *Computer Aided Chemical Engineering,* 15**,** 1020-1025.

SANCHEZ-FERNÁNDEZ, A., FUENTE, M. J. & SAINZ-PALMERO, G. I. Fault detection in wastewater treatment plants using distributed PCA methods. 2015 IEEE 20th Conference on Emerging Technologies & Factory Automation (ETFA), 8-11 Sept. 2015 2015. 1-7.

SIVATHANU, A. K. & SUBRAMANIAN, S. 2018. Extended Kalman filter for fouling detection in thermal power plant reheater. *Control Engineering Practice,* 73**,** 91-99.

SUN, L., CONG, Y. & KUANG, J. 2014. Asymptotic behavior of nonlinear delay differential-algebraic equations and implicit Euler methods. *Applied Mathematics and Computation,* 228**,** 395-403.

TAN, C. K., WARD, J., WILCOX, S. J. & PAYNE, R. 2009. Artificial neural network modelling of the thermal performance of a compact heat exchanger. *Applied Thermal Engineering,* 29**,** 3609-3617.

TJOA, I.-B. & BIEGLER, L. T. 1991. Simultaneous solution and optimization strategies for parameter estimation of differential-algebraic equation systems. *Industrial & Engineering Chemistry Research,* 30**,** 376-385.

TREETRONG, J., SINHA, J., GU, F. & BALL, A. 2012. *Parameter Estimation for Electric Motor Condition Monitoring*.

VARAH, J. M. 1982. A spline least squares method for numerical parameter estimation in differential equations. *SIAM Journal on Scientific and Statistical Computing,* 3**,** 28-46.

VARZIRI, M. S., POYTON, A. A., MCAULEY, K. B., MCLELLAN, P. J. & RAMSAY, J. O. 2008. Selecting optimal weighting factors in iPDA for parameter estimation in continuous-time dynamic models. *Computers and Chemical Engineering,* 32**,** 3011-3022.

VASSILIADIS, V. S., SARGENT, R. W. H.,PANTELIDES, C. C. 1994. Solution of a Class of Multistage Dynamic Optimization Problems. 1. Problems without

Path Constraints. *Industrial & Engineering Chemistry Research,* 33**,** 2111-2122.

VENKATASUBRAMANIAN, V., RENGASWAMY, R. & KAVURI, S. N. 2003a. A review of process fault detection and diagnosis: Part II: Qualitative models and search strategies. *Computers & Chemical Engineering,* 27**,** 313-326.

VENKATASUBRAMANIAN, V., RENGASWAMY, R., KAVURI, S. N. & YIN, K. 2003b. A review of process fault detection and diagnosis: Part III: Process history based methods. *Computers & Chemical Engineering,* 27**,** 327-346.

VENKATASUBRAMANIAN, V., RENGASWAMY, R., YIN, K. & KAVURI, S. N. 2003c. A review of process fault detection and diagnosis Part I: Quantitative model-based methods. *Computers & Chemical Engineering,* 27**,** 293-311.

VILLADSEN, J. B. N. 1982. A family of collocation based methods for parameter estimation in differential equations. *The Chemical Engineering Journal,* 23**,** 1-13.

WIMBERGER, D. & VERDE, C. 2008. Fault diagnosticability for an aerobic batch wastewater treatment process. *Control Engineering Practice,* 16**,** 1344-1353.

WITHERS, P. 1996. Ultrasonic, acoustic and optical techniques for the non invasive detection of fouling in food processing equipment. *Trends in Food Science and Technology,* 7**,** 293-298.

XING-GANG, Y. & EDWARDS, C. Robust sliding mode observer-based actuator fault detection and isolation for a class of nonlinear systems. Proceedings of the 44th IEEE Conference on Decision and Control, 15-15 Dec. 2005 2005. 987-992.

XUAN, J., XU, Z. & SUN, Y. 2015. Selecting the Number of Principal Components on the Basis of Performance Optimization of Fault Detection and Identification. *Industrial & Engineering Chemistry Research,* 54**,** 3145-3153.

ZAREI, J. & SHOKRI, E. 2014. Robust sensor fault detection based on nonlinear unknown input observer. *Measurement,* 48**,** 355-367.

ZHANG, X., POLYCARPOU, M. M. & PARISINI, T. 2010. Fault diagnosis of a class of nonlinear uncertain systems with Lipschitz nonlinearities using adaptive estimation. *Automatica,* 46**,** 290-299.

ZHANG, Y. & JIANG, J. 2008. Bibliographical review on reconfigurable fault-tolerant control systems. *Annual Reviews in Control,* 32**,** 229-252.

ZHAO, Z., GU, X. & JIANG, W. 1999. Fault Detection Based on Wavearx Neural Network. *IFAC Proceedings Volumes,* 32**,** 7826-7831.

APPENDIX A: ARTIFICIAL NEURAL NETWORK-BASED FORMULATION

The nonlinear ODE model is converted into algebraic equations using the ANN as described next. A basic structure of ANN is shown in Figure A.1. Nodes are represented by small circles and each layer consists of one or more nodes. The lines between the nodes indicate the flow of information from one node to the next. In this feedforward of the NN, the information flows from the input to the output.

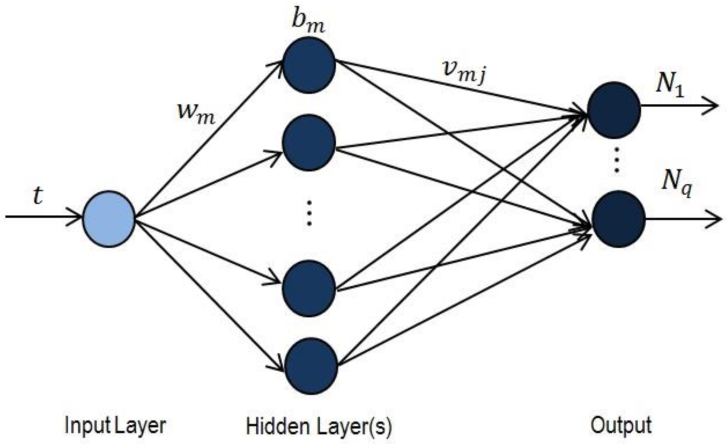

Figure A.1 ANN framework

For given values of $\mathbf{u}$ and $\boldsymbol{\theta}$, the solution of the ODE model (Equation (3.2) to Equation (3.4)) can be obtained. The output from the ANN is given by Dua and Dua (2011):

$$N_q = \sum_m v_{mq} \sigma_m \tag{A.1}$$

where

$$\sigma_m = \frac{1}{1+e^{-am}} \tag{A.2}$$

where

$$a_m = \sum_p w_m t + b_m \tag{A.3}$$

where subscripts p, q and m represent the input of ANN, output of ANN and hidden layer nodes, respectively. Here, only one hidden layer is used. The output from the ANN, N_q, is dependent on v_{mq}, which is representing the weights from the hidden nodes to the outputs, and the sigmoidal transformation, σ_m. The activation function of the node, a_m, is dependent on the input signal, t, which is adjusted by weight from the input nodes to the hidden nodes, w_m, and summed up with the bias on the hidden nodes, b_m.

A trial solution of the ODE model is postulated as:

$$x_j^{ANN} = x_j^0 + tN_q \tag{A.4}$$

where an output of ANN model, N_q, is considered for each trial solution x_j^{ANN}. A trial solution of the ODEs (Equation (A.4)) is constructed such that it satisfies the system's initial condition given by Equation (3.3). The ANN time-dependent solution is represented in Equation (A.5) and the change in the ANN outputs with time is given by Equation (A.6).

$$\frac{dx_j^{ANN}}{dt} = N_q + t\frac{dN_q}{dt} \tag{A.5}$$

$$\frac{dN_q}{dt} = \sum_m v_m w_{mp} \sigma_m \tag{A.6}$$

Therefore, the solution of the ODE model (Equation (3.2)) for given values of $\mathbf{u}$ and $\boldsymbol{\theta}$ can be formulated as the following NLP problem as follows:

Problem A.1:

$$\varepsilon_{ODE} = \min_{x_j^{ANN}, N, \sigma, w, v, a, b} \sum_{j \in J} \sum_{i \in I} \left(\frac{dx_j^{ANN}(t_i)}{dt} - f_j(\mathbf{x}(t_i), \mathbf{u}(t_i), \boldsymbol{\theta}, t) \right)^2 \tag{A.7}$$

Subject to:

Equations (A.1) to (A.6)

APPENDIX B: RUNGE-KUTTA FOURTH-ORDER FORMULATION

The RK method achieves the accuracy of a Taylor series approach without requiring the calculation of higher derivatives. The most popular RK method is fourth order as given as follows (Chapra and Canale, 2009):

$$x_j(t_{i+1}) = x_j(t_i) + \frac{1}{6}(k_1 + 2k_2 + 2k_3 + k_4)h \tag{B.1}$$

where

$$k_1 = f_j\left(x_j(t_i), t_i\right) \tag{B.2}$$

$$k_2 = f_j\left(x_j(t_i) + \frac{1}{2}k_1 h, t_i + \frac{1}{2}h\right) \tag{B.3}$$

$$k_3 = f_j\left(x_j(t_i) + \frac{1}{2}k_2 h, t_i + \frac{1}{2}h\right) \tag{B.4}$$

$$k_4 = f_j\left(x_j(t_i) + k_3 h, t_i + h\right) \tag{B.5}$$

where k is the slope approximation and h is the time step of the approximation. Therefore, the numerical solution of nonlinear ODEs in Equation (3.2) is given in Equation (B.1).